GRIFFITH UNIVERSITY

-

GOLD COAST CAMPUS

COMPRESSIBILITY CHARACTERISTICS OF SOUTH EAST QUEENSLAND SOFT CLAYS

by

Ross Pyke

A thesis submitted in partial fulfilment of the requirements for the Bachelor of Engineering in Civil Engineering

Supervisor: Prof. A.S. Balasubramaniam

October, 2003

DECLERATION

I certify that the activities and documentation of this Thesis have been undertaken by myself, and that the content is the direct result of my own effort except where contribution data and external assistance has been acknowledged.

Name: .....

Student Number: .....

Date: .....

Supervisor: .....

Date: .....

ACKNOWLEDGEMENTS

I wish to express my sincerest appreciation and gratitude to my supervisor Prof. Balasubramaniam and co-supervisor Erwin Yan-Nam Oh for their support and direction during the thesis period.

I am also grateful to Mr. Vasantha Wijeyakulasuriya at the Queensland Department of Main Roads (Material and Geotechnical Service Branch at Herston), for his assistance in providing the necessary soil data and the associated internal reports as used in this research work.

THESIS BRIEF

Student Name: Ross Pyke
Student Number: 1420454
Course: 4091ENG Thesis
Date: 19/03/03
Title of Project: Compressibility Characteristics of South East Queensland Soft Clays
Supervisor: Professor Balasubramaniam

BACKGROUND

Several motorways and tall buildings are constructed in Brisbane and on the Gold Coast. Associated with these activities are the soil profiles and laboratory and field test data available with the Queensland Main roads and other private sector organisations.

It would be worthwhile if this data was collected and analysed in a form suitable for academic research and private sector activities. Emphasis will be made on the engineering properties of the soft clay deposits, but in addition the field test data on other layers which are of importance in foundation engineering will also be collected and analysed.

OBJECTIVES

The strength and compressibility characteristics of the Brisbane and Gold Coast sub-soils as determined from the laboratory and field tests will be used to characterise their engineering behaviour.

Useful correlations will be established between these engineering properties and the index properties.

ABSTRACT

There is extensive soft clay in the South East Queensland region. Associated with soft clays are problems that arise from settlement. Compressibility characteristics of soft clays in the Gold Coast Highway, the Sunshine Motorway, and the Port Brisbane Motorway have been investigated.

The soft clays encountered were generally estuarine and swamp deposits, coastal mangrove and tidal deposits of varying depths. The deposits examined mainly comprised of extremely soft, recently deposited, estuarine silty clay being generally very soft to firm, compressible silty clays of medium to high plasticity.

The data of moisture content (w_n), liquid limit (w_L) and plasticity index (I_p) were used to construct the statistical distribution for the soil properties and has been correlated with the compression index (C_c).

TABLE OF CONTENTS

LIST OF FIGURES

LIST OF TABLES

NOTATION

C_c	Compression index
C_c*	Intrinsic compression index
c_v	Coefficient of consolidation
m_v	Coefficient of volume compressibility
e	Void ratio
e_o	In-situ void ratio
e_L	Void ratio at liquid limit
e_{100}*	Void ratio for $\sigma_v9 = 100$ kPa
σ_v9	Effective vertical stress
$\sigma_{vo}9$	Effective overburden pressure
w_L	Liquid limit
I_p	Plasticity index
w_n	Natural moisture content
G_s	Specific gravity of soil
I_v	Void index

1. CHAPTER 1 - INTRODUCTION

1.1 BACKGROUND

There are extensive deposits of soft clay in the South East Queensland region. Associated with these soft clays are problems that arise from settlement. In determining these settlements accurately, accurate determination of the compressibility of the soft clay is important. Measuring the compressibility of soft clay is an uncertain endeavour due to variations in the soil strata, methods of soil sampling, choice of testing methods, and variation between field and laboratory test conditions. It is therefore necessary to have reliable methods of determining the compressibility characteristics of soft clays.

There are several motorways that are constructed in the South East Queensland region. Associated with these construction activities are the soil profiles along with the laboratory and field test data which is available from the Queensland Department of Main Roads and other private sector organisations. The data collected and analysed in this thesis has been done so that the soft clay properties are documented for future use.

Compression of the soil results in a volume change and vertical displacement. This settlement is referred to as consolidation settlement. The compressibility of a soft clay can be measured by the oedometer consolidation test. This test finds the parameter that defines the settling time, the coefficient of consolidation (c_v). The parameter used to estimate the settlement magnitude is the coefficient of volume change (m_v), this parameter is calculated from the void ratio (e) versus log effective vertical stress ($\sigma_v 9$) relationship which is derived from the oedometer consolidation test. It is well known that the plasticity index (I_p) governs the mechanical properties of soft clays and has been correlated with the compressibility and strength of the soil.

1.2 OBJECTIVES

It is the purpose of this thesis to show the consolidation characteristics of South East Queensland soft clays. This will be done by characterising the consolidation properties of the soft clay deposits through the use of data obtained from laboratory testing on undisturbed samples.

The soft clay data were obtained from three sites: the Brisbane Port Road, the Sunshine Motorway, and the Gold Coast Highway. Most of the time was spent in acquiring the consolidation test data from the voluminous reports available from the Queensland Department of Main Roads such that only little time was available to comprehensively analyse the data.

1.3 OUTLINE OF THESIS

In this thesis an introduction which covers the background of the research and identifies the objective of the thesis is given in Chapter 1. An illustration of the relevant work that has been done recently by others is given in Chapter 2, and gives a review of the related work. A general outline of the data obtained from the three sites and the methods used to analyse them is given in Chapter 3. Chapter 4 gives the analysed results and the discussion of the findings, and Chapter 5 gives the conclusions and recommendations for further work arising from the findings.

1.4 COLLECTION OF DATA

A total of three reports have been collected. A summary of the reports collected can be seen in Table 3.1.

Table 1.1 Summary of reports

Report No.	Project Name	Number of Boreholes	Number of Oedometer Consolidation Tests
R1828	Gold Coast Highway – Helensvale Interchange to Arundel Drive	12	7
R1746	Sunshine Motorway Stage 2 – Area 2	31	33
R3197	Port Brisbane Motorway - Stage 2 Investigation	12	11

2. CHAPTER 2 – LITERATURE REVIEW

2.1 GENERAL

The term consolidation refers to the volume change of a soil due to the drainage of excess pore water. The most basic form is one-dimensional consolidation where there is zero lateral strain. The vertical displacement due to volume change arising from the process of consolidation is referred to as consolidation settlement. The process of consolidation will continue until all the excess pore water pressure has dissipated.

There are three main parameters that concern the compressibility characteristics of a soft clay:

1. Compression index (C_c)
2. Coefficient of consolidation (c_v)
3. Coefficient of volume compressibility (m_v)

The oedometer consolidation test enables the values of c_v and m_v to be directly measured for a soil sample in the laboratory. The test involves applying a vertical load to a saturated soil at time intervals until the compression recorded appears steady. The load is increased after every increment. Plots of void ratio (e) against the effective vertical stress (σ_v9) are derived from the oedometer consolidation test and can be seen in Figure 2.1. The compression index (C_c) is equal to the slope of the linear portion of the line which is defined by the following equation:

$$C_c = \frac{e_o - e_1}{\log(\sigma_1 / \sigma_0)} \quad \text{..... (2.1)}$$

The coefficient of volume compressibility (m_v) is defined as the volume change per unit volume per unit increase in effective stress (m^2/MN). The coefficient of volume compressibility decreases with the increase in the stress. The other parameter is the coefficient of consolidation (c_v). This parameter describes the rate at which the consolidation occurs i.e. (m^2/year). For the settlement due to consolidation to be known these parameters are required. Refer to Appendix D for theory of one-dimensional consolidation.

2.2 COMPRESSIBILITY OF CLAYS

There are a number of benefits in finding correlations between the index properties of the soft clay and its compressibility characteristics. Many researchers have investigated the correlation between the compression index (C_c) and the liquid limit (w_L), but have also established correlations with other index properties of the soil. Some of these empirical relationships can be seen in Table 2.1.

Table 2.1 Empirical relations for compression index

Reference	Relation	Comments
Terzaghi & Peck (1967)	$C_c = 0.009(w_L - 10)$	Undisturbed clay
	$C_c = 0.007(w_L - 10)$	Remoulded clay
	w_L = liquid limit (%)	
Azzouz *et al*. (1976)	$C_c = 0.01 w_N$	Chicago clay
	w_N = natural moisture content (%)	
	$C_c = 0.0046(w_L - 9)$	Brazilian clay
	$C_c = 1.21 + 1.005(e_o - 1.87)$	Motley clays from Sao Paulo city
	e_o = in situ void ratio	
	$C_c = 0.208 e_o + 0.0083$	Chicago clay
	$C_c = 0.0115 w_N$	Organic soil, peat
Nacci *et al*. (1975)	$C_c = 0.02 + 0.014(I_p)$	North Atlantic clay
	I_p = plasticity index (%)	
Rendon-Herrero (1983)	$C_c = 0.141 G_s^{1.2}\left(\frac{1+e_o}{G_s}\right)^{2.38}$	
	G_s = specific gravity of soil	
Nagaraj & Murty (1985)	$C_c = 0.2343\left(\frac{LL}{100}\right)G_s$	

Skempton (1970) investigated the consolidation of twenty natural clays by gravitational compaction. Skempton (1970) drew the following conclusions from relating the in situ void ratio e_o and the effective overburden pressure $\sigma_{vo}9$.

a) The relationship between e_o and log $\sigma_{vo}9$ (i.e. the sedimentation compression curve) is essentially linear for any particular clay.
b) At a given value of $\sigma_{vo}9$ the void ratio of a normally consolidated natural clay depends on the nature and amount of clay minerals present, as indicated by the liquid limit. The higher the liquid limit the higher is the void ratio.
c) A most striking observation is the converging pattern formed by the various compression curves.
d) When plotted in terms of liquidity index, rather than void ratio, the results lie within a moderately narrow band. Clays with a high sensitivity lie towards the upper part of the band while those with low sensitivity lie towards the lower part of the band.

Burland (1990) has investigated the compressibility characteristics of reconstituted clays, i.e. a clay that has been thoroughly mixed at a water content equal to or greater than the liquid limit. Figure 2.1 shows the one-dimensional compression curves for a number of

clays with varying plasticity. Burland observed that e_L (void ratio at the liquid limit) is a more fundamental parameter in determining the compressibility of a clay than w_L. This observation was established from comparing the Kleinbelt Ton and Argile Plastique clays. Both of these clays have the same liquid limit, but Argile Plastique has a lower e_L due to a lower specific gravity.

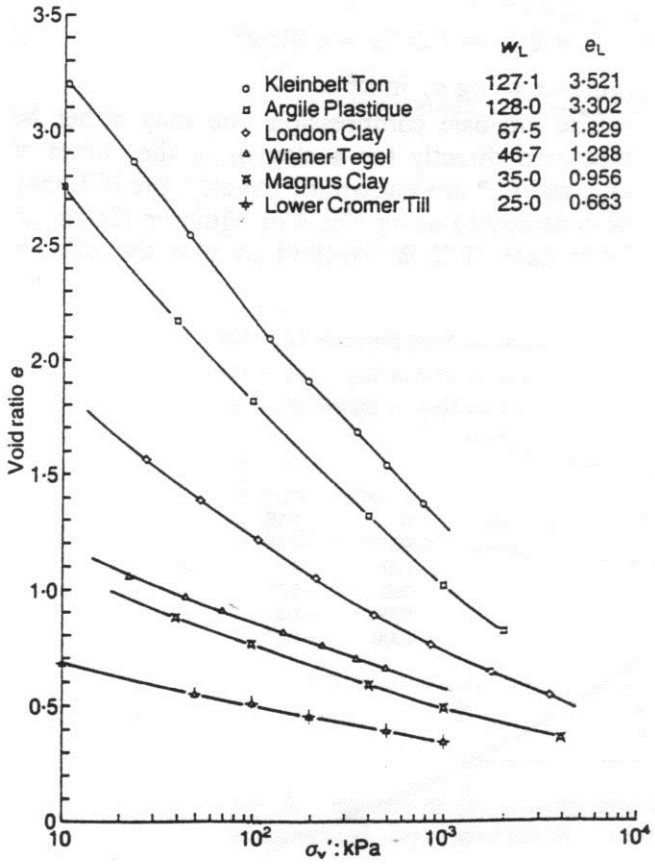

Figure 2.1 One-dimensional compression curves for various reconstituted clays (Burland, 1990)

Burland introduced the term 'intrinsic properties'. This term refers to the properties of reconstituted clays as described earlier. This term was chosen since it refers to the basic, or inherent, properties of a given soil prepared in a specific manner and which are independent of its natural state (Burland, 1990). The intrinsic properties can be used as a reference to evaluate the undisturbed behaviour of natural soils and therefore, the influence of soil structure on the resulting behaviour may be determined (Lutenegger & Cerato, 2003).

Burland (1990) normalised the curves in Figure 2.1 by assigning fixed values to e_{100}* and e_{1000}* and can be seen in Figure 2.2. The quantities e_{100}* and e_{1000}* are the void ratios corresponding to $\sigma_v 9$ = 100 kPa and 1000 kPa respectively and the asterisk denotes an intrinsic property. The void index (I_v) is the normalising parameter and is defined by Equation 2.2 (Burland, 1990).

$$I_v = \frac{e - e_{100}^*}{e_{100}^* - e_{1000}^*} = \frac{e - e_{100}^*}{C_c^*} \quad \text{..... (2.2)}$$

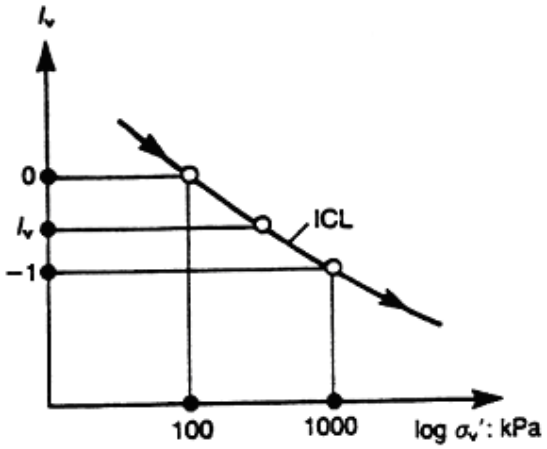

Figure 2.2 Normalised compression curves by the use of void index, I_v (Burland, 1990).

The intrinsic compression index C_c^* is defined as $e_{100}^* - e_{1000}^*$. When $e = e_{100}^*$, $I_v = 0$ and when $e = e_{1000}^*$, $I_v = -1$. Burland (1990) replotted three of the intrinsic compression curves with varying liquid limits and pressures from Figure 2.1 in terms of void index I_v versus log $\sigma_v 9$ and can be seen in Figure 2.3. The line achieved from the plot is termed the intrinsic compression line (ICL). Burland (1990) represented the ICL by the following equation.

$$I_v = 2.45 - 1.285x + 0.015x^3 \quad \text{..... (2.3)}$$

Where x = log $\sigma_v 9$ in kPa.

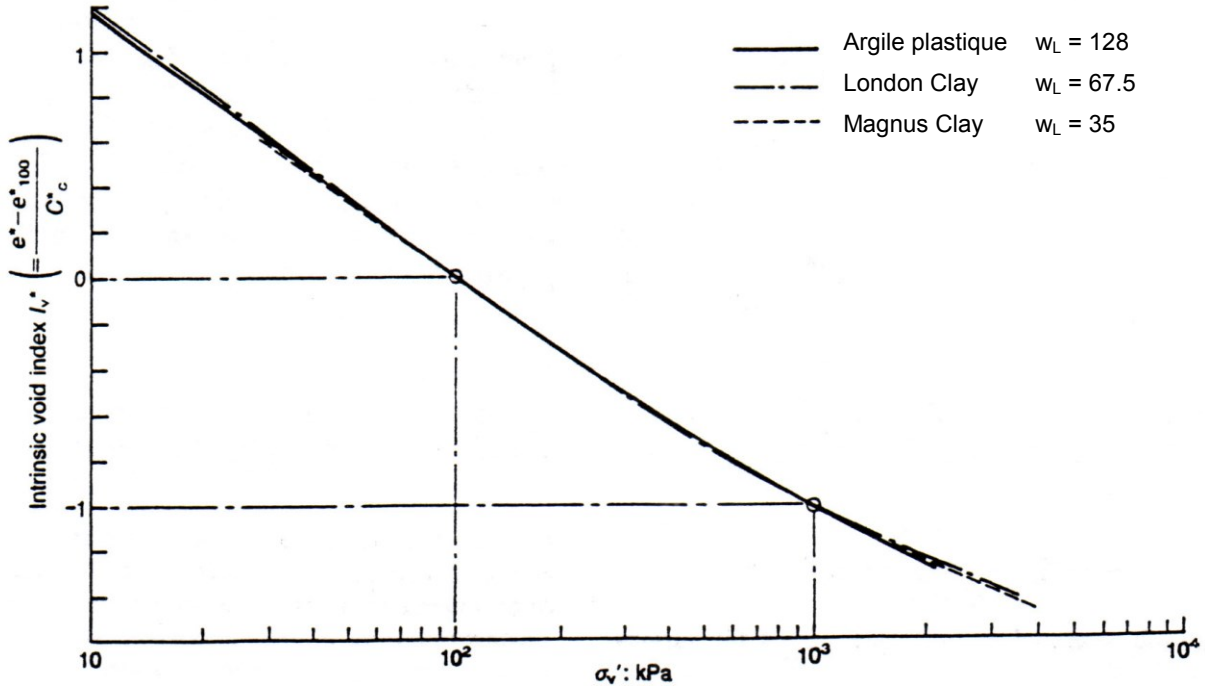

Figure 2.3 Normalised intrinsic compression curves (Burland, 1990).

The intrinsic compression line may either be measured directly for a clay or, if the values of e_{100}* and C_c* are known for the clay, the ICL may be constructed using Figure 2.3 or Equation 2.3 (Burland, 1990).

The geotechnical engineering deals with natural processes and material properties of geological formations which must be interpreted from limited observations and few data availability. Several soil properties exhibit relatively large spatial variability, even within the so called homogeneous zones. Deterministic descriptions of this spatial variability are not feasible due to prohibitive cost of sampling and to uncertainties induced by measurement errors. Consequently, the reliable settlement and differential settlement of a structure can not proceed from a deterministic approach. Thus, for the settlement and differential settlement analysis, the use of probabilistic approaches allows modelling of the uncertainties by analysing their dispersion effect on the global behaviour of the structure.

Uncertainties have long been appreciated in evaluating the capacity of soil foundations, at least in a qualitative manner. However, in the overwhelming majority of soil foundation texts and courses, after making the observation that uncertainty is an important factor, it is then relegated to a minor position, and the remainder of the text/course is evaluated in a traditional deterministic fashion. The uncertainty of calculation models is addressed elsewhere (e.g., Prakoso and Kulhawy 2002).

In this context, the stochastic finite element method, was efficiently used in solving complex structural systems (Shinuzuka 1972, Cambou 1975, Vanmarcke et al. 1983, and Liu et al. 1986) with some parametric uncertainties. In the geotechnical area, it has been

also applied, and one notes mainly the contributions of Baecher and Ingra (1981) to predict settlement, Ishiu and Suzuki (1987) for slope stability reliability analysis, Righetti and Harrop-Williams (1988) for analysing a random soil media, Paice et al. (1996) for finite element modelling of settlements on spatially random soil, Fenton and Vanmarcke (1998) for investigating the spatial variation in liquefaction risk, Rahman and Yeh (1999) for studying the variability of seismic response of soils, Griffiths and Fenton (2001) for bearing capacity of spatially random soil and, Nour et al. (2001) for the seismic behaviour of heterogeneous soil profile via stochastic finite element analysis.

2.3 CORRELATIONS

When the ICL could not be measured directly, Burland (1990) established correlations between e_L (void ratio at the liquid limit) and e_{100}* and C_c* to measure the ICL. Regression analyses defined the best fit regression lines as (Burland, 1990).

$$e_{100}* = 0.109 + 0.679e_L - 0.089e_L^2 + 0.016e_L^3 \quad \text{..... (2.4)}$$

$$C_c* = 0.25e_L - 0.04 \quad \text{..... (2.5)}$$

Equations showed an excellent correlation, with correlation factors of 0.991 and 0.985 respectively. Burland (1990) stipulates that for the equations to correlate well, they should only be used for values of e_L within the range 0.6 to 4.5 and for soils with Atterberg limits lying above the A line.

Tanaka (2000) investigated the relationship between the compression index (C_c) and the liquid limit (w_L) and confirmed the empirical relationship established by Terzaghi & Peck (1967) can be applied to reconstituted or remoulded soils, i.e.

$$C_c = 0.009(w_L - 10) \quad \text{..... (2.6)}$$

This means that when the pressure becomes larger than the yield pressure, the C_c for the reconstituted or remoulded soil becomes the same as the C_c for the in-situ soil.

3. CHAPTER 3 – SOIL CHARACTERISTICS AT THREE SITES IN SE QLD

3.1 GOLD COAST HIGHWAY SITE

The Gold Coast Highway is the major route through the Gold Coast of Queensland. Due to the increased traffic, it has become necessary to upgrade the existing two lane road to a four lane facility. There is an important wetland reserve adjacent to this section of highway which has environmental significance. The section of highway traverses a swamp of soft clay up to 13.5 m deep.

The soils and rocks along the highway belong to the Neranleigh-Fernvale Group of the Silurian Age. The rocks are mainly greywacks with some interbedded argillite. Quaternary alluvium is present in valleys between the ridges. This alluvium consists of clays and silty clay overlain by soft organic clays. The boreholes indicated a subsurface profile of consolidated alluvium or argillite below soft to very soft estuarine clays. The soft clay deposit is a maximum 13.5m deep towards the centre of the plain, thinning to a minimum of 3m at the outer edges.

Field and laboratory tests were performed to investigate the geotechnical properties of the subsurface profile. The field testing was to investigate the general subsurface profile and to perform the field vane shear test. The laboratory testing included the standard classification and the tests involved in determining the engineering properties of the soils. The soils were classified using the Unified Soil Classification System.

The moisture content ranges from 20% to 172%. The wet density (ρ_{wet}) of the clays was determined at all depths and ranged from 1.5 t/m^3 to a high of 1.9 t/m^3. The dry density (ρ_{dry}) of the clays ranged from a low of 0.5 t/m^3 to a high of 1.6 t/m^3. The moisture content generally decreases with depth as can be seen in Figure 3.1. The liquid limit and plasticity index are generally uniform with depth.

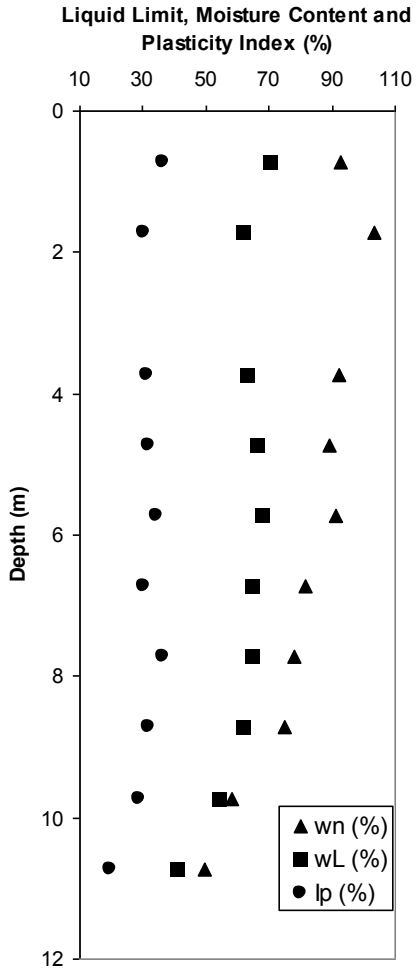

Figure 3.1 Index properties in relation to depth for Gold Coast Highway

3.2 SUNSHINE MOTORWAY SITE

The Sunshine Motorway is the main connection between the Sunshine Coast and Brisbane. Test data from a number of soft soil and swampy areas along the alignment were collected. Included were the consolidation parameters, classifications, Atterberg limits and shear strengths.

The scope of the report is directed at Area 2 of the Sunshine Motorway. This area extends through cane farm lowlands, a minor swamp section adjacent to the Maroochy River, then higher terrain south of West Coolum Road, before another swamp area and more cane farm lowlands.

This alignment of the Motorway predominantly traverses low lying unconsolidated sediments including;

- Estuarine swamp and lagoonal deposits

- Pleistocene to Holocene deposits consisting of soft organic clay, mud, sand-clay mixtures and fine sand.

- Coastal mangrove and tidal deposits
  - Holocene deposits consisting of very soft fine grained clay/silt mixtures which contain minor sand.

These sediments are from the Quaternary Age.

The moisture content ranges from 16.4% to 162.8%. The wet density (ρ_{wet}) of the clays was determined at all depths and ranged from 1.1 t/m^3 to a high of 2.8 t/m^3. The dry density (ρ_{dry}) of the clays ranged from a low of 0.5 t/m^3 to a high of 1.9 t/m^3. The plasticity index, liquid limit, and moisture content are generally uniform with depth and can be seen in Figure 3.2.

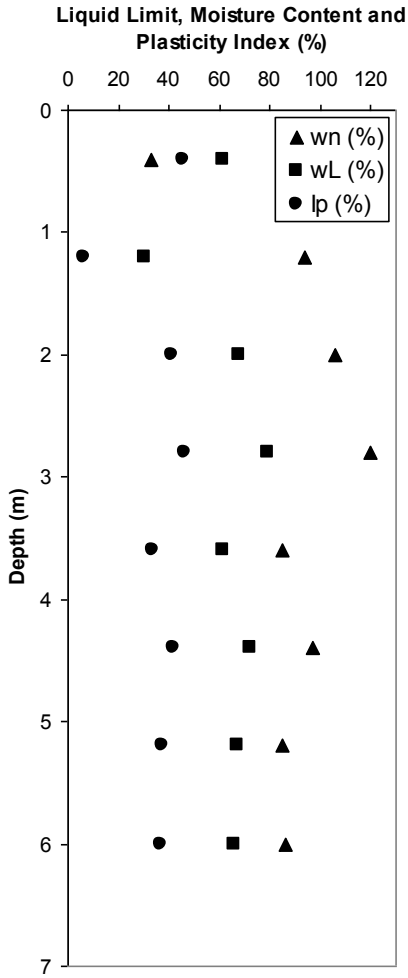

Figure 3.2 Index properties in relation to depth for Sunshine Motorway

3.3 PORT BRISBANE MOTORWAY SITE

The Port Brisbane Motorway connects the Gateway Motorway to the Port of Brisbane. The Gateway Motorway is the western end of the road and the Port of Brisbane is the eastern end. The route generally traverses flat low lying estuarine terrain. However, at the western end it traverses sloping residual terrain.

The estuarine deposits encountered were generally dark grey to dark brown, very soft to firm, moist to wet, compressible silty clays of medium to high plasticity. It was found that the Oxbow creek bed comprised of extremely soft, recently deposited, estuarine silty clay which overlies young deposits of soft to firm estuarine silty clay and silty sand. This very soft soil thickness varies up to 5m depth. These deposits overlie old beds of residual and alluvial soils and bedrock belonging to the Tingalpa Formation. The layer thicknesses vary across the site with a maximum depth of 26.5m. The upper silty clay alluvial layer was found continuously along the alignment except the western end. This alluvial silty clay has low plasticity compared to the estuarine silty clay. The residual soils exhibit the engineering properties of a moist, stiff to hard sandy clay/sandy silty clay.

The road traverses estuarine and residual soils with varying thicknesses. The moisture content ranges from 22% to 108%. The wet density (ρ_{wet}) of the clays was determined at all depths and ranged from 1.2 t/m^3 to a high of 2.0 t/m^3. The dry density (ρ_{dry}) of the clays ranged from a low of 0.7 t/m^3 to a high of 1.6 t/m^3. It can be seen in Figure 3.3 that the plasticity index, liquid limit, and moisture content are generally uniform with depth.

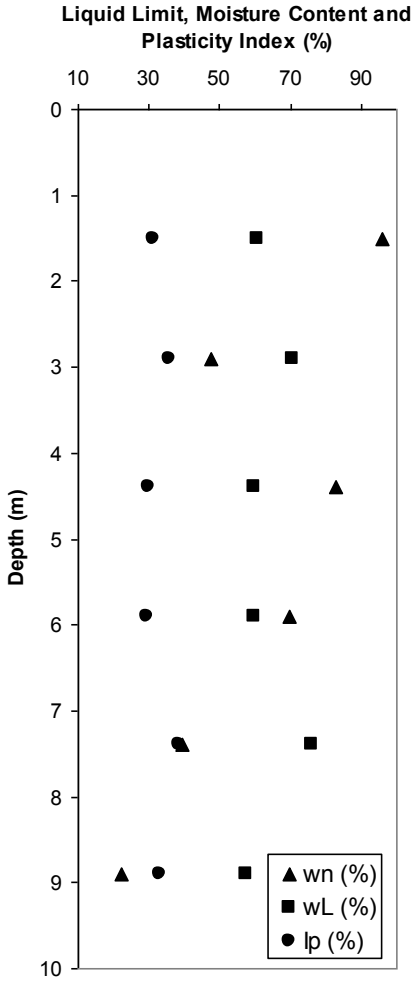

Figure 3.3 Index properties in relation to depth for Brisbane Port Road

3.4 STATISTICAL METHODS

Three soil parameters are evaluated: moisture content (w_n, %), liquid limit (w_L, %), and plasticity index (I_p, %). Further, empirical equations for the Compression Index are established based on the relation with liquid limit and plasticity index. The data was also analysed statistically using frequency distribution diagrams.

4. CHAPTER 4 – RESULTS AND ANALYSIS

4.1 INTRODUCTION

The data for the Gold Coast Highway, Sunshine Motorway and the Port Brisbane Motorway sites are presented here.

4.2 GOLD COAST HIGHWAY

4.2.1 STATISTICAL DISTRIBUTION

In reality, there is no way that a soil property can be predetermined. Having established the random nature of the soft clay property from previous tests, it is clear that every soil parameter will be associated with some statistical numbers.

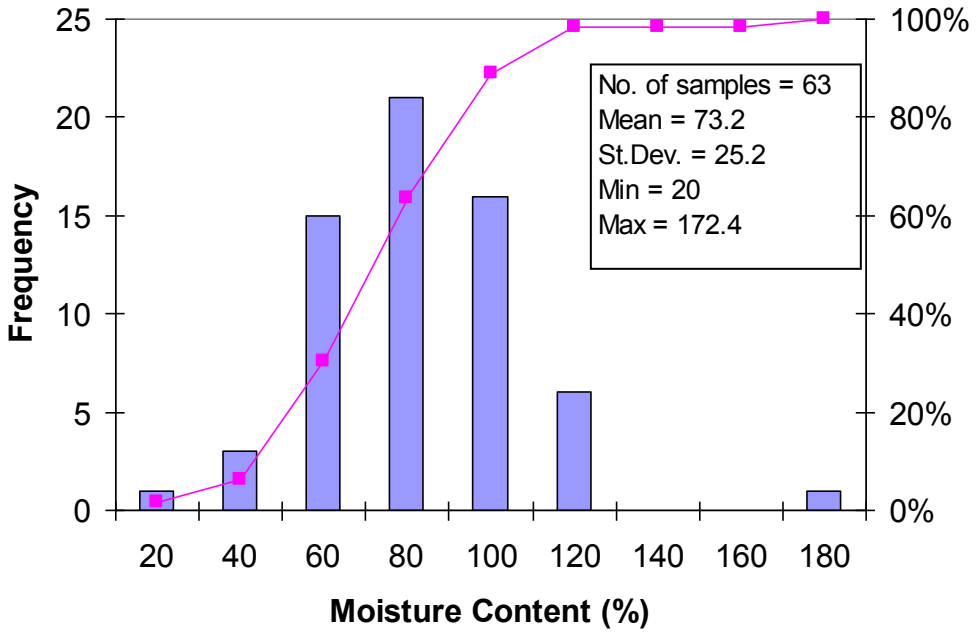

Figure 4.1 Moisture content histogram with cumulative frequency

The data of moisture content (w_n), liquid limit (w_L) and plasticity index (I_p) were used to construct the statistical distributions for the soil properties. Figure 4.1 shows the histogram of the moisture content in the Gold Coast Highway. As shown in the figure, 63 samples were analysed, and the w_n ranges from 20 to 172.4%. Most of the soil samples have a w_n of 60 to 100%. This shows the soft clay has high water content.

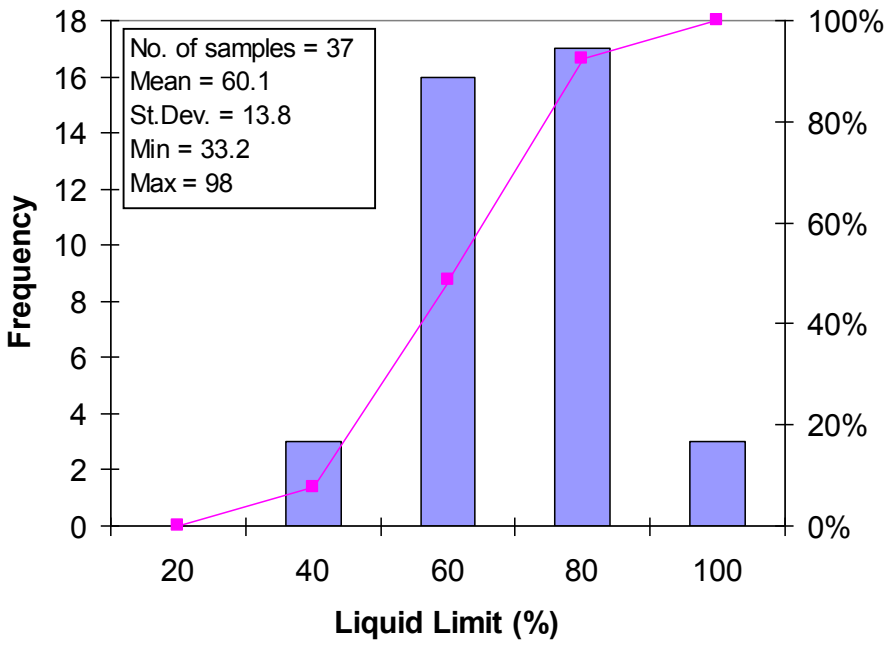

Figure 4.2 Liquid limit histogram with cumulative frequency

Figure 4.2 shows the histogram of liquid limit from 37 samples, and has a mean of 60.1% with most of the values ranging between 60 and 80%. Figure 4.3 shows the histogram of plasticity index and Table 4.1 lists their parameters.

Table 4.1 Statistical distribution for the moisture content, w_L, and I_p.

	No. of samples	Mean (%)	Std. Dev. (%)	Min (%)	Max (%)	Median (%)
Moisture content	63	73.2	25.2	20	172.4	72.8
I_p	37	31.3	9.3	15.2	61.4	31.2
w_L	37	60.1	13.8	33.2	98	61

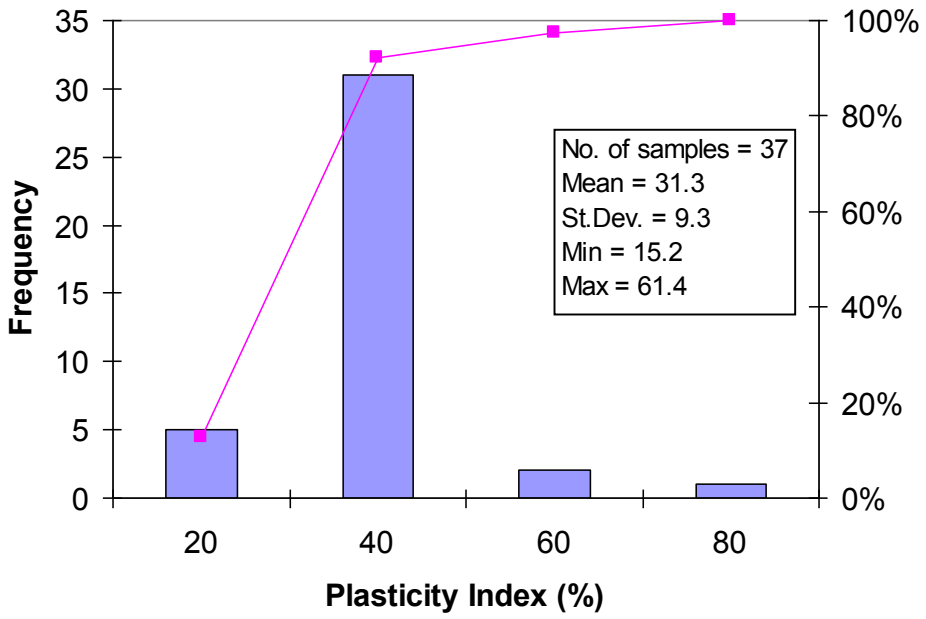

Figure 4.3 Plasticity index histogram with cumulative frequency

4.2.2 COMPRESSIBILITY CHARACTERISTICS

The consolidation characteristics of the soft clay in the Gold Coast Highway were determined by the laboratory oedometer consolidation test. The parameters normally required are: (i) The compressibility of soil, which is expressed in terms of coefficient of volume compressibility (m_v), and (ii) The compression index (C_c), which allows the calculation of the magnitude of primary consolidation, and (iii) The time parameter, which is illustrated by the coefficient of consolidation (c_v). These parameters will measure the amount of compression of the soil when it is loaded, and indicate the rate of compression.

A total of seven, one-dimensional oedometer consolidation tests (data given in Appendix A) were established on the soft clay to estimate the deformation parameters and the stress history of the samples. Six or seven loading increments (depending on the depth of sample) and two unloading steps were applied. The test results provide information on the pre-consolidation pressure (or maximum past pressure) and the loading or unloading behaviour of the samples under controlled conditions.

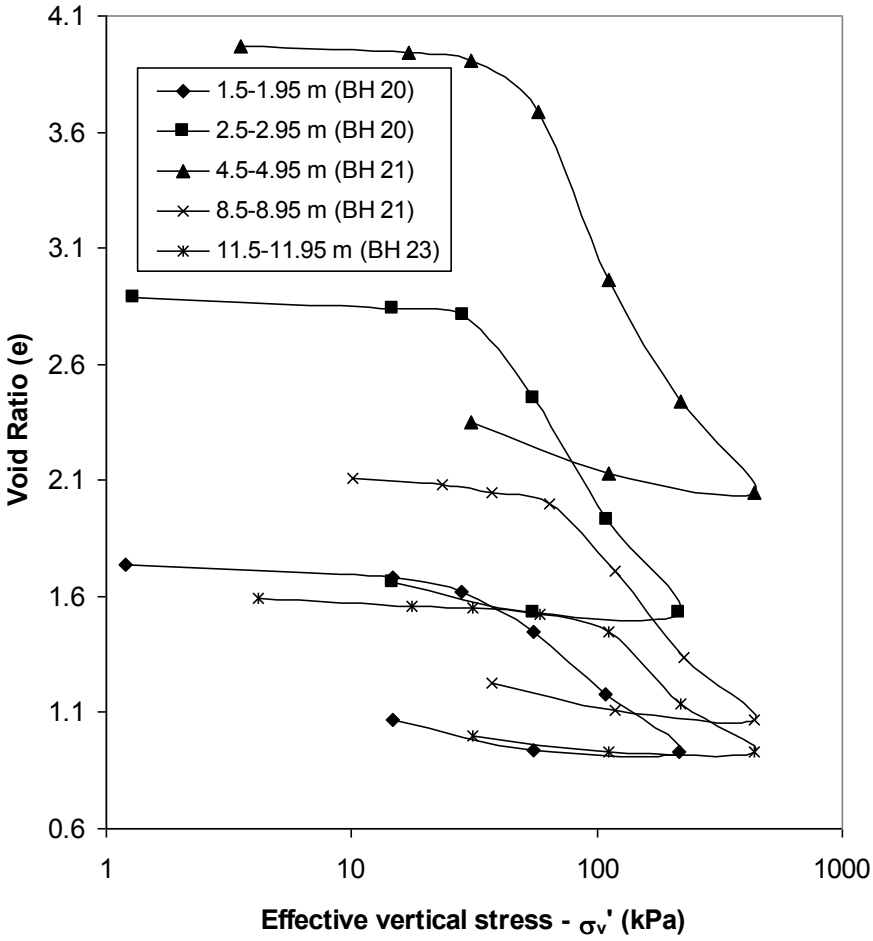

Figure 4.4 Consolidation curves at varying depth (Gold Coast Highway)

Figure 4.4 shows the e-log σ_v9 relationships for different depths. The relationships representing samples deeper than 4.5m appear geometrically similar. The e-log σ_v9 relationships resemble that of sensitive clay. The figure gives the compression indexes (C_c) and the pre-consolidation pressures, and is assessed in Table 4.2.

Figure 4.5 illustrates the coefficient of volume compressibility (m_v) for different soil depths. Based on the results, the compressibility of the soft clays ranges from 0.5 to 3.5 m^2/MN. The m_v profile shows that the soft clay deposit becomes less compressible with depth.

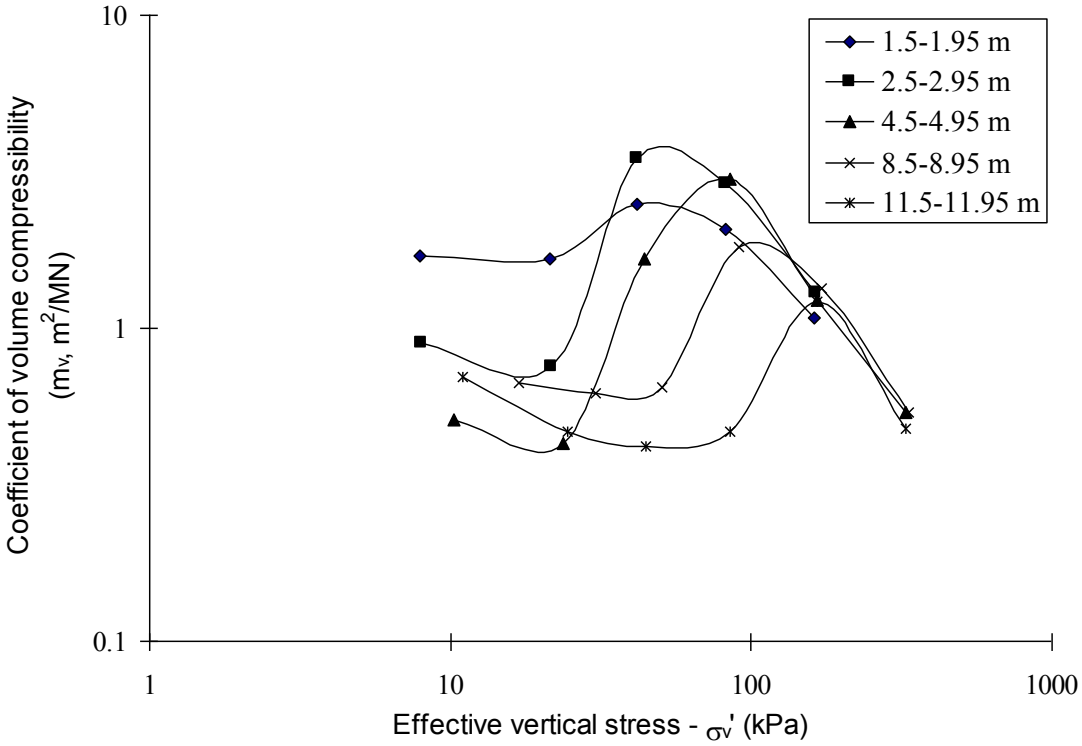

Figure 4.5 Coefficient of volume compressibility curves at varying depth

Following the results of the oedometer tests, the coefficient of consolidation (c_v) is given in Figure 4.6. For stress ranges less than the interpreted pre-consolidation pressure, the c_v values vary widely from 2.24 to 12.97 m^2/year. For stress ranges greater than the interpreted pre-consolidation pressure, the c_v values vary from 0.17 to 2.68 m^2/year, with the majority of values between 0.2 to 0.3 m^2/year.

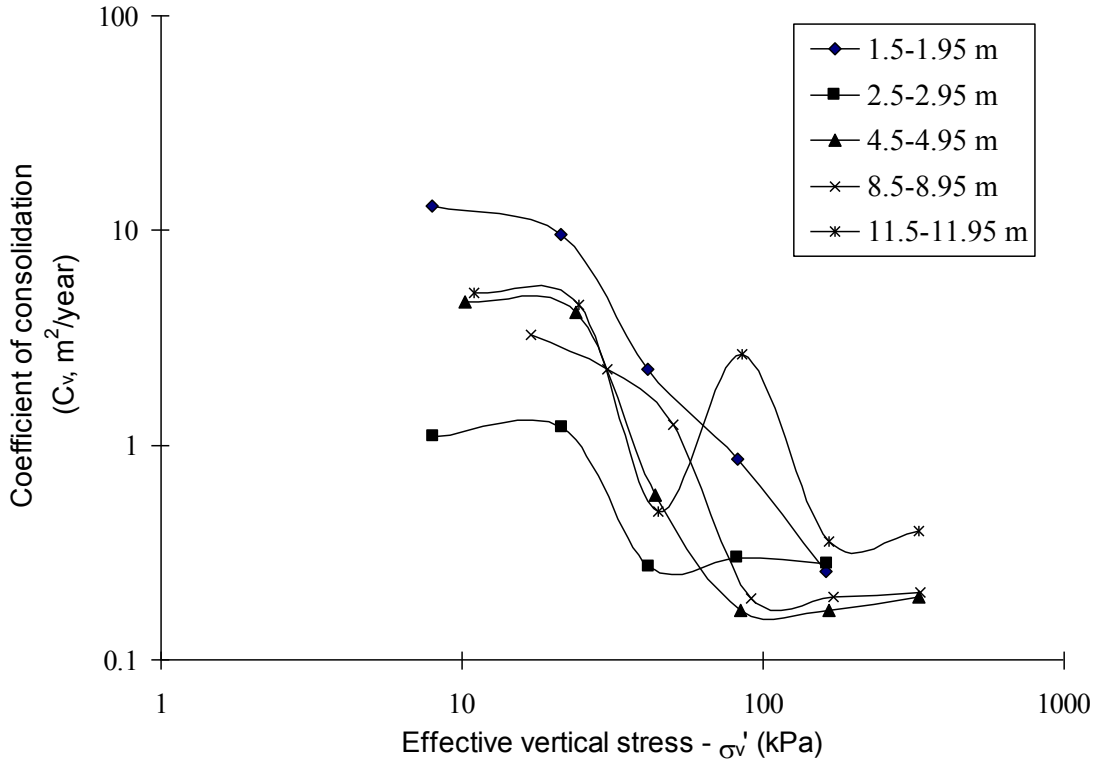

Figure 4.6 Coefficient of consolidation curves at varying depth

Table 4.2 Estimation of pre-consolidation pressure from e vs. log σ_v9 curves.

Soil depth (m)	pre-consolidation pressure (kPa)	Compression index (C_c)
1.5-2.0	35	0.78
2.5-3.0	36	1.45
4.5-5.0	54	1.87
8.5-9.0	71	1.11
11.5-12.0	110	0.89

The compressibility index (C_c), being the important compressibility characteristic, was regressed with the liquid limit (w_L) and the plasticity index (I_p). These regressions are shown in Figures 4.7 and 4.8 respectively. The regression equations are summarised in Table 4.3.

Table 4.3 Compression index correlations

Site	No of samples	Regression equation	R
Gold Coast Highway	5	$C_c = 0.0126(w_L + 20.53)$	0.933
Gold Coast Highway	6	$C_c = 0.0182(I_p + 20.46)$	0.847

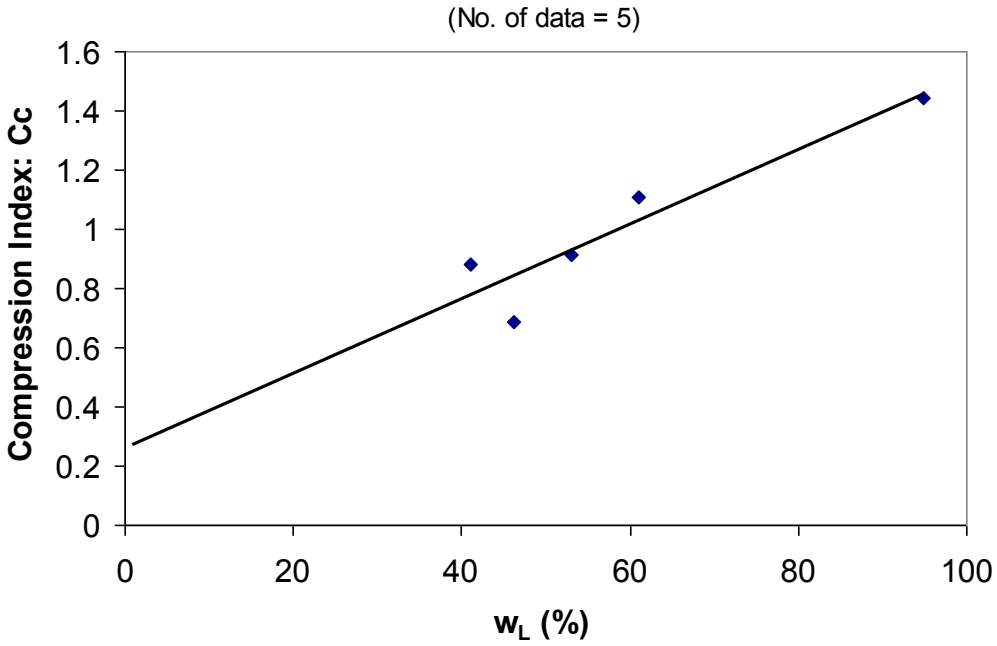

Figure 4.7 Compression index correlated with liquid limit

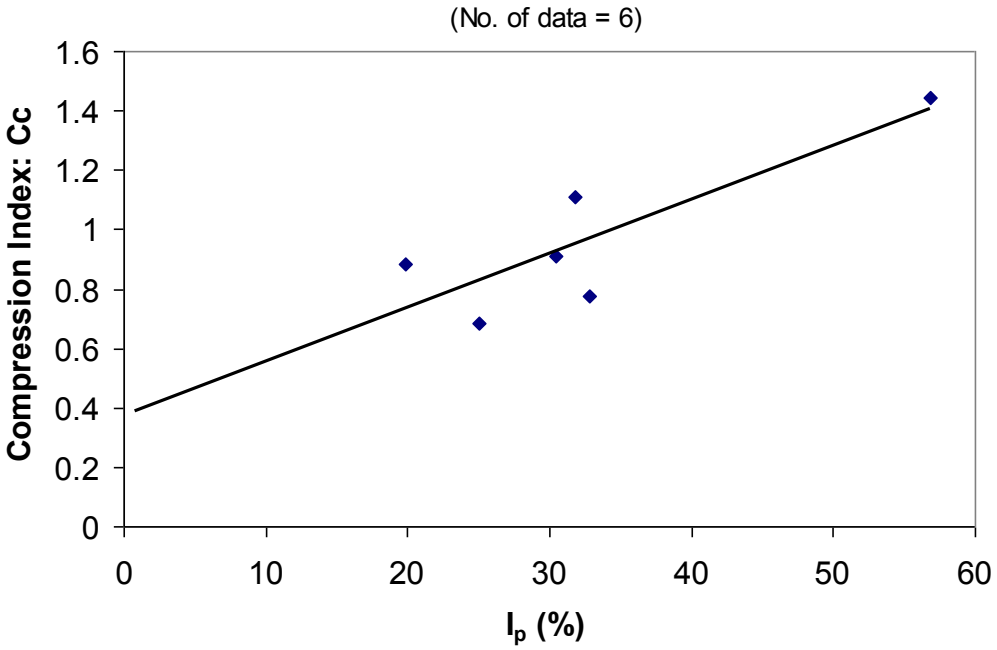

Figure 4.8 Compression index correlated with plasticity index

4.3 SUNSHINE MOTORWAY

4.3.1 STATISTICAL DISTRIBUTION

The data of moisture content (w_n), liquid limit (w_L) and plasticity index (I_p) were used to construct the statistical distributions for the soil properties. Figure 4.9 shows the histogram of the moisture content in the Sunshine Motorway. As shown in the figure, 190 samples were analysed, and the w_n ranges from 16.4 to 162.8%. Most of the soil samples have a w_n of 40 to 140%. This shows the soil has high moisture content.

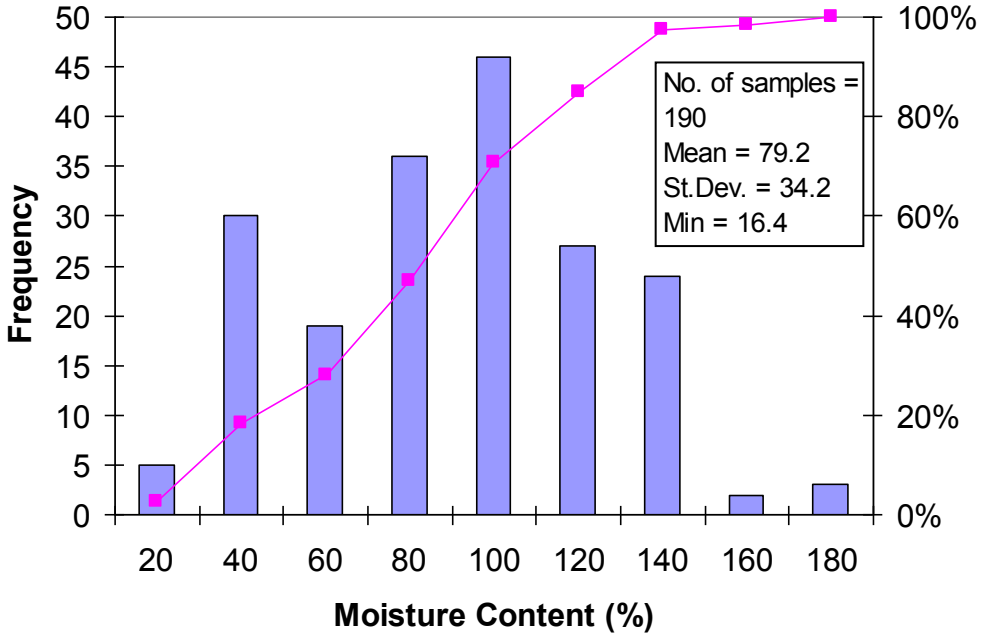

Figure 4.9 Moisture content histogram with cumulative frequency

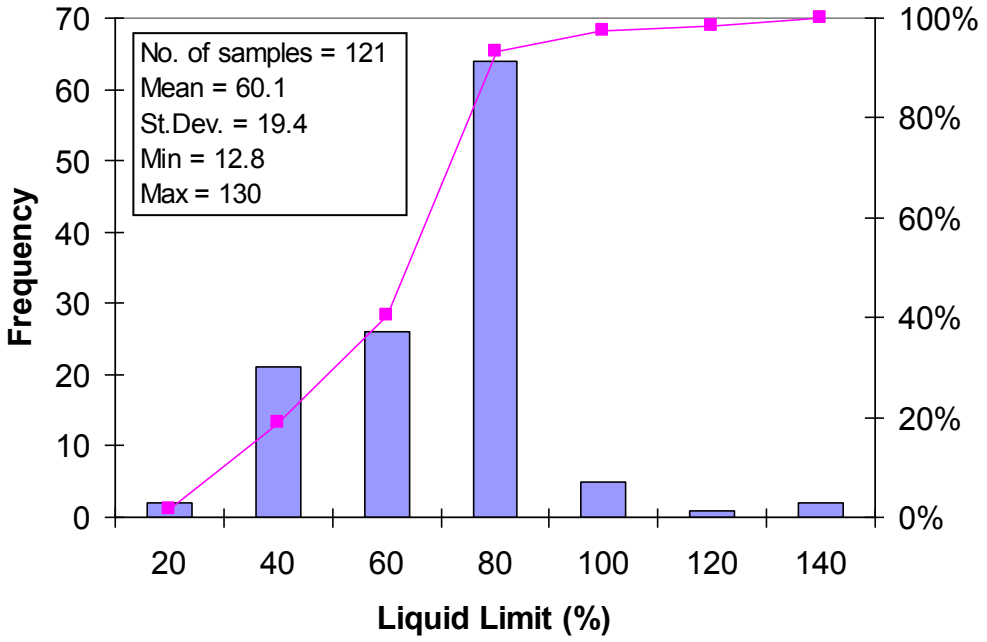

Figure 4.10 Liquid limit histogram with cumulative frequency

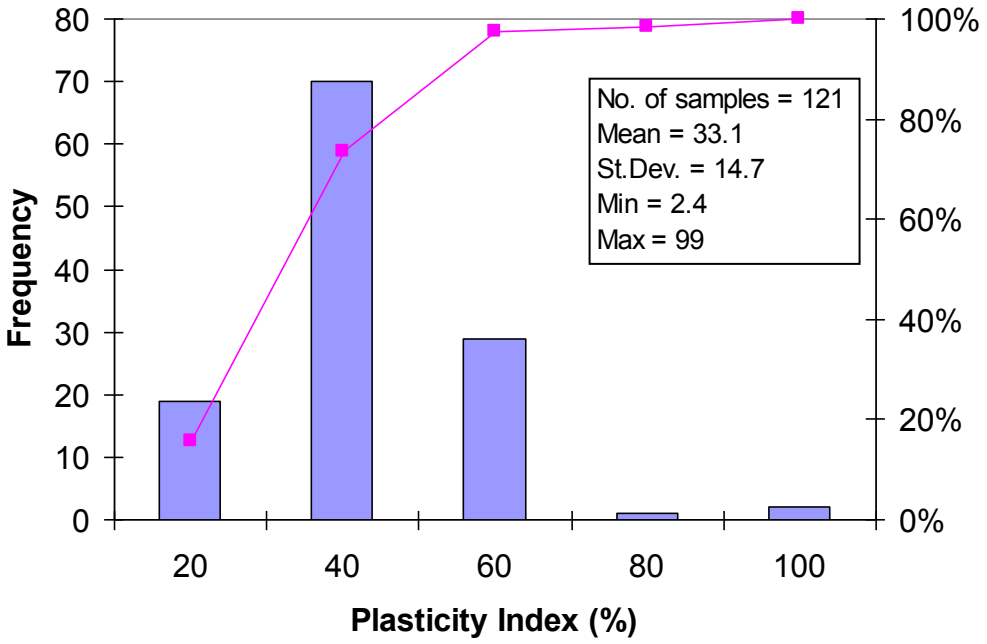

Figure 4.11 Plasticity index histogram with cumulative frequency

Figure 4.10 shows the histogram of liquid limit from 121 samples, and has a mean of 60.1% with most of the values ranging between 40 and 80%. Figure 4.11 shows the histogram of plasticity index and Table 4.4 lists their parameters.

Table 4.4 Statistical distribution for the moisture content, w_L, and I_p.

	No. of samples	Mean (%)	Std. Dev. (%)	Min (%)	Max (%)	Median (%)
Moisture content	190	79.2	34.2	16.4	162.8	83.7
I_p	121	60.1	19.4	12.8	130	63.2
w_L	121	33.1	14.7	2.4	99	34.8

4.3.2 COMPRESSIBILITY CHARACTERISTICS

The consolidation characteristics of the soft clay in the Sunshine Motorway were determined by the laboratory oedometer consolidation test. A total of thirty three, one-dimensional oedometer consolidation tests (data given in Appendix B) were established on the soft clay to estimate the deformation parameters and the stress history of the samples. Six or seven loading increments (depending on the depth of sample) and two unloading steps were applied. The test results provide information on the pre-consolidation pressure (or maximum past pressure) and the loading or unloading behaviour of the samples under controlled conditions.

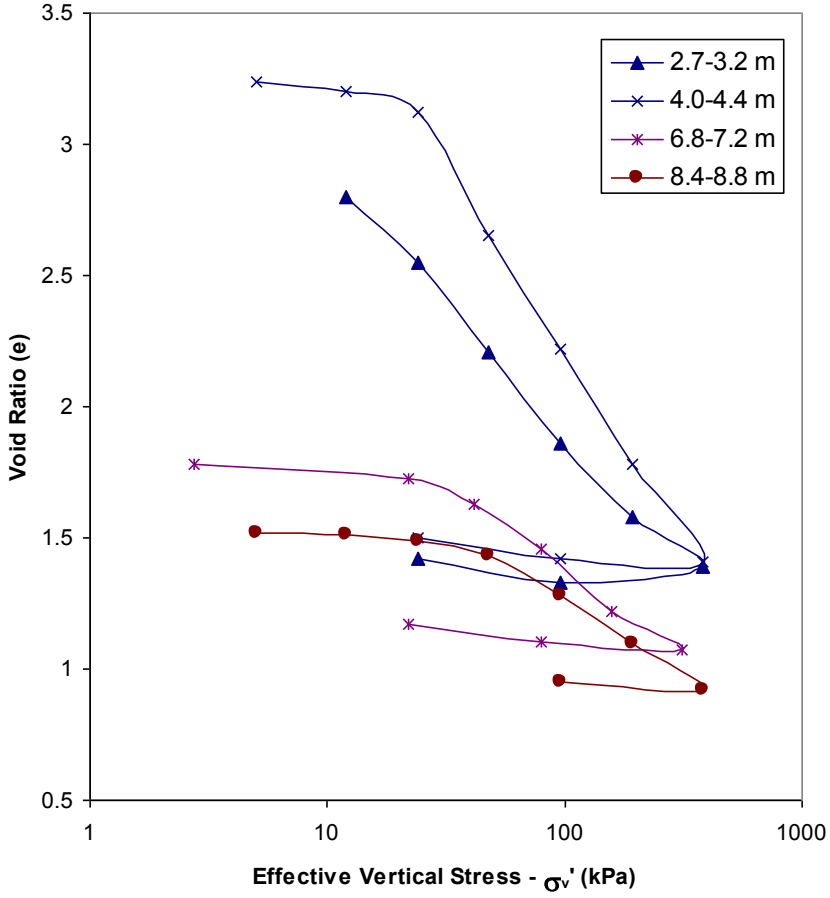

Figure 4.12 Consolidation curves at varying depth

Figure 4.12 the e-log $\sigma_v 9$ relationships for different depths. The relationships representing samples deeper than 6.8m appear geometrically similar. The e-log $\sigma_v 9$ relationships resemble that of sensitive clay. The figure gives the compression indexes (C_c) and the pre-consolidation pressures, and is assessed in Table 4.5.

Figure 4.13 illustrates the coefficient of volume compressibility (m_v) for different soil depths. Based on the results, the compressibility of the soft clays ranges from 0.04 to 5.6 m^2/MN. The m_v profile shows that the soft clay deposit becomes less compressible with depth.

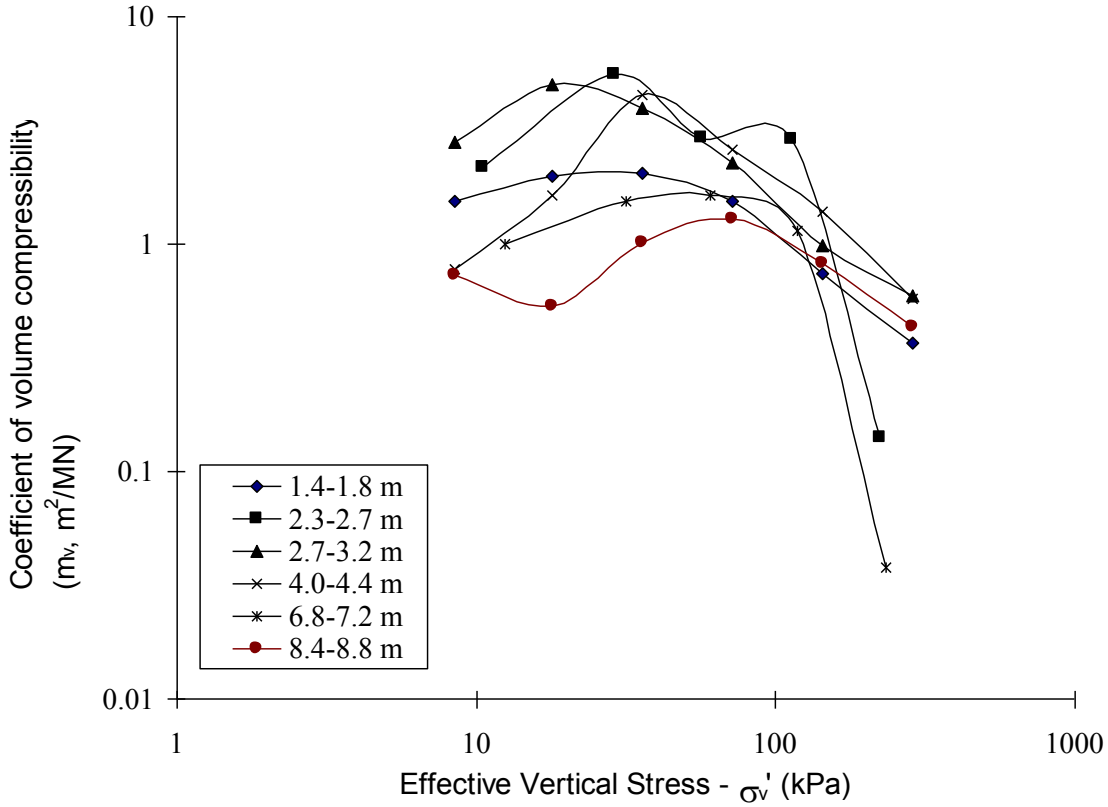

Figure 4.13 Coefficient of volume compressibility curves at varying depth

Following the results of the oedometer tests, the coefficient of consolidation (c_v) is given in Figure 4.14. For stress ranges less than the interpreted pre-consolidation pressure, the c_v values vary widely from 0.19 to 10.5 m^2/year. For stress ranges greater than the interpreted pre-consolidation pressure, the c_v values vary from 0.17 to 1.32 m^2/year, with the majority of values between 0.2 to 0.48 m^2/year.

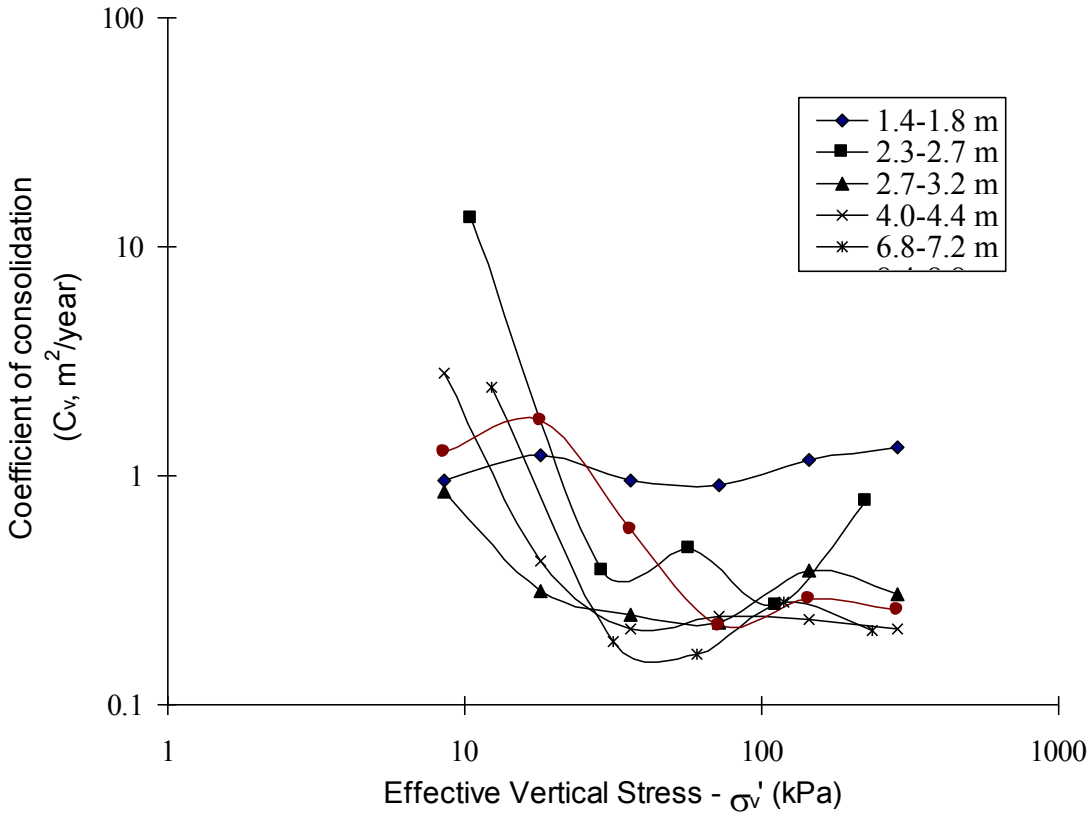

Figure 4.14 Coefficient of consolidation curves at varying depth

Table 4.5 Estimation of pre-consolidation pressure from e vs. log σ_v9 curves.

Soil depth (m)	pre-consolidation pressure (kPa)	Compression index (C_c)
1.4-1.8	25	0.50
2.3-2.7	26	1.87
2.7-3.2	12	0.96
4.0-4.4	25	1.42
6.8-7.2	30	0.63
8.4-8.8	49	0.56

The compressibility index (C_c), being the important compressibility characteristic, was regressed with the liquid limit (w_L) and the plasticity index (I_p). These regressions are shown in Figures 4.15 and 4.16 respectively The regression equations are summarised in Table 4.6.

Table 4.6 Compression index correlations

Site	No. of samples	Regression equation	R
Sunshine Motorway	19	$C_c = 0.0165(w_L - 14.17)$	0.913
Sunshine Motorway	19	$C_c = 0.0248(I_p + 3.00)$	0.903

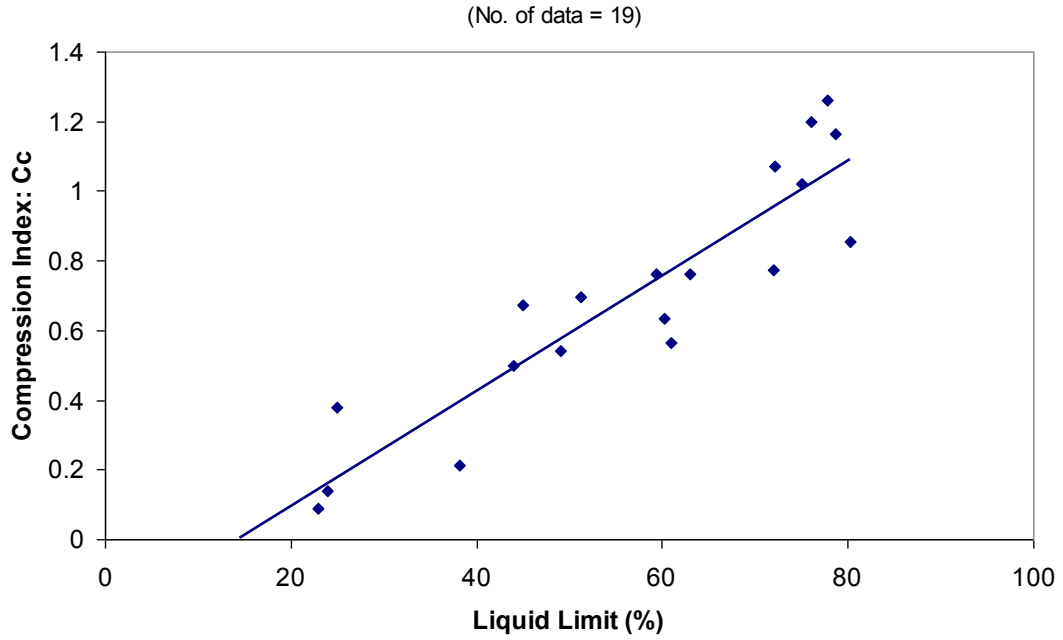

Figure 4.15 Compression index correlated with liquid limit

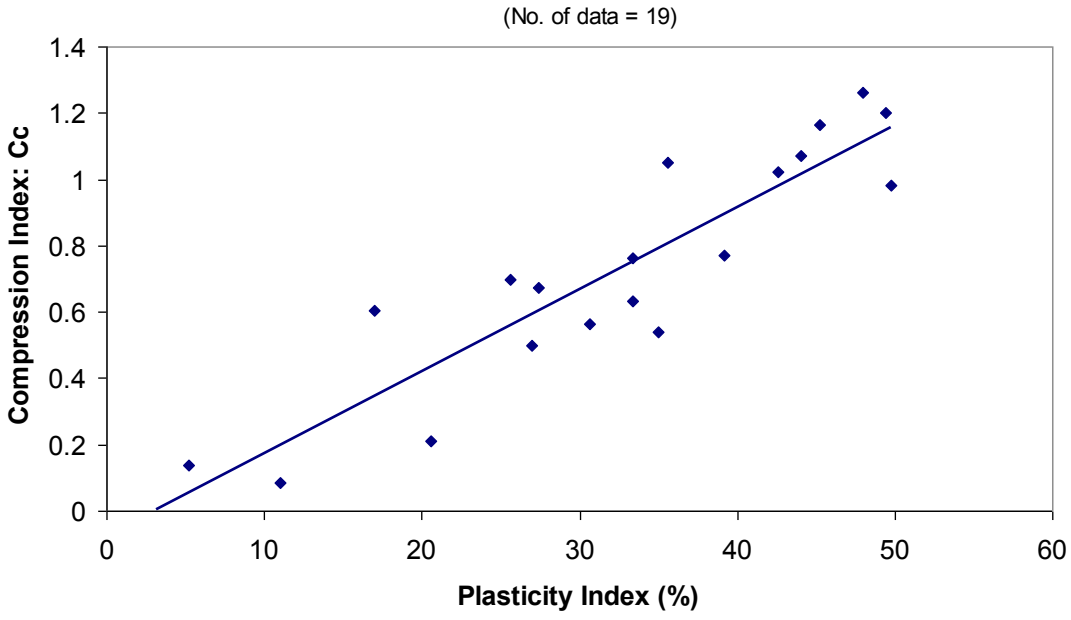

Figure 4.16 Compression index correlated with plasticity index

4.4 PORT BRISBANE MOTORWAY

4.4.1 STATISTICAL DISTRIBUTION

The data of moisture content (w_n), liquid limit (w_L) and plasticity index (I_p) were used to construct the statistical distributions for the soil properties. Figure 4.17 shows the histogram of the moisture content in the Port Brisbane Motorway. As shown in the figure, 55 samples were analysed, and the w_n ranges from 22.2 to 108.2%. Most of the soil samples have a w_n of 60 to 80%. This shows the soil has high moisture content.

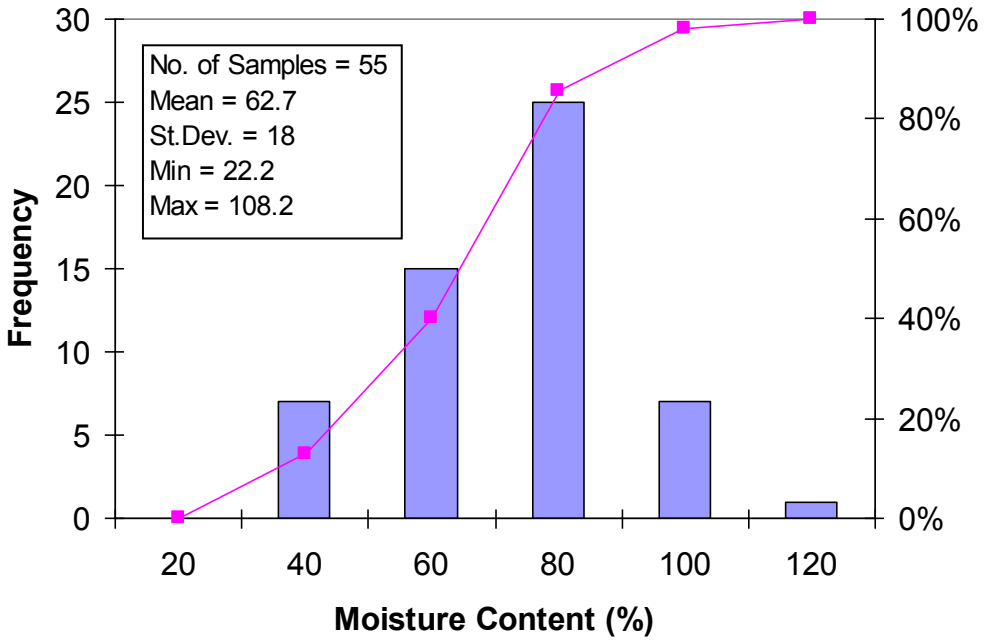

Figure 4.17 Moisture content histogram with cumulative frequency

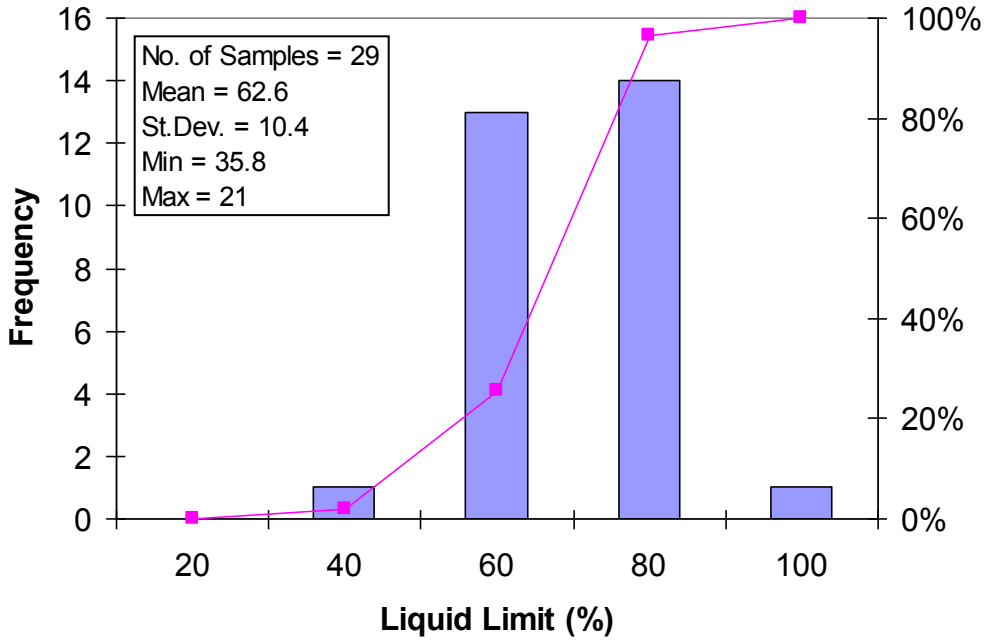

Figure 4.18 Liquid limit histogram with cumulative frequency

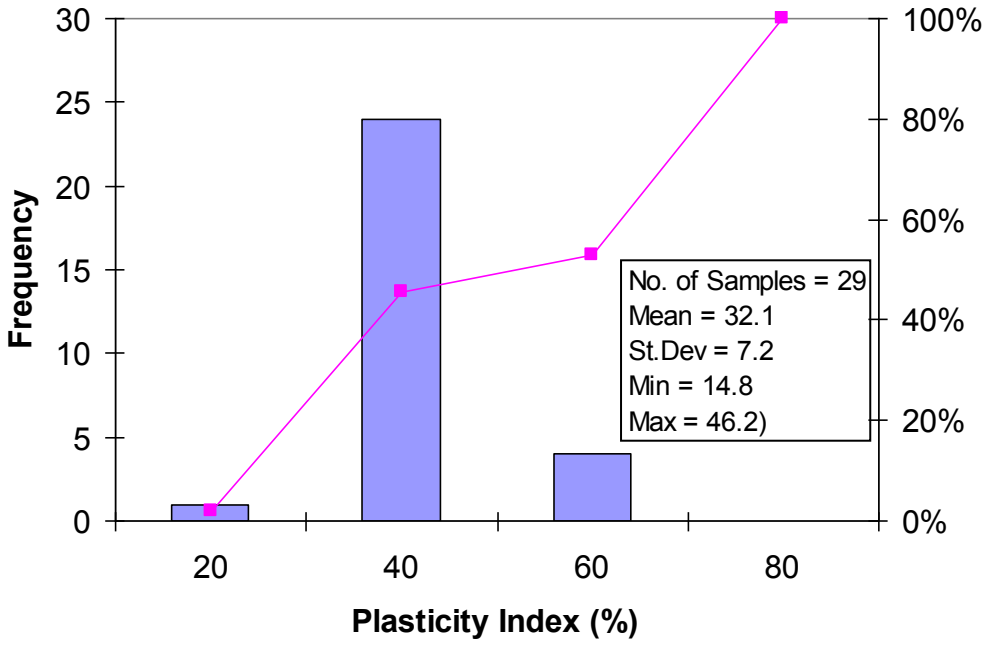

Figure 4.19 Plasticity index histogram with cumulative frequency

Figure 4.18 shows the histogram of liquid limit from 29 samples, and has a mean of 62.6% with most of the value ranges between 60 and 80%. Figure 4.19 shows the histogram of plasticity index and Table 4.7 lists their parameters.

Table 4.7 Statistical distribution for the moisture content, w_L, and I_p.

	No. of samples	Mean (%)	Std. Dev. (%)	Min (%)	Max (%)	Median (%)
Moisture content	29	62.7	18	22.2	108.2	63.6
I_p	29	62.6	10.4	35.8	21	31.4
w_L	29	32.1	7.2	14.8	46.2	60.6

4.4.2 COMPRESSIBILITY CHARACTERISTICS

The consolidation characteristics of the soft clay in the Port Brisbane Motorway were determined by the laboratory oedometer consolidation test. A total of eleven, one-dimensional oedometer consolidation tests (data given in Appendix C) were established on the soft clay to estimate the deformation parameters and the stress history of the samples. Six or seven loading increments (depending on the depth of sample) were applied. The samples were then unloaded and reloaded with a further six to seven increments. The test results provide information on the pre-consolidation pressure (or maximum past pressure) and the loading or unloading behaviour of the samples under controlled conditions.

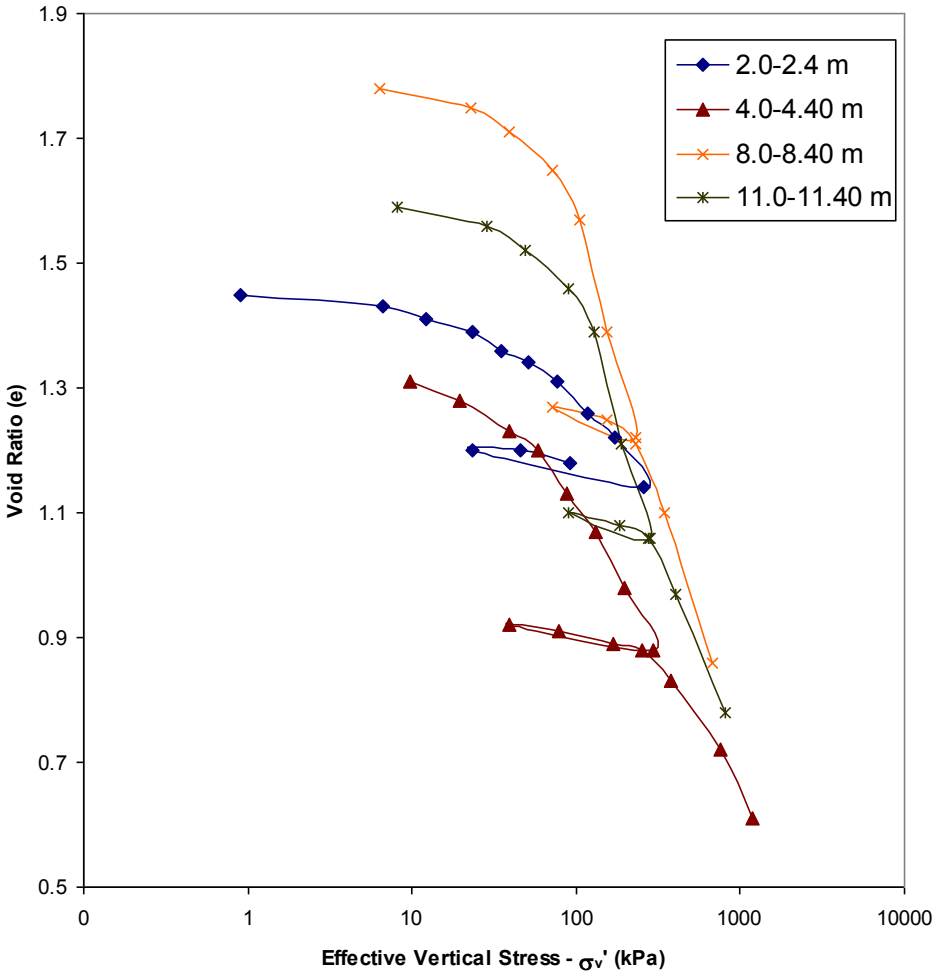
1.9
1.7
1.5
1.3
1.1
0.9
0.7
0.5
Void Ratio (e)
0
1
10
100
1000
10000
Effective Vertical Stress - σv' (kPa)
2.0-2.4 m
4.0-4.40 m
8.0-8.40 m
11.0-11.40 m

(a)

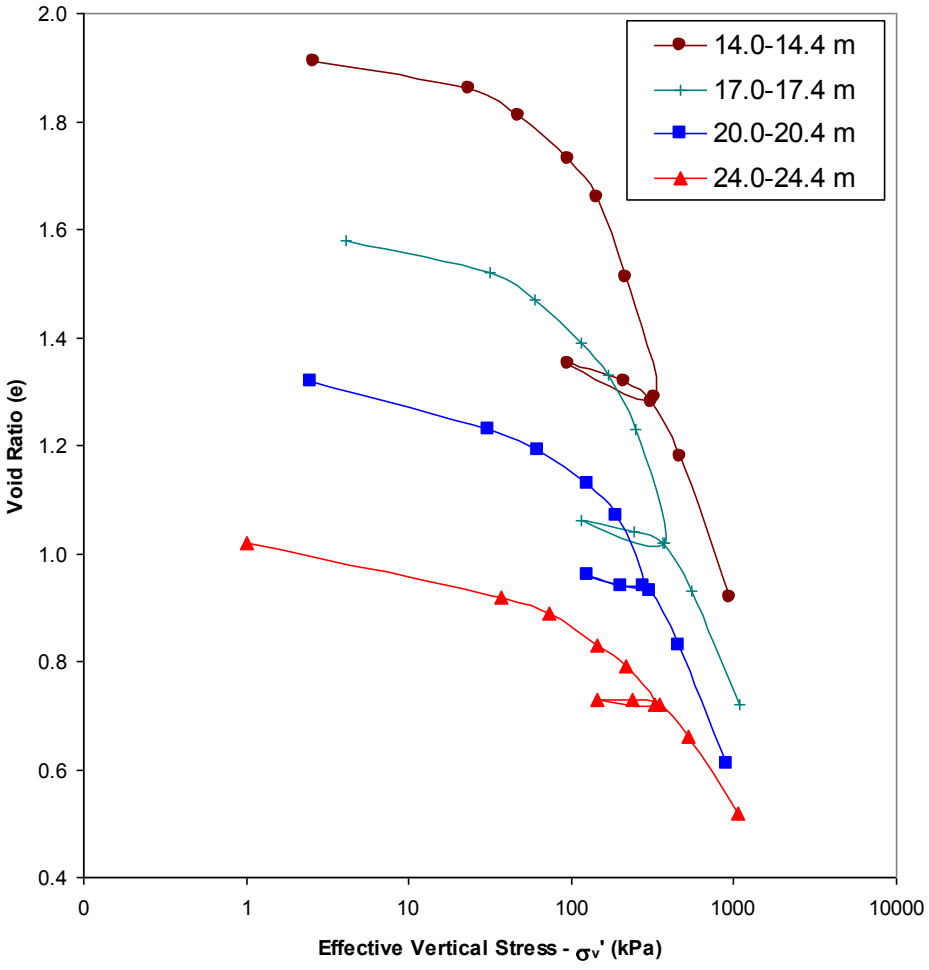

(b)

Figure 4.20 (a) Consolidation curves at varying depth (14.0-24.4m) (b) Consolidation curves at varying depth (2.0-11.4m)

Figure 4.20 shows the e-log $\sigma_v 9$ relationships for different depths. The relationships representing samples deeper than 14.0m appear geometrically similar. The e-log $\sigma_v 9$ relationships resemble that of sensitive clay. The figure gives the compression indexes (C_c) and the pre-consolidation pressures, and is assessed in Table 4.8.

Figure 4.21 illustrates the coefficient of volume compressibility (m_v) for different soil depths. Based on the results, the compressibility of the soft clays ranges from 0.16 to 1.23m^2/MN. The m_v profile shows that the soft clay deposit becomes less compressible with depth.

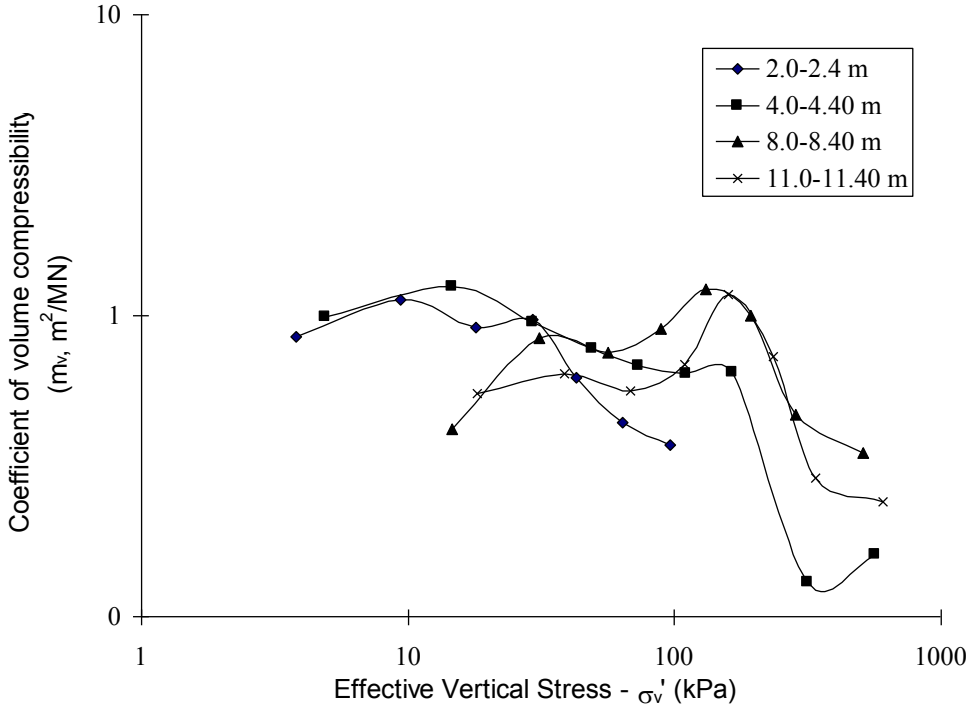

(a)

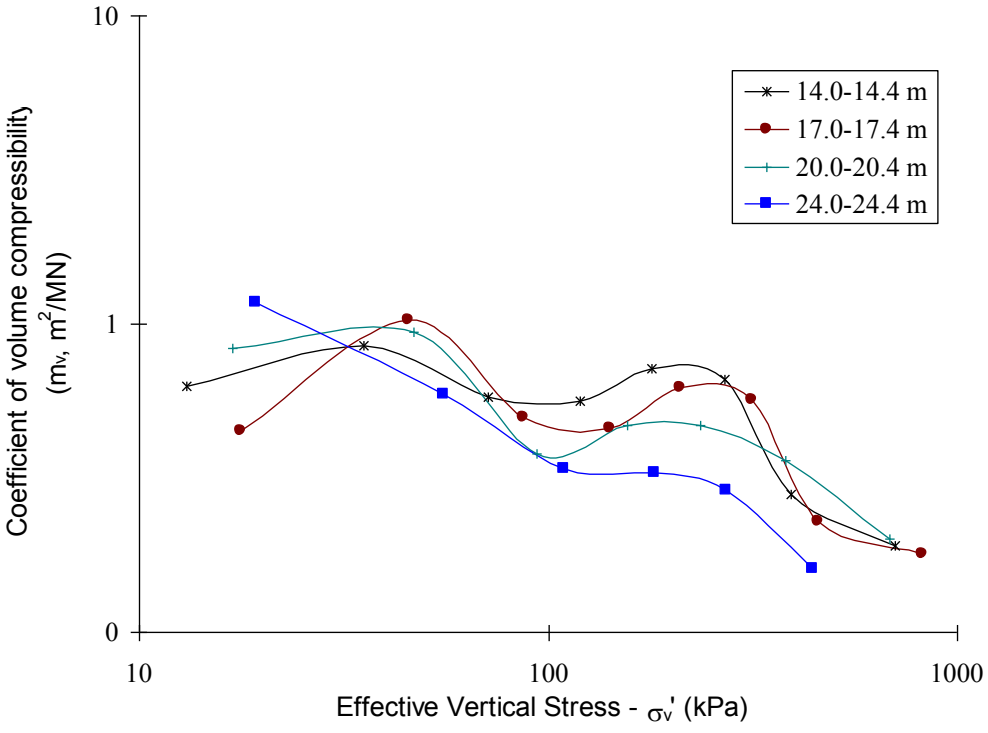

(b)

Figure 4.21 (a) Coefficient of volume compressibility curves for depths 2-11.4m (b) Coefficient of volume compressibility curves for depths 14-24.4m

Following the results of the oedometer tests, the coefficient of consolidation (c_v) is given in Figure 4.22. For stress ranges less than the interpreted pre-consolidation pressure, the c_v values vary widely from 0.3 to 100.6 m^2/year. For stress ranges greater than the interpreted pre-consolidation pressure, the c_v values vary from 0.1 to 110.3 m^2/year, with the majority of values between 0.2 to 0.6 m^2/year.

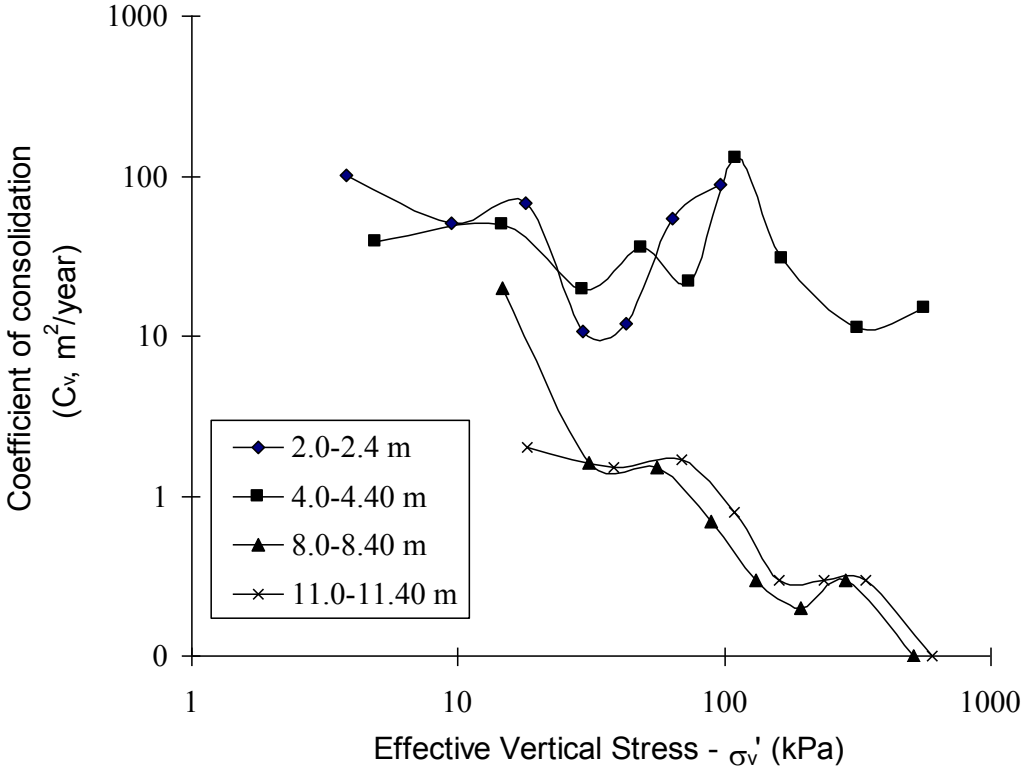

(a)

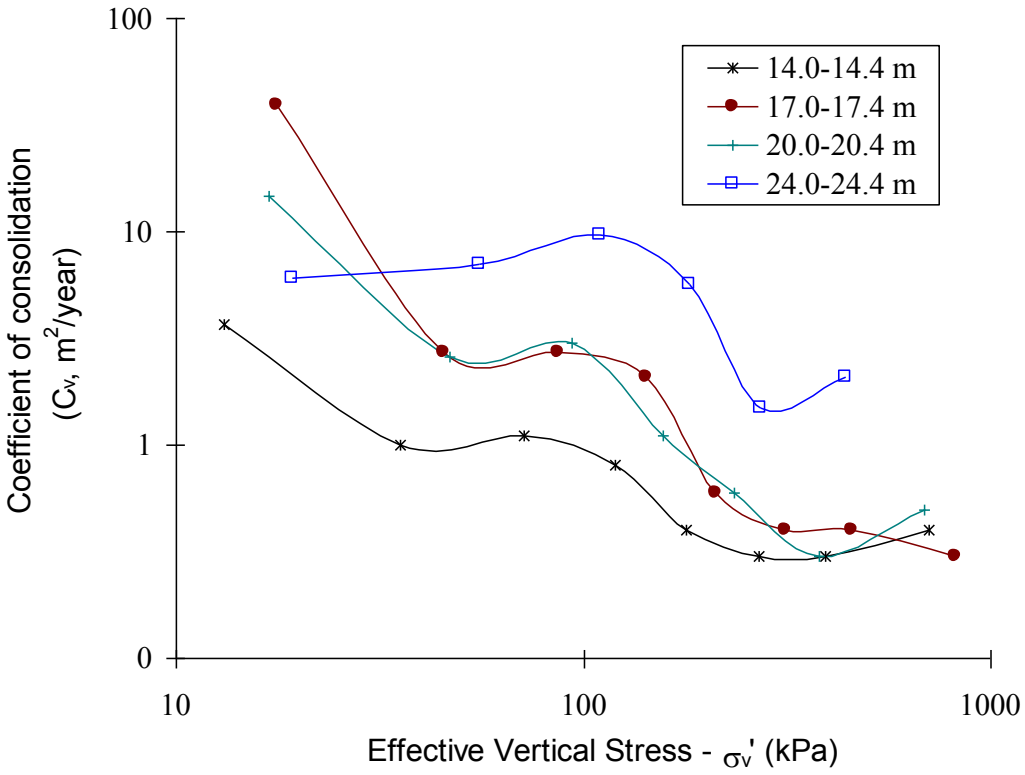

(b)

Figure 4.22 (a) Coefficient of consolidation curves for depths 2-11.4m (b) Coefficient of consolidation curves for depths 14-24.4m

Table 4.8 Estimation of pre-consolidation pressure from e vs. log σ_v9 curves.

Soil depth (m)	pre-consolidation pressure (kPa)	Compression index (C_c)
2.0-2.4	75	0.24
4.0-4.4	75	0.45
8.0-8.4	100	0.88
11.0-11.4	170	0.71
14.0-14.4	175	0.90
17.0-17.4	170	0.68
20.0-20.4	180	0.67
24.0-24.4	150	0.36

4.5 CONCLUDING REMARKS

The consolidation characteristics of the soft clays were determined by the laboratory oedometer test. The compressibility curves (e-log σ_v9 relationships) for different depths are presented for the three sites. The coefficient of consolidation (c_v) and the coefficient of volume compressibility (m_v) with different soil depths are illustrated. Finally, regression equations for compression index (C_c) and liquid limit (w_L) are established and can be seen in Table 4.9. The correlation coefficients (R) are also illustrated in Table 4.9.

Based on the three case studies, the conclusions can be made and are presented in Chapter 5.

Regression equations for the Port Brisbane Motorway were not established due to the lack of liquid limit and plasticity index parameters for the corresponding oedometer consolidation tests.

Table 4.9 Regression equations for compression index.

Site	No of samples	Regression equation	R
Gold Coast Highway	5	$C_c = 0.0126(w_L + 20.53)$	0.933
Gold Coast Highway	6	$C_c = 0.0182(I_p + 20.46)$	0.847
Sunshine Motorway	19	$C_c = 0.0165(w_L - 14.17)$	0.913
Sunshine Motorway	19	$C_c = 0.0248(I_p + 3.00)$	0.903

5. CHAPTER 5 – CONCLUSIONS AND RECOMMENDATIONS

5.1 CONCLUSIONS

The consolidation characteristics of the soft clays for the three case studies were determined by using laboratory oedometer consolidation test data at various depths for each borehole. The soft clays encountered were generally estuarine and swamp deposits, coastal mangrove and tidal deposits of varying depths. The deposits mainly comprised of extremely soft, recently deposited, estuarine silty clay which overlie young deposits of soft to firm estuarine silty clay and silty sand. The estuarine deposits were generally very soft to firm, compressible silty clays of medium to high plasticity.

1. The data of moisture content (w_n), liquid limit (w_L) and plasticity index (I_p) were used to construct the statistical distribution for the soil properties. The distributions were generally skewed.

2. The plasticity index, liquid limit, and moisture content were found to be generally uniform with depth. The majority of moisture content and liquid limit values were distributed in the 60-80% region and plasticity index values in the 40-60% region. However, the distribution of moisture content values in the Sunshine Motorway was in the range of 40-140%.

3. The e-log σ_v9 relationships generally resembled those of clays of high sensitivity. The relationships also show that the clays became less compressible with depth.

4. For stress ranges greater than the interpreted pre-consolidation pressure, the coefficient of consolidation (c_v) values are distributed in the range of 0.5-3.5 m^2/year and the coefficient of volume compressibility (m_v) values distributed in the range of 0.2-0.6 m^2/MN.

5. The most important compressibility characteristic, the compressibility index (C_c), was calculated from the e-log σ_v9 relationships and were regressed with the liquid limit (w_L) and the plasticity index (I_p) with the equations given in Table 4.9. The correlation between the compression index and the liquid limit gave correlation coefficients of 0.913 to 0.933. The correlation coefficient for the compression index and the plasticity index is 0.847 to 0.903. Data that showed excess scatter were removed for these correlations.

5.2 RECCOMENDATIONS FOR FUTURE WORK

Most of the time was spent on acquiring the consolidation test data such that little time was available for a comprehensive analysis. It is recommended that the further tasks be undertaken.

(1) Based on the results, further investigations can be done in evaluating the secondary consolidation.

(2) Probability approach in determining the long term settlement can be done by further analysis.

(3) The results should be compared with the long term field monitoring data.

REFERENCES

[1]Prakoso, W.A. & Kulhawy, F.H. (2002): Uncertainty in capacity models for foundations in rock. Proc. 5th North American Rock Mech. Symp., Toronto. 1241-1248.

[2] Shinuzuka M. Monte Carlo simulation of structural dynamics. International Journal Computer and Structures 1972;2:855–74.

[3] Cambou B. Application of first-order uncertainty analysis in the finite element method in linear elasticity. In: Proceeding of the second International Conference on Application of Statistics and Probability in Soil and Structural Engineering. Aachen, West Germany; 1975. p. 67–87.

[4] Vanmarcke E, Grigoriu M. Stochastic finite element analysis of simple beams. Journal of Engineering Mechanics ASCE 1983;109(5):1203–14.

[5] Liu WK, Belytsuchko T, Mani A. Probabilistic finite elements for nonlinear structural dynamics. Computer methods in Applied Mechanics and Engineering 1986;56:61–81.

[6] Baecher GB, Ingra TS. Stochastic FEM in settlement predictions. Journal of the Geotechnical Engineering Division ASCE 1981;107(GT4):449–63.

[7] Ishii K, Suzuki M. Stochastic finite element method for slope stability analysis. Structural Safety 1987;4:111–29.

[8] Righetti G, Harrop-Williams K. Finite element analysis of random soil media. Journal of Geotechnical Engineering ASCE 1988;104(1):59–75.

[9] Paice GM, Griffiths DV, Fenton GA. Finite element modelling of settlements on spatially random soil. Journal of Geotechnical Engineering ASCE 1996;122(9):777–9.

[10] Fenton GA, Vanmarcke EH. Spatial variation in liquefaction risk. Geotechnique 1998; 48(6):819–31.

[11] Rahman MS, Yeh CH. Variability of seismic response of soils using stochastic finite element method. Soil Dynamics and Earthquake Engineering 1999;18:229–45.

[12] Griffths DV, Fenton GA. Bearing capacity of spatially random soil: the undrained clay Prandtl problem revisited. Geotechnique 2001;51(4):351–9.

[13] Nour A, Laouami N, Tabbouche B. Seismic behaviour of heterogeneous soil profile via stochastic finite element analysis. In: Proceeding of the 15th International Conference on Soil Mechanics and Geotechnical Engineering, Lessons learned from Recent Strong Earthquakes, Earthquake Geotechnical Engineering Satellite Conference, Istambul (Turkey) 25 August Ed. Ansal A., 2001. p. 173–6.

[14] Burland, J.B. 1990. On the compressibility and shear strength of natural clays. Geotechnique, 40: 329-378.

[15] Skempton, A.W. 1970. The consolidation of clays by gravitational compaction. Q.J. Geology Society, 125: 373-411.

[16] Tanaka, H. 2000. Re-examination of established relations between index properties and soil parameters. Port and Harbour Research Institute, Yokusuka, Japan.

[17] Hong, Z., Tsuchida, T. 2000. Compressibility of sensitive Ariake clays. Port and Harbour Research Institute, Yokusuka, Japan.

[18] Lutenegger, A.J., Cerato, A.B. 2003. Intrinsic compressibility of fine-grained soils. ASCE Journal of Geotechnical and Geoenvironmental Engineering.

[19] Queensland Department of Main Roads (QDMR), (1993): Gold Coast Highway (Helensvale - Southport): Helensvale Interchange to Arundel Drive Section Geotechnical Investigation, R1828, Australia.

[20] Queensland Department of Main Roads (QDMR), (1991): Sunshine Motorway Stage 2 – Area 2 Geotechnical Investigation, R1746, Australia.

[21] Queensland Department of Main Roads (QDMR), (2000): Brisbane Port Road Stage 2 Investigation, R3197, Australia.

APPENDIX A - GOLD COAST HIGHWAY

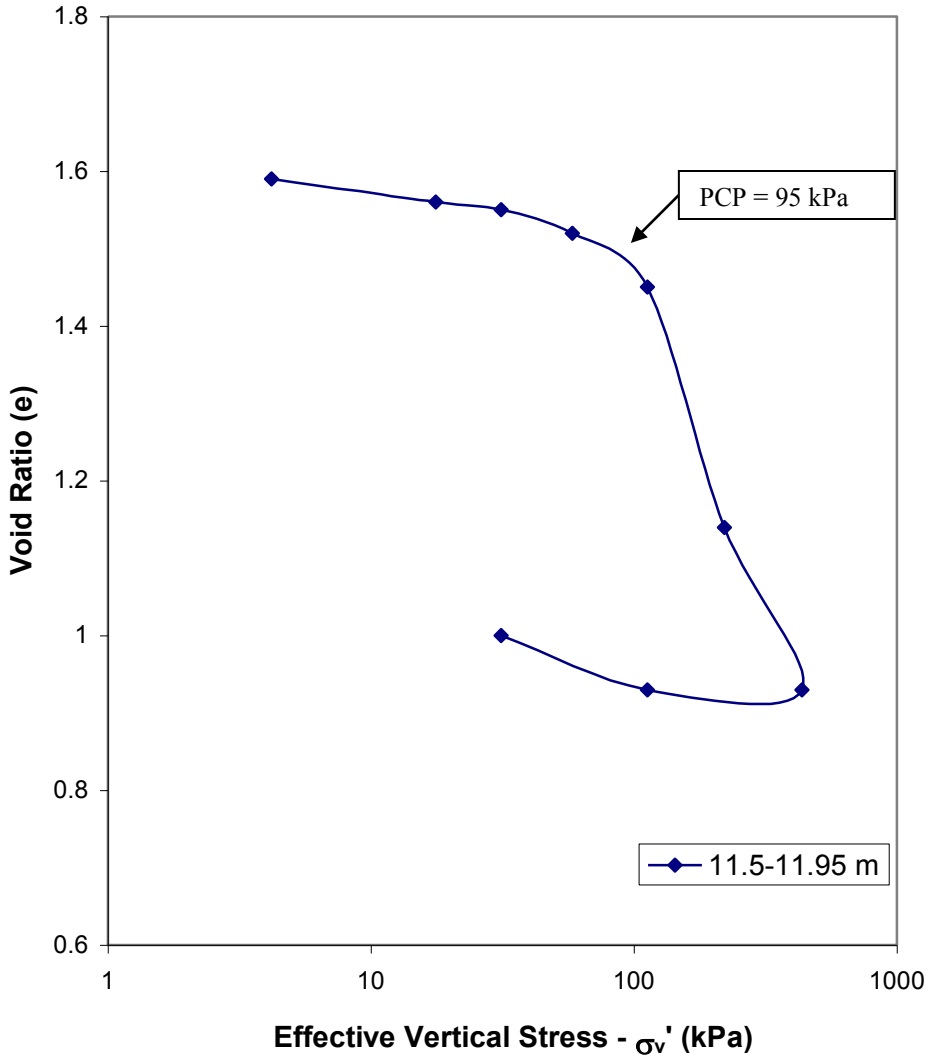

Figure A.1: Pressure versus void ratio plot for borehole 23M

Table A.1: Test results for borehole 23M

Av. Pressure (kPa)	10.94	24.44	44.71	85.22	166.24	328.24
m_v (m^2/MN)	0.7	0.47	0.42	0.47	1.22	0.48
c_v (m^2/year)	5.127	4.532	0.494	2.648	0.353	0.398
Description: Grey Sl. SANDY CLAY						

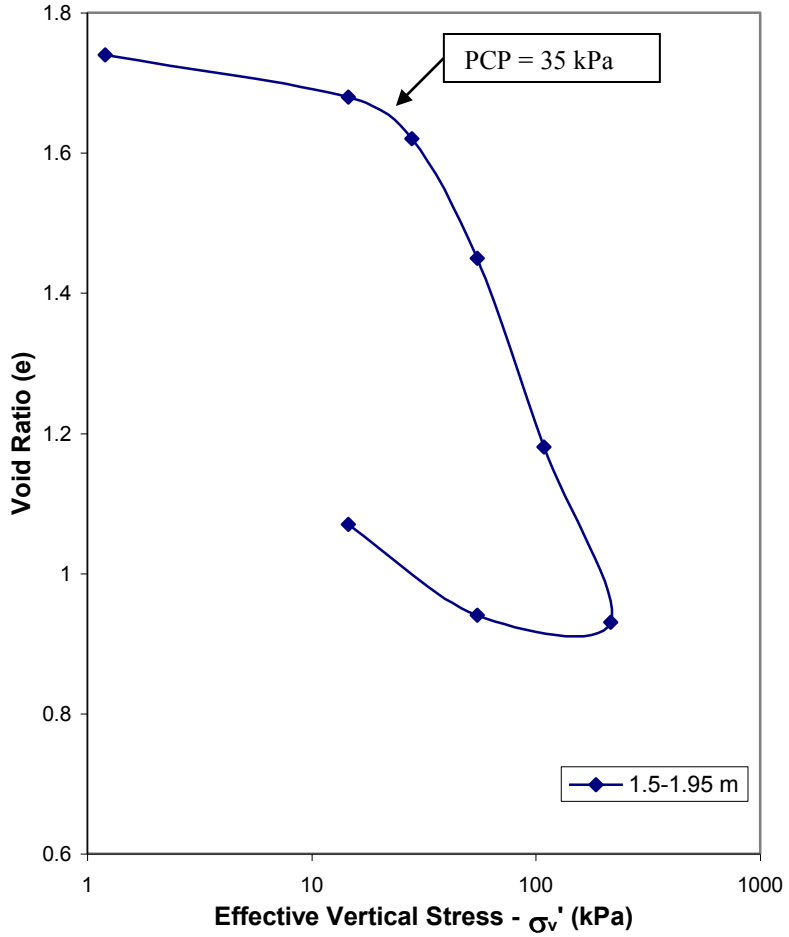

Figure A.2: Pressure versus void ratio plot for borehole 20A

PCP = Pre-consolidation Pressure

Table A.2: Test results for borehole 20A

Av. Pressure (kPa)	7.91	21.35	41.52	81.84	162.49
m_v (m^2/MN)	1.7	1.66	2.5	2.07	1.08
c_v (m^2/year)	12.97	9.6	2.24	0.86	0.26
Description: Dark Grey CLAY					

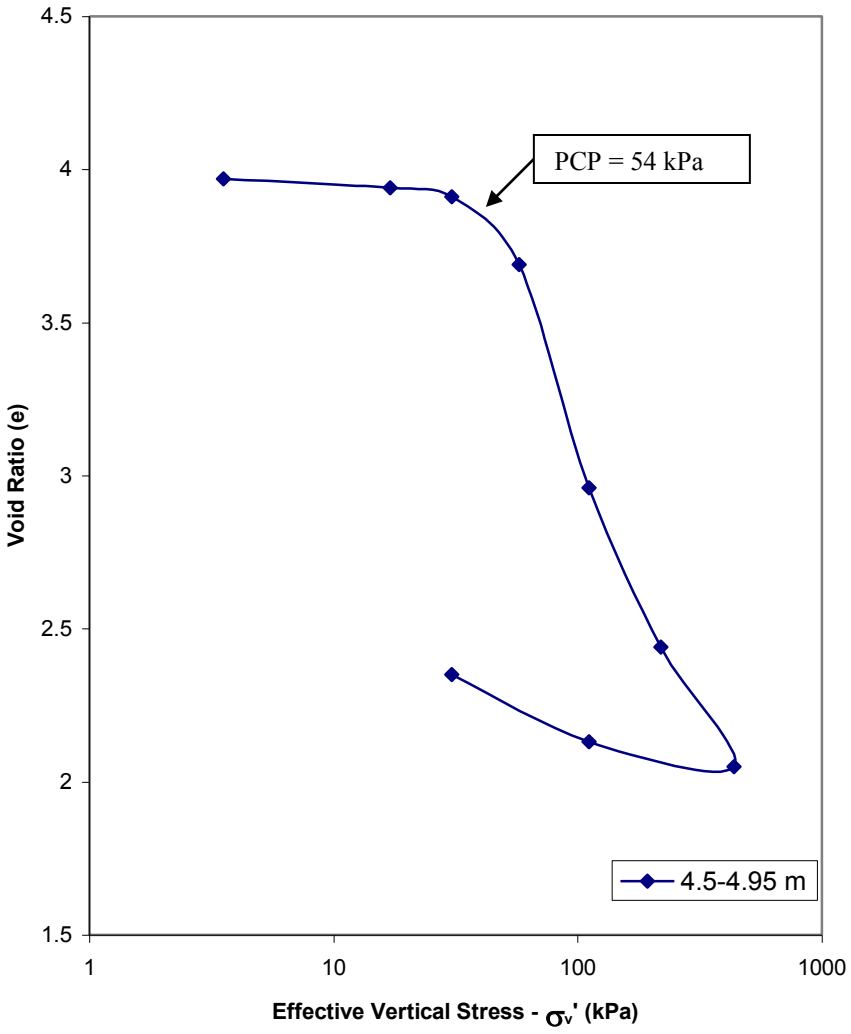

Figure A.3: Pressure versus void ratio plot for borehole 21E

Table A.3: Test results for borehole 21E

Av. Pressure (kPa)	10.29	23.79	44.06	84.57	165.59	327.64
m_v (m^2/MN)	0.51	0.43	1.67	3.01	1.23	0.54
c_v (m^2/year)	4.651	4.166	0.582	0.17	0.169	0.196
Description: Grey CLAY (Shell Fragments)						

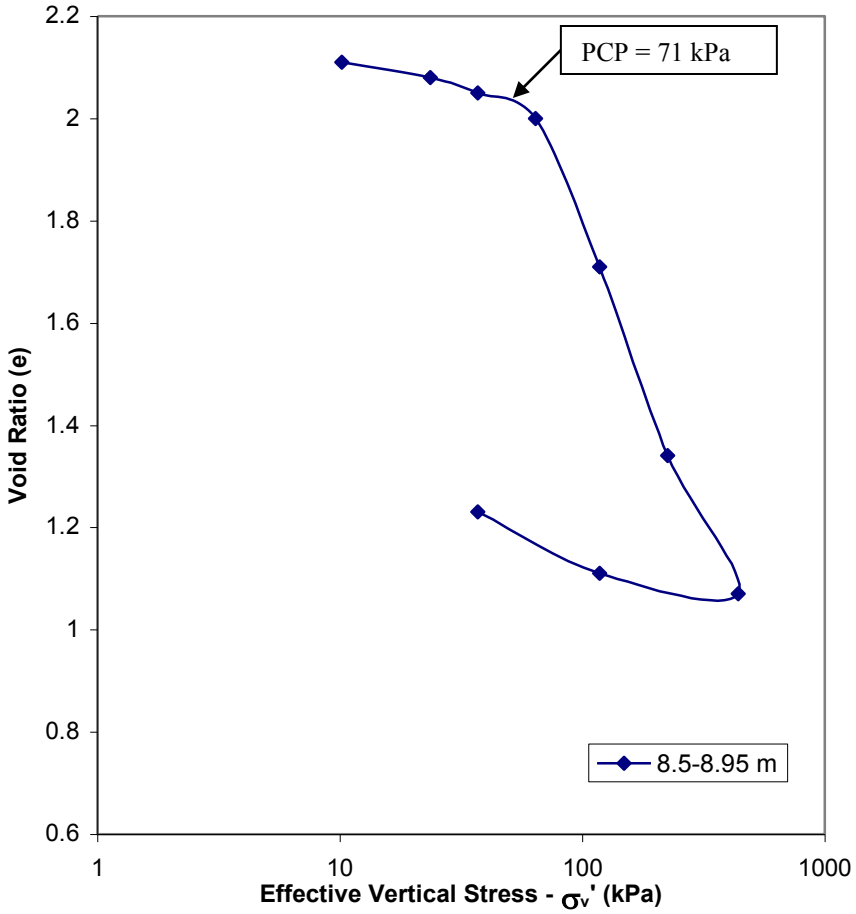

Figure A.4: Pressure versus void ratio plot for borehole 21J

Table A.4: Test results for borehole 21J

Av. Pressure (kPa)	16.87	30.31	50.48	90.8	171.45	332.73
m_v (m^2/MN)	0.67	0.62	0.65	1.81	1.34	0.54
c_v (m^2/year)	3.287	2.255	1.255	0.194	0.196	0.207
Description: Grey CLAY (Shell Fragments)						

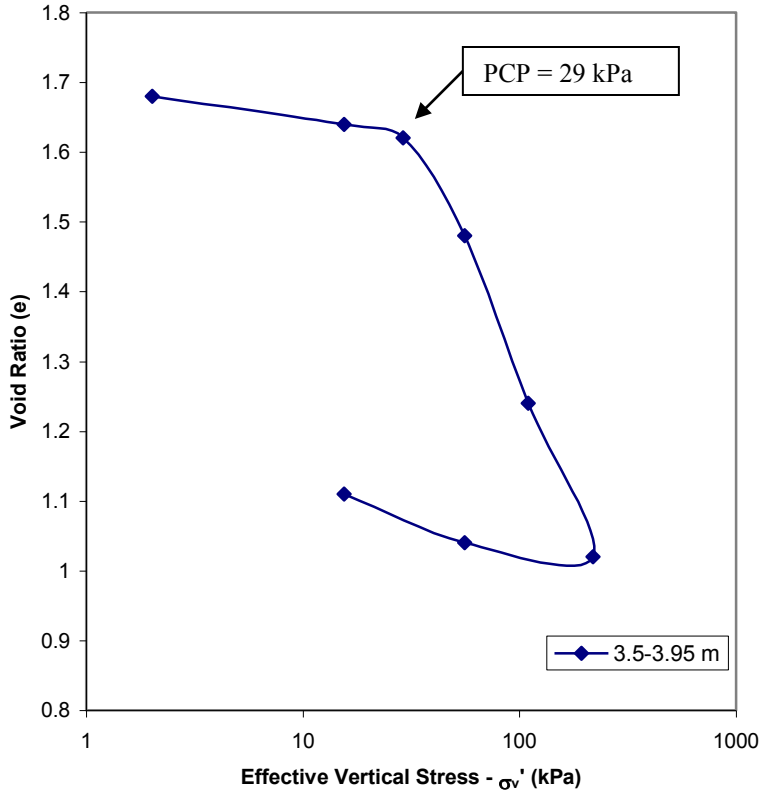

Figure A.5: Pressure versus void ratio plot for borehole 18D

Table A.5: Test results for borehole 18D

Av. Pressure (kPa)	8.77	22.27	42.54	83.05	164.07
m_v (m^2/MN)	1.14	0.76	2	1.77	0.92
c_v (m^2/year)	8.34	5.57	1.438	0.34	0.32
Description: Grey CLAY					

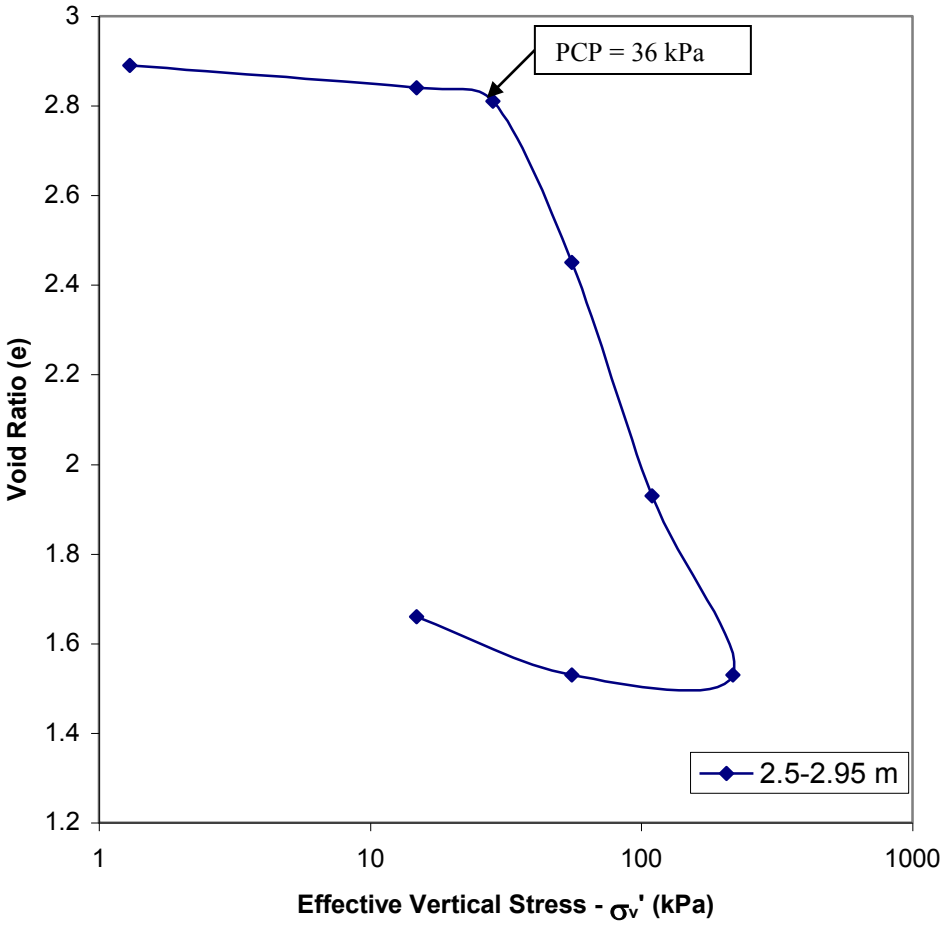

Figure A.6: Pressure versus void ratio plot for borehole 20C

Table A.6: Test results for borehole 20C

Av. Pressure (kPa)	8.05	21.55	41.82	82.33	163.35
m_v (m^2/MN)	0.9	0.75	3.48	2.9	1.3
c_v (m^2/year)	1.09	1.2	0.27	0.3	0.28
Description: Dark Grey SILTY CLAY					

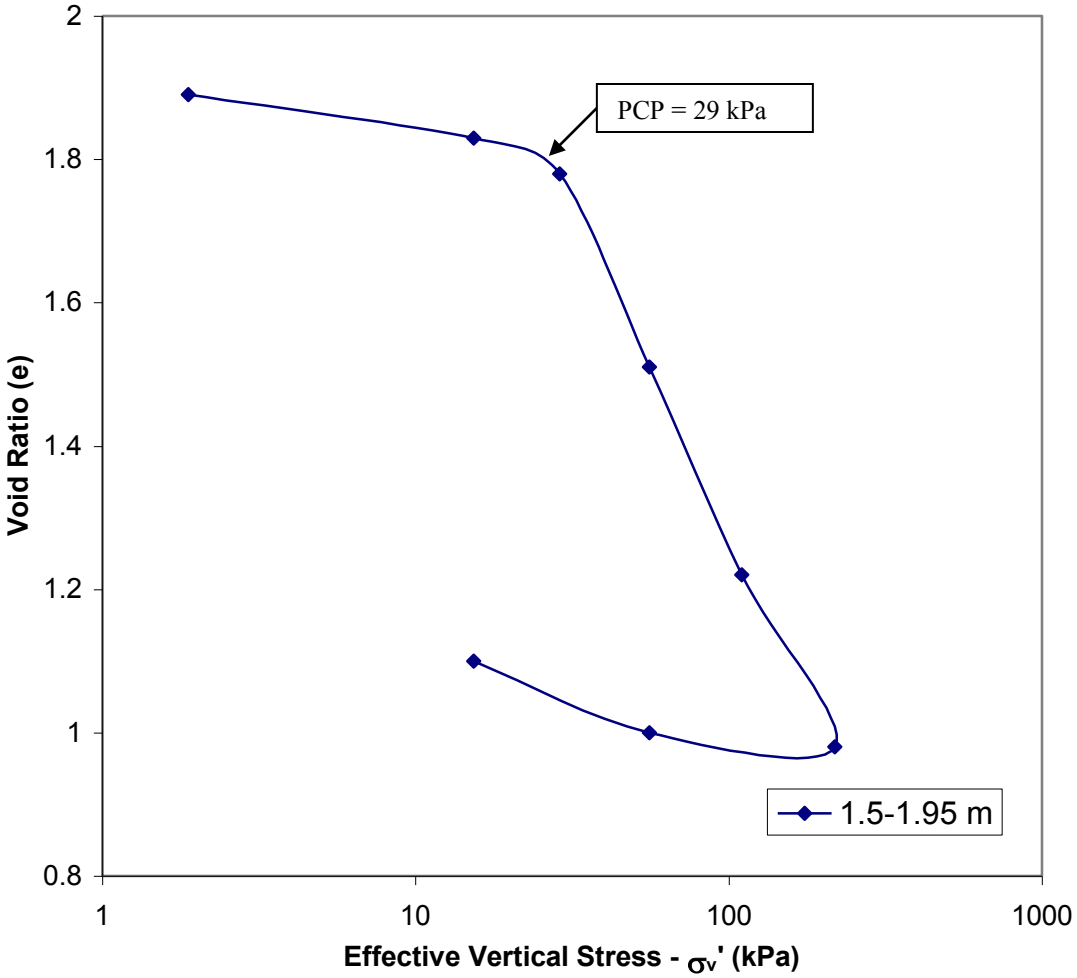

Figure A.7: Pressure versus void ratio plot for borehole 16B

Table A.7: Test results for borehole 16B

Av. Pressure (kPa)	8.63	22.13	42.4	82.91	163.93
m_v (m^2/MN)	1.53	1.32	3.69	2.19	1.01
c_v (m^2/year)	12.18	5.47	0.39	0.4	0.3
Description: Dark Grey CLAY (OH) with Shells					

Table A.8: Summary of test results for Gold Coast Highway

LOCATION/ DEPTH (m)	w_n (%)	WET DENSITY (t/m^3)	DRY DENSITY (t/m^3)	w_L (%)	I_p (%)	C_c	SPECIMEN DESCRIPTION / (UNIFIED SOIL CLASSIFICATION)
0.5-0.95	56	1.68	1.08	54	32.4		Dark grey moist very soft SILTY CLAY (OH)
1.5-1.95	73.4	1.6	0.92	53	30.4	0.911588	Dark grey moist very soft sl. Sandy CLAY (OH+Shells)
1.5-1.95	74	1.5	0.86	53	30.4		Dark grey moist very soft sl. Sandy CLAY (OH+Shells)
2.5-2.95	51			35.8	17.8		Dark grey moist very soft Sandy CLAY (OH+Shells)
0.5-1.0	74			58	32.2		Dark grey moist very soft CLAY (OH)
1.5-2.0	72.8	1.6	0.92	57.8	29.2		Dark grey moist very soft sl. Sandy CLAY (OH)
2.5-2.95	39.6			34.6	18.4		Dark grey moist soft Sandy CLAY
3.5-3.95	30.2	1.92	1.46	33.2	17.6		Dark grey moist mod. Dense Clayey SAND (Shells)
0.5-0.95	56.6			55.8	27.8		Dark grey moist very soft CLAY (OH)
1.5-1.95	46.4						Dark grey moist very soft sl. Sandy CLAY (Shells)
2.5-2.95	56			48.6	25.8		Dark grey moist very soft Silty CLAY (Shells)
3.5-3.95	61	1.7	1.06			0.685112	Grey moist soft CLAY
3.5-3.95	61	1.62	1.6	46.2	25		Grey moist soft CLAY
5.5-5.95	46	1.84	1.26				Dark grey moist soft sl. Sandy CLAY (Shells)
6.5-6.95	20						Light grey moist firm sl. Sandy CLAY
1.0-1.4							Light brown moist firm CLAY
3.0-3.4							Light mottled brown Silty CLAY
1.25	62.8						Dark grey moist soft CLAY (OH)
2.2	61.2						Dark grey moist sl. Sandy CLAY (Shells)
3.2	62.2						Dark grey moist soft CLAY (Shells)
4.2	62.2						Grey moist soft CLAY
5.2	49.8						Grey moist soft CLAY
1	95						Grey moist soft CLAY
1.8	87						Grey moist soft CLAY
2.8	74.4						Grey moist soft CLAY

3.8	60.6						Grey moist soft CLAY
4.8	60.8						Grey moist soft CLAY
0.5	84.6						Dark grey moist soft CLAY (OH)
1.5	56.6						Grey moist soft CLAY (Shells)
2.5	54						Grey moist soft CLAY (Shells)
3.5	44.6						Grey moist soft CLAY (Shells)
1	97.69						Dark grey moist soft CLAY (OH)
2	92.4						Dark grey moist soft CLAY (OH)
3	74.2						Dark grey moist soft clay (Shells)
4	64.2						Dark grey moist soft clay (Shells)
5	57.6						Dark grey moist soft clay (Shells)
6	60.8						Dark grey moist soft clay (Shells)
0.5-0.95	52.8	1.46	0.96	67.2	32.8	0.77829	Dark brown moist soft CLAY (OH)
1.5-1.95							Dark grey moist soft CLAY (OH+Shells)
2.5-2.95	110	1.46	0.7	94.8	56.8	1.445936	Dark grey moist soft silty CLAY (Shells)
3.5-3.95							Dark grey moist soft silty CLAY (Shells)
4.5-4.95	96.4			98	61.4		Dark grey moist soft silty CLAY (Shells)
5.5-5.95							Dark grey moist soft CLAY (Shells)
6.5-6.95	23.4			45.2	25.8		Dark grey moist soft clay into firm/stiff grey/green CLAY
7.5-7.95							Grey/green Sandy CLAY (Jar sample)
2.0-2.35							Pale grey/brown moist hard clayey SILT
0.5-0.95	92.6			70.4	36.4		Dark grey moist soft CLAY (OH)
1.5-1.95	103.4			61.8	30.2		Dark grey moist very soft CLAY (OH)
2.5-2.95	82.4			55.6	25.4		Dark grey moist very soft CLAY (OH)
3.5-3.95	92.2			63.2	31.2		Grey moist soft CLAY (Shells)
4.5-4.95	89			66.4	32		Grey moist soft CLAY (Shells)
5.5-5.95	91.4			67.8	34.4		Grey moist firm CLAY (Shells)
6.5-6.95	81.4			65	30.4		Grey moist firm CLAY
7.5-7.95	78.2			64.8	36.2		Grey moist firm CLAY
8.5-8.95	74.8			61.8	31.6		Grey moist firm CLAY

9.5-9.95	58			54.2	28.6		Grey moist firm CLAY
10.5-10.95	49.6			41	19.8		Grey moist firm CLAY
11.5-11.95						0.881901	Grey moist firm Sl. Sandy CLAY
12.5-12.95							Grey moist soft CLAY
0.5-0.95	72.6			68.8	36		Grey moist firm CLAY
1.5-1.95	113.6			68.2	35.4		Grey moist very soft CLAY (Shells)
2.5-2.95	97			69	36		Grey moist very soft Silty CLAY (Shells)
3.5-3.95	100			58	28.4		Brown moist very soft CLAY (OH)
4.5-4.95	172.4	1.48	0.54	69.6	34.4	1.865678	Dark grey moist very soft CLAY (OH)
5.5-5.95	104.2			69	36		Grey moist very soft CLAY (Shells)
6.5-6.95	85.8			66.6	35.8		Grey moist very soft CLAY
7.5-7.95	83.8			64.8	34.2		Grey moist firm CLAY
8.5-8.95	79.8	1.56	0.86	61	31.8	1.109702	Grey moist firm CLAY (Shells)
9.5-9.95	65.8			48.2	25		Grey moist firm CLAY (Shells)
10.5-10.95	55.4			82.2	49		Grey moist firm CLAY
0.5-0.95	114			59.4	22.6		Brown moist very soft CLAY (OH)
1.5-1.95	110.6			50	15.2		Dark grey moist very soft CLAY (OH)

73.19508	1.618333	1.018333	60.05128	31.27692	1.096887	<- Average
172.4	1.92	1.6	98	61.4	1.865678	<- Max
20	1.46	0.54	33.2	15.2	0.685112	<- Min
72.8	1.6	0.94	61	31.2	0.911588	<- Median
63	12	12	39	39	7	<-No. sample
25.02108	0.140821	0.288728	13.63192	9.156487	0.389992	<- Standard Deviation

APPENDIX B - SUNSHINE MOTORWAY

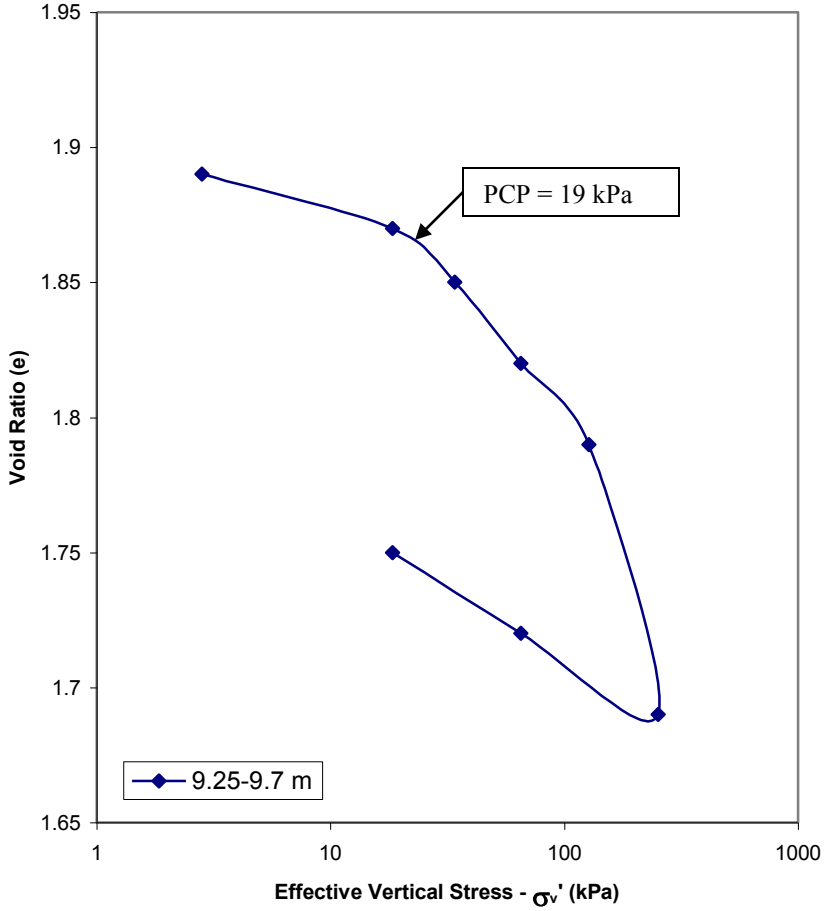

Figure B.1: Pressure versus void ratio plot for borehole 4N

Table B.1: Test results for borehole 4N

Av. Pressure (kPa)	10.61	26.2	49.63	96.47	190.12
m_v (m^2/MN)	0.52	0.25	0.23	0.18	0.23
c_v (m^2/year)	4.082	4.823	6.33	3.708	1.039
Description: Sandy Silt (MH)					

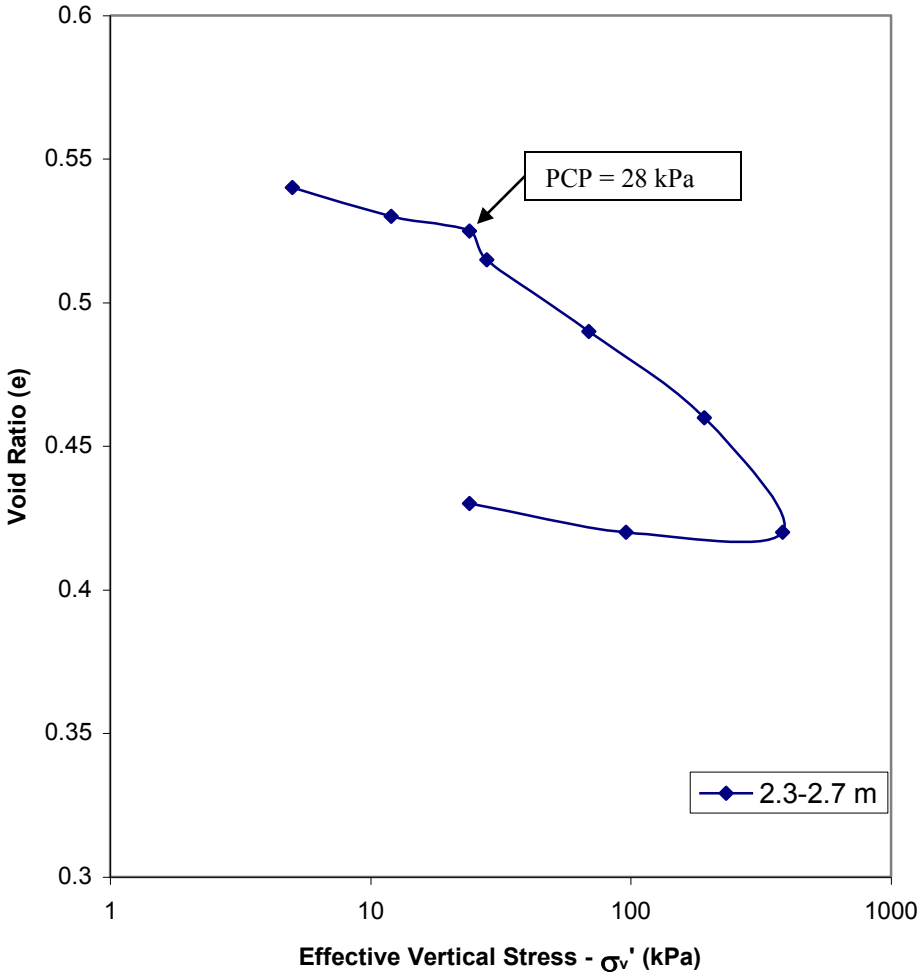

Figure B.2: Pressure versus void ratio plot for borehole 5AF

Table B.2: Test results for borehole 5AF

Av. Pressure (kPa)	8.5	18	36	72	144	288
m_v (m^2/MN)		0.464	0.38	0.409	0.275	0.216
c_v (m^2/year)	4.6	11.55	4.88	9.81	19.19	27.46
Description: Clayey Sand (SC)						

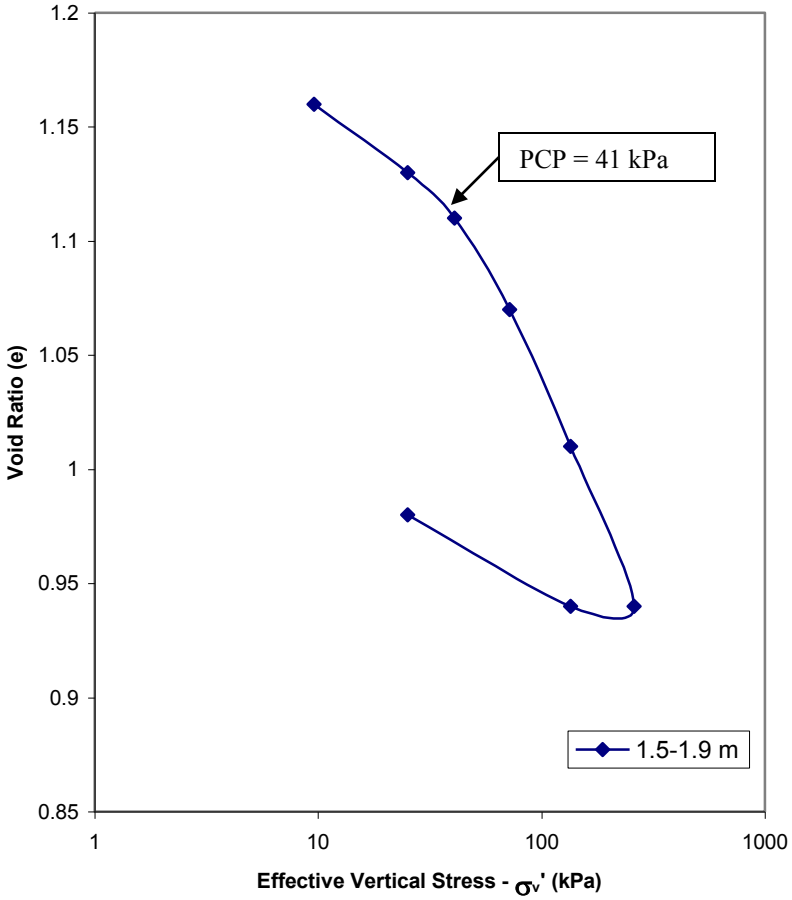

Figure B.3: Pressure versus void ratio plot for borehole 9A

Table B.3: Test results for borehole 9A

Av. Pressure (kPa)	17.41	33.04	56.53	103.48	197.36
m_v (m^2/MN)	0.95	0.46	0.47	0.4	0.25
c_v (m^2/year)	21.35	8.33	5.39	2.57	2.4
Description: Silty Sandy Clay (CL)					

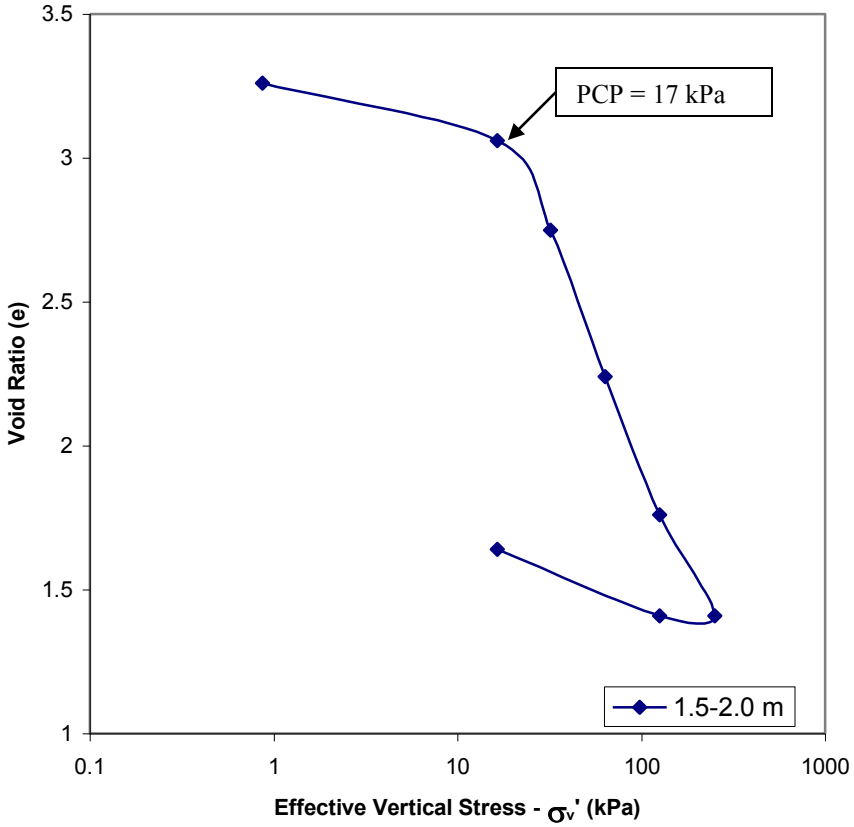

Figure B.4: Pressure versus void ratio plot for borehole 11B

Table B.4: Test results for borehole 11B

Av. Pressure (kPa)	8.66	24.25	47.68	94.52	188.17
m_v (m^2/MN)	2.97	4.38	3.88	1.95	0.95
c_v (m^2/year)	3.01	0.315	0.208	0.175	0.138
Description: Clayey Silt (MH)					

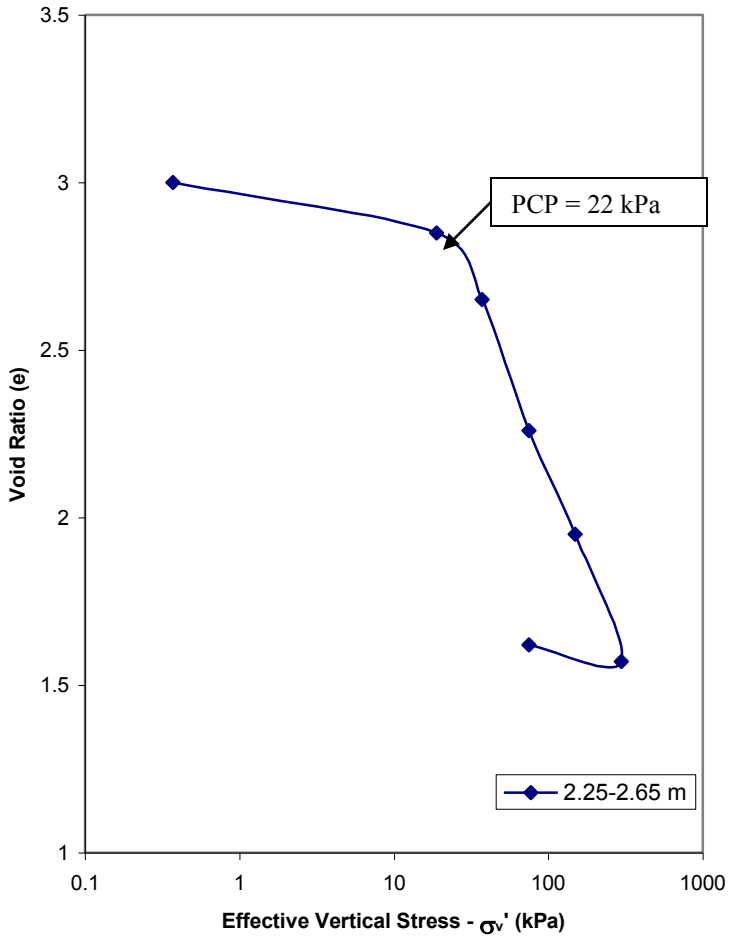

Figure B.5: Pressure versus void ratio plot for borehole 12C

Table B.5: Test results for borehole 12C

Av. Pressure (kPa)	9.61	28.13	55.97	111.63	222.9	185.81
m_v (m^2/MN)	2.05	2.68	2.74	1.13	0.81	0.13
c_v (m^2/year)	3.172	1.446	0.245	0.535	0.223	
Description: Silty Clay (CH)						

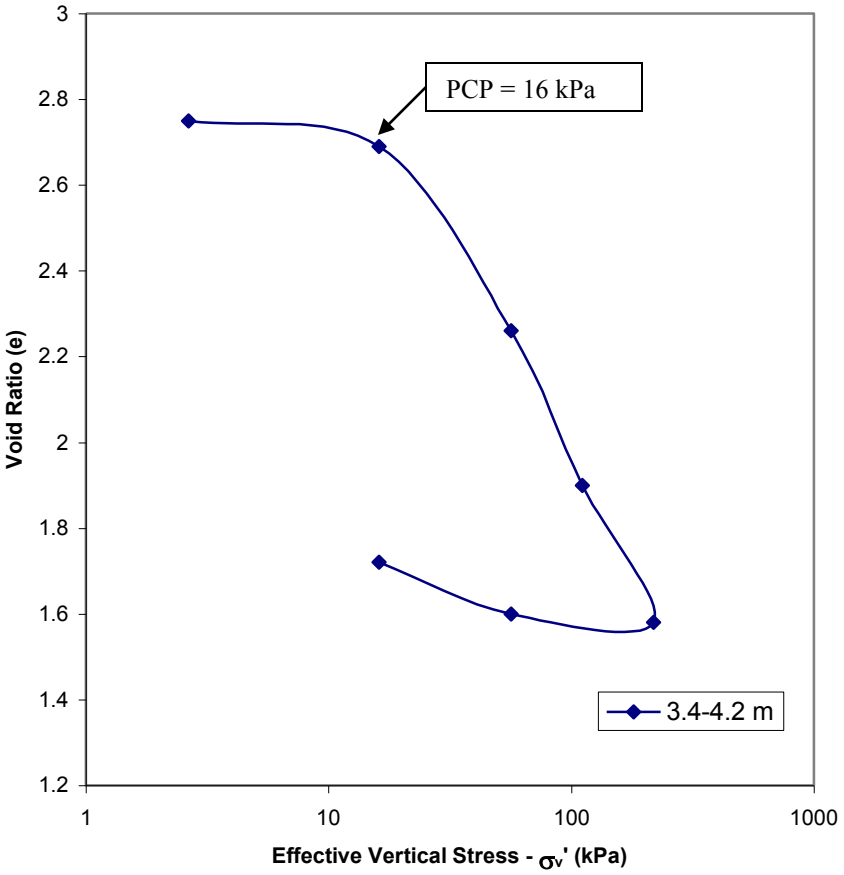

Figure B.6: Pressure versus void ratio plot for borehole 20E

Table B.6: Test results for borehole 20E

Av. Pressure (kPa)	9.39	36.43	83.75	164.86	137.82
m_v (m^2/MN)	1.26	2.25	1.79	0.82	0.18
c_v (m^2/year)	4.497	0.169	0.243	0.238	0.285
Description: Silty Clay (CH)					

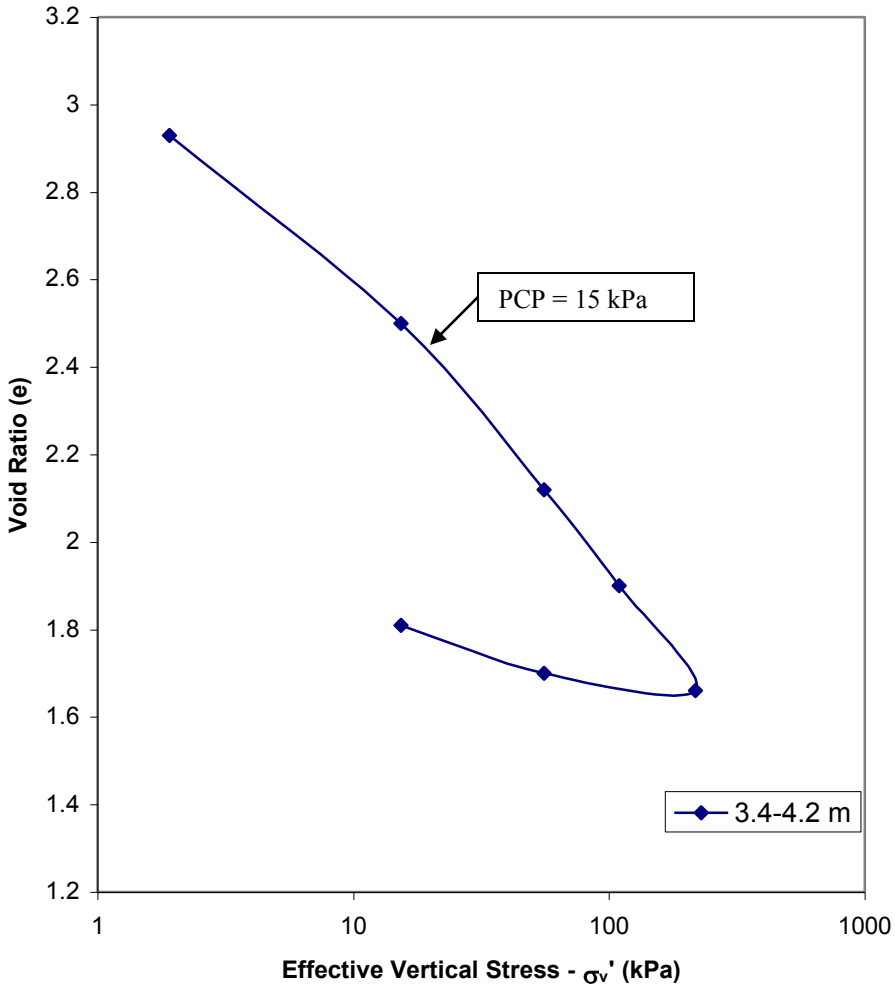

Figure B.7: Pressure versus void ratio plot for borehole 20E,1

Table B.7: Test results for borehole 20E,1

Av. Pressure (kPa)	8.63	35.56	82.68	163.45
m_v (m^2/MN)	8.11	2.5	2.24	1.29
c_v (m^2/year)	0.21	0.147	0.234	0.173
Description: Silty Clay (CH)				

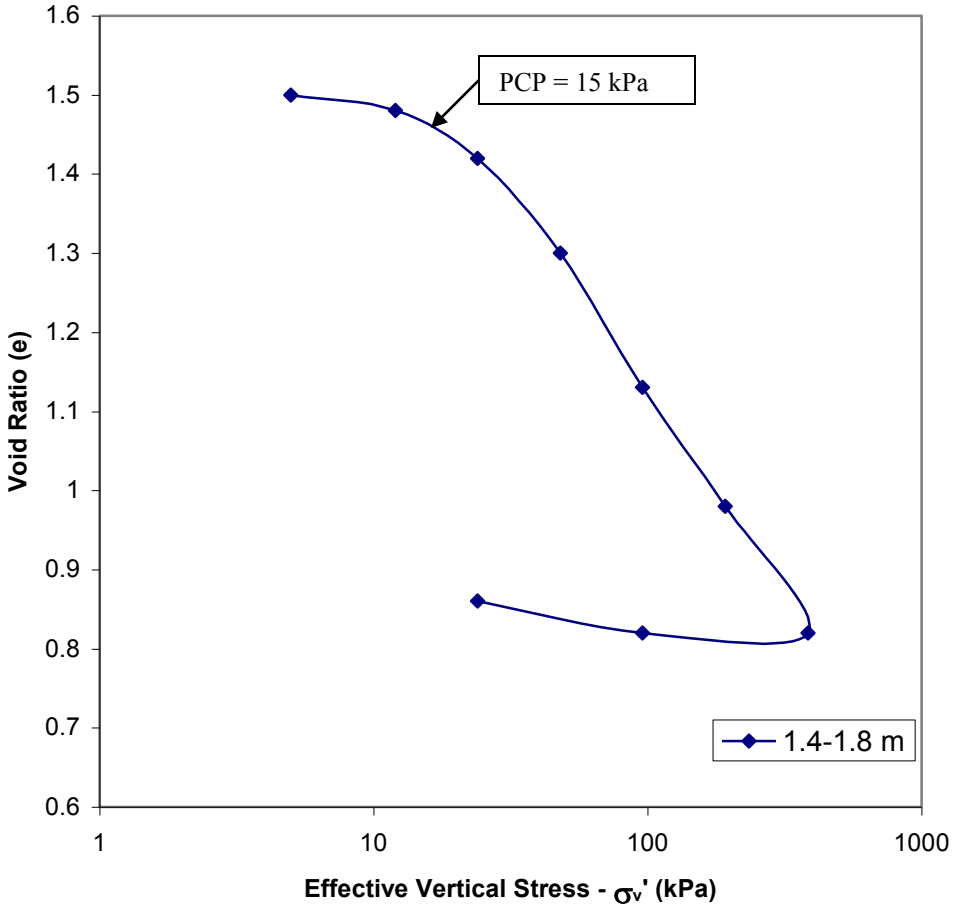

Figure B.8: Pressure versus void ratio plot for borehole 22C

Table B.8: Test results for borehole 22C

Av. Pressure (kPa)	8.5	18	36	72	144	288
m_v (m^2/MN)	1.542	1.987	2.036	1.533	0.739	0.369
c_v (m^2/year)	0.95	1.23	0.959	0.902	1.166	1.324
Description: Clayey Silty Sand (SM)						

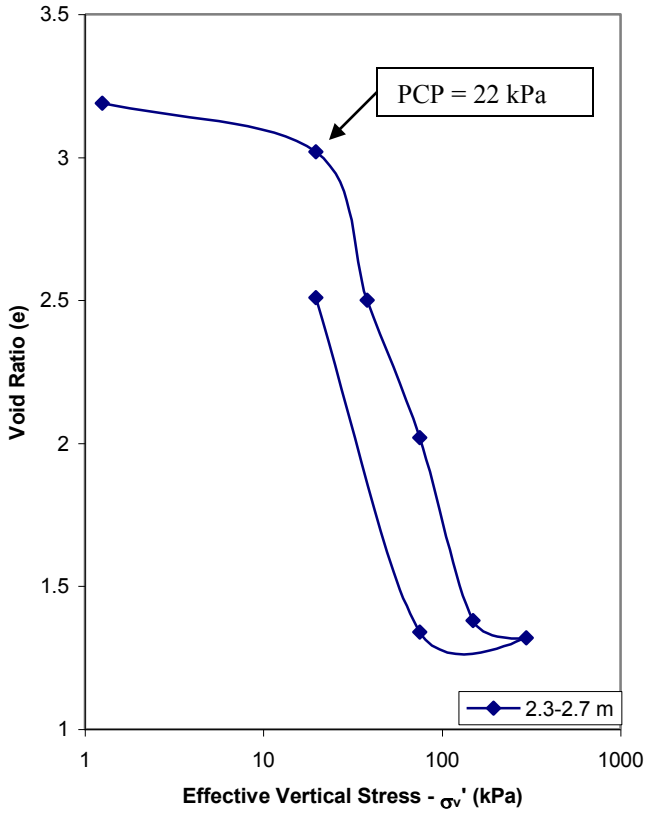

Figure B.9: Pressure versus void ratio plot for borehole 22E

Table B.9: Test results for borehole 22E

Av. Pressure (kPa)	10.48	28.96	56.74	112.28	223.31
m_v (m^2/MN)	2.19	5.59	2.92	2.87	0.14
c_v (m^2/year)	13.26	0.386	0.483	0.273	0.774
Description: Clayey Sandy Silt (MH)					

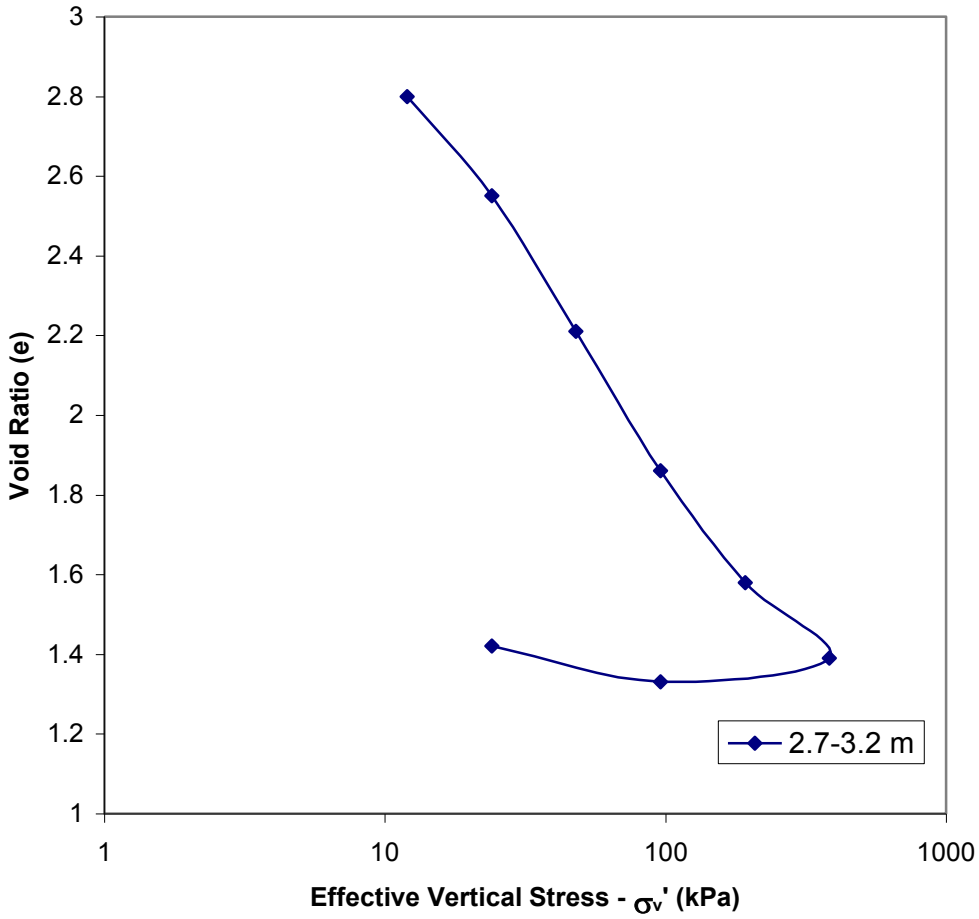

Figure B.10: Pressure versus void ratio plot for borehole 22F

Table B.10: Test results for borehole 22F

Av. Pressure (kPa)	8.5	18	36	72	144	288
m_v (m^2/MN)	2.82	5	3.95	2.28	0.978	0.592
c_v (m^2/year)	0.85	0.314	0.247	0.229	0.386	0.304
Description: Silty Clay (CH)						

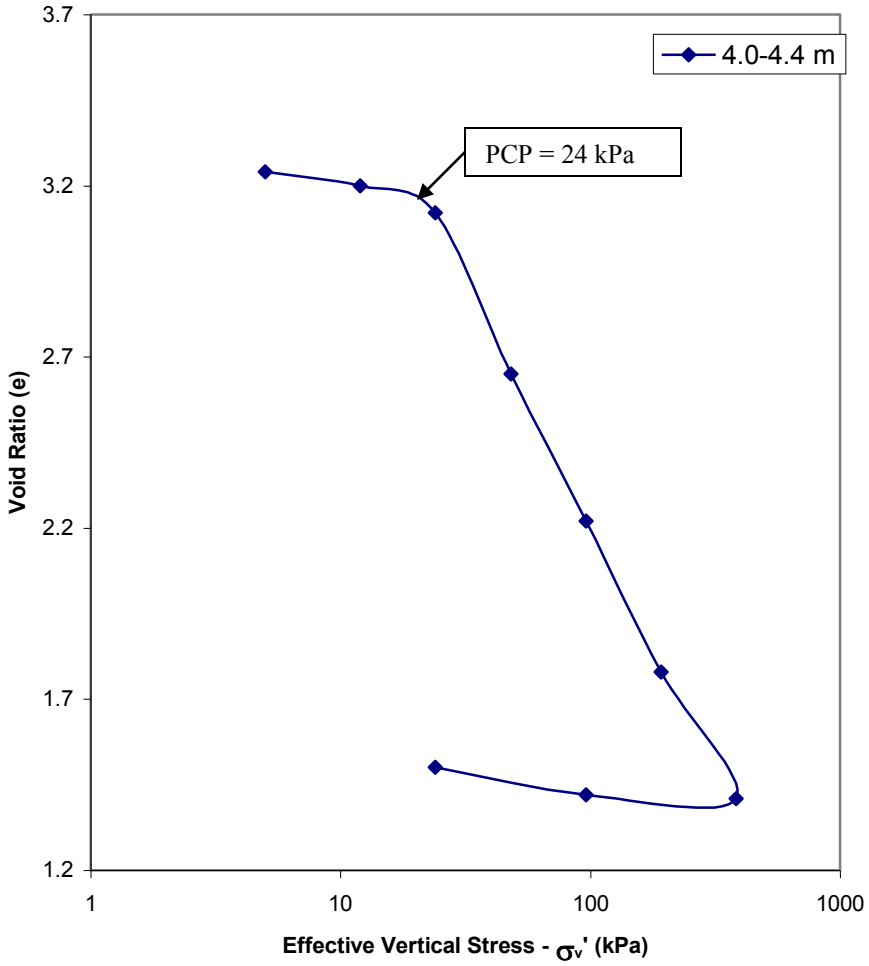

Figure B.11: Pressure versus void ratio plot for borehole 22J

Table B.11: Test results for borehole 22J

Av. Pressure (kPa)	8.5	18	36	72	144	288
m_v (m^2/MN)	0.778	1.647	4.504	2.604	1.388	0.572
c_v (m^2/year)	2.823	0.427	0.214	0.244	0.234	0.214
Description: Sandy Silty Clay (CH)						

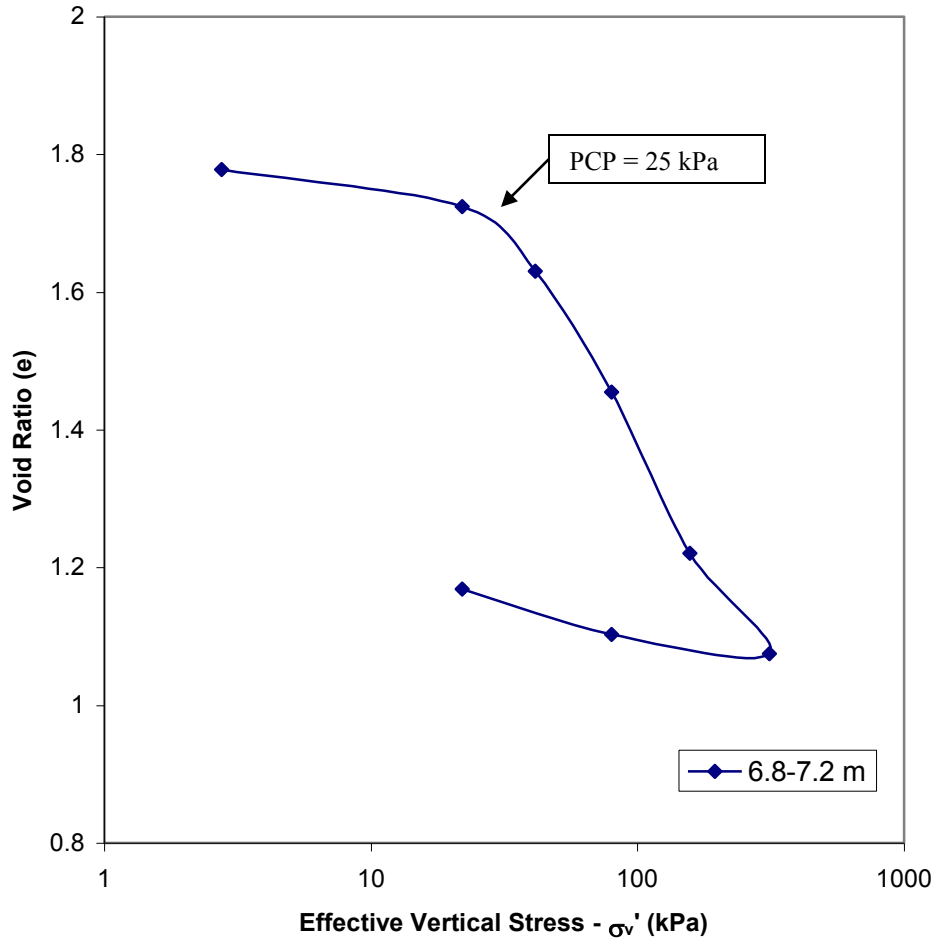

Figure B.12: Pressure versus void ratio plot for borehole 22M

Table B.12: Test results for borehole 22M

Av. Pressure (kPa)	12.39	31.7	60.72	118.73	234.7
m_v (m^2/MN)	1.007	1.544	1.636	1.152	0.0379
c_v (m^2/year)	2.441	0.188	0.166	0.28	0.211
Description: Clay Silt Mixture (CH-MH)					

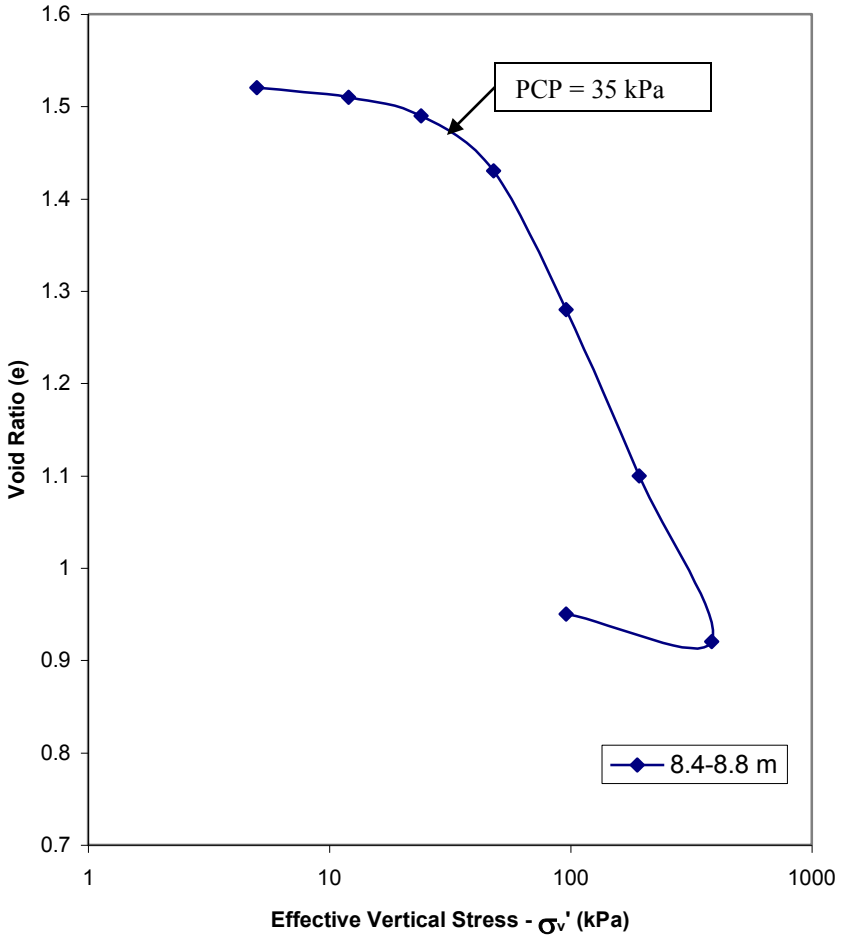

Figure B.13: Pressure versus void ratio plot for borehole 22P

Table B.13: Test results for borehole 22P

Av. Pressure (kPa)	8.5	18	36	72	144	288
m_v (m^2/MN)	0.736	0.531	1.019	1.284	0.826	0.436
c_v (m^2/year)	1.265	1.751	0.585	0.222	0.292	0.258
Description: Clayey Silt (CH/MH)						

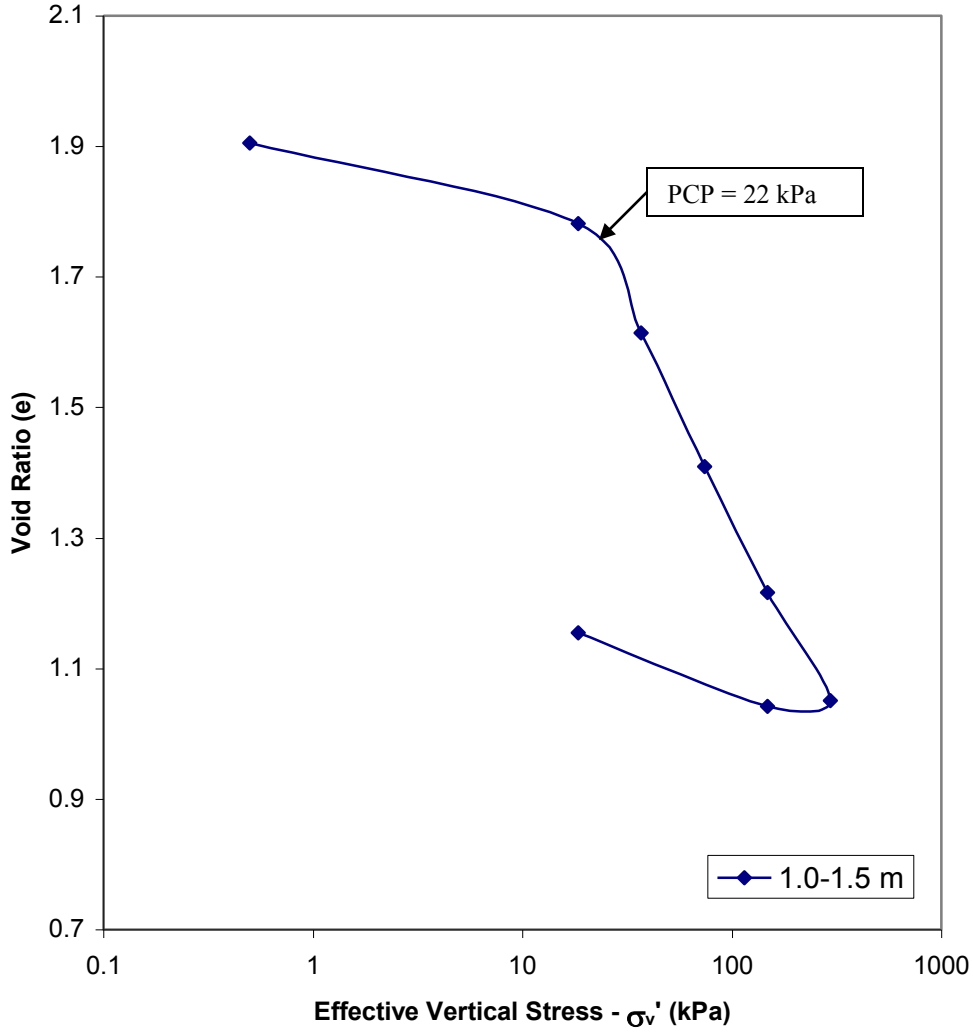

Figure B.14: Pressure versus void ratio plot for borehole 23B

Table B.14: Test results for borehole 23B

Av. Pressure (kPa)	9.48	27.71	55.49	111.03	222.06
m_v (m^2/MN)	2.364	2.963	1.903	0.944	0.439
c_v (m^2/year)	2.166	0.341	0.294	0.311	0.353
Description: Clayey Silty Sand (SC)					

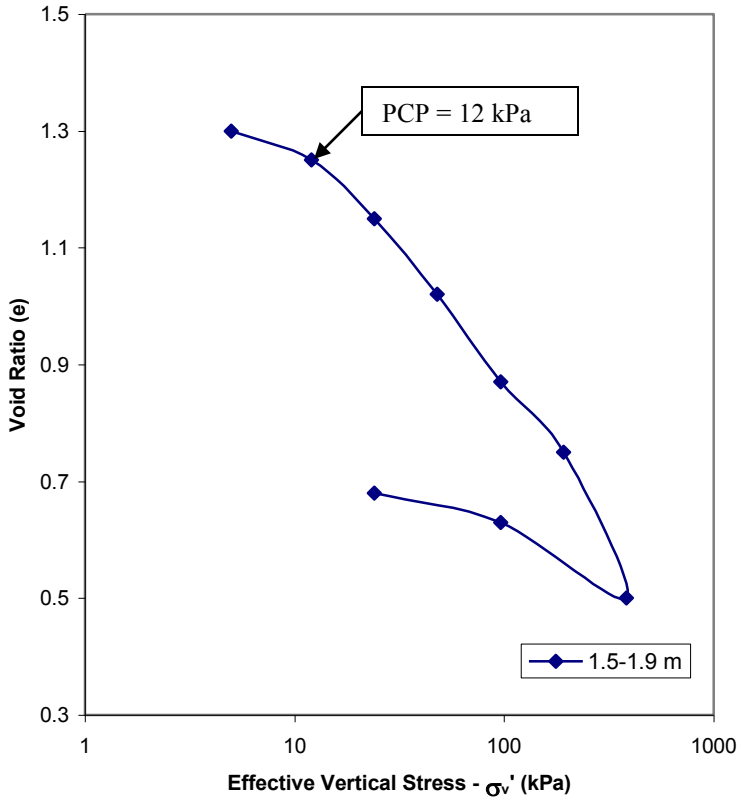

Figure B.15: Pressure versus void ratio plot for borehole 23C

Table B.15: Test results for borehole 23C

Av. Pressure (kPa)	8.5	18	36	72	144	288
m_v (m^2/MN)	4.84	3.92	2.58	1.46	0.71	0.35
c_v (m^2/year)	0.1	0.14	0.33	0.33	0.54	0.81
Description: Sandy Silty Clay (CH)						

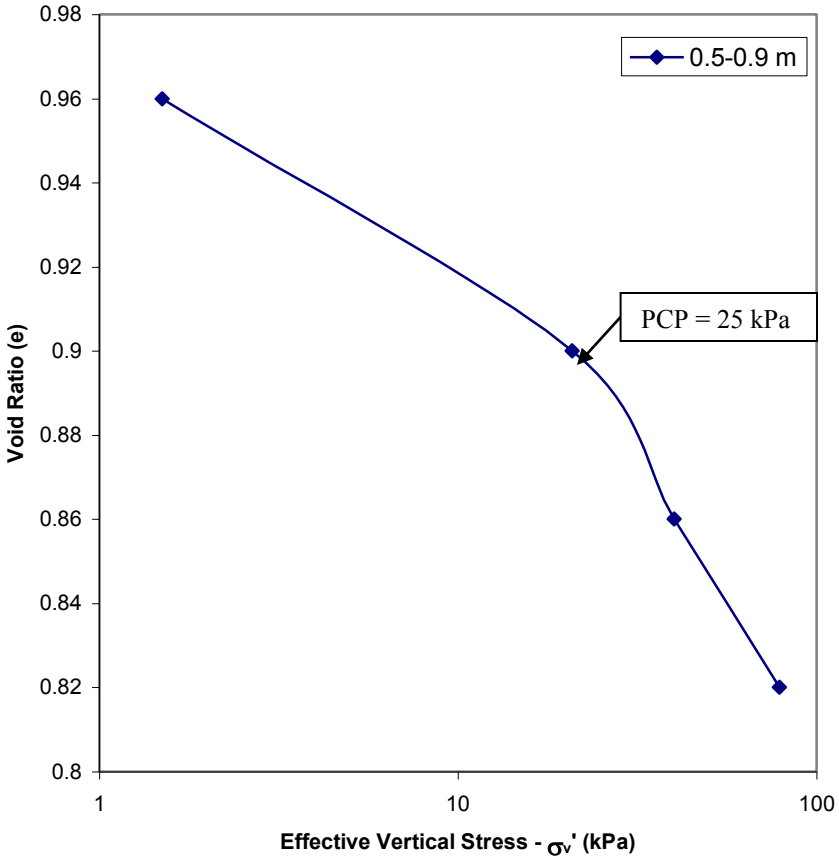

Figure B.16: Pressure versus void ratio plot for borehole 24A

Table B.16: Table results for borehole 24A

Av. Pressure (kPa)	11.15	30.46	59.48
m_v (m^2/MN)	1.47	0.82	0.4
c_v (m^2/year)	14.04	2.65	6.8
Description: Clayey Silty Sand (SC)			

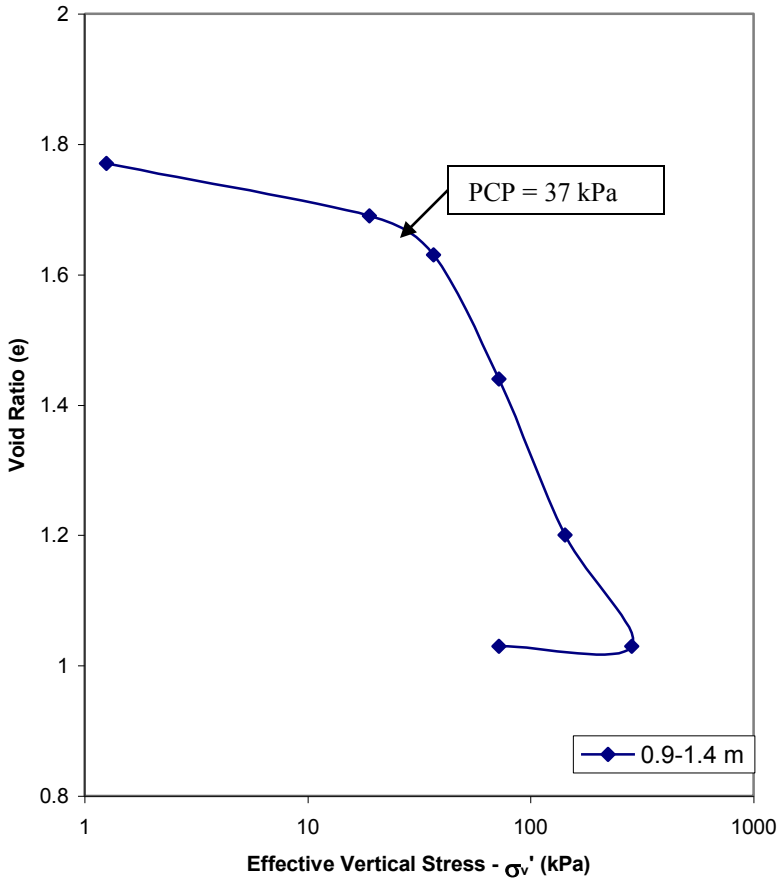

Figure B.17: Pressure versus void ratio plot for borehole 24B

Table B.17: Test results for borehole 24B

Av. Pressure (kPa)	10.07	27.75	54.31	107.41	213.57
m_v (m^2/MN)	1.73	0.99	1.5	0.99	0.46
c_v (m^2/year)	25.282	10.718	2.564	0.705	0.598
Description: Silty Clayey Sand (SC)					

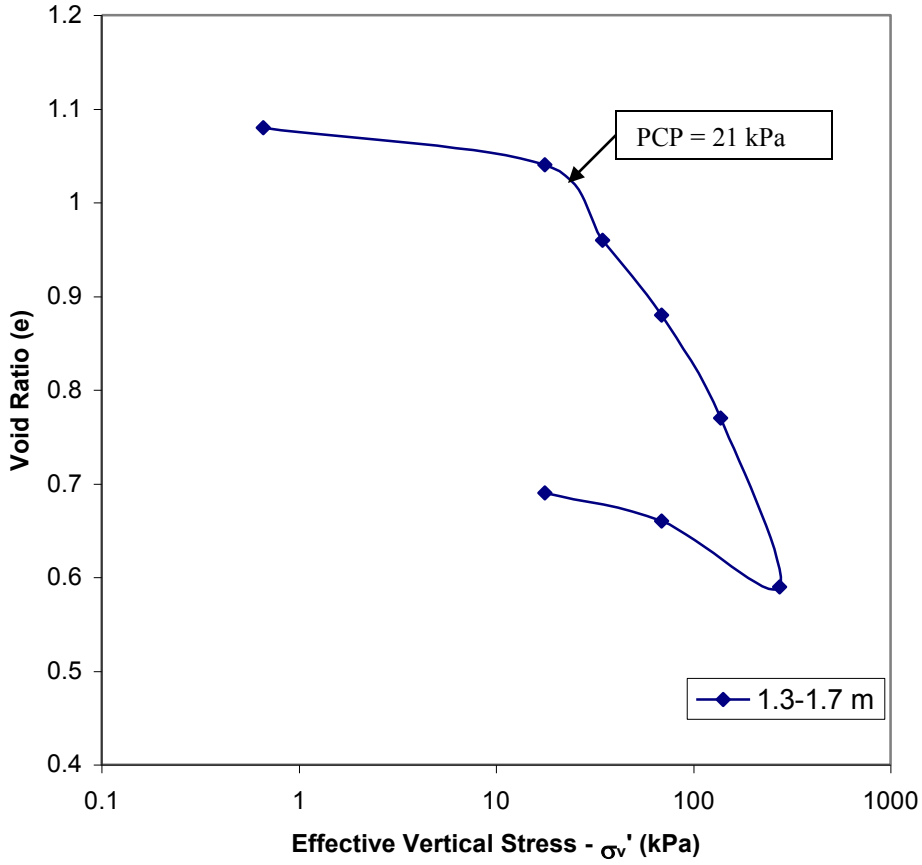

Figure B.18: Pressure versus void ratio plot for borehole 25C

Table B.18: Test results for borehole 25C

Av. Pressure (kPa)	91.16	26.18	51.76	102.9	205.44
m_v (m^2/MN)	1.27	1.59	0.92	0.76	0.68
c_v (m^2/year)	15.405	4.115	4.205	4.002	4.073
Description: Sandy Clay (CL)					

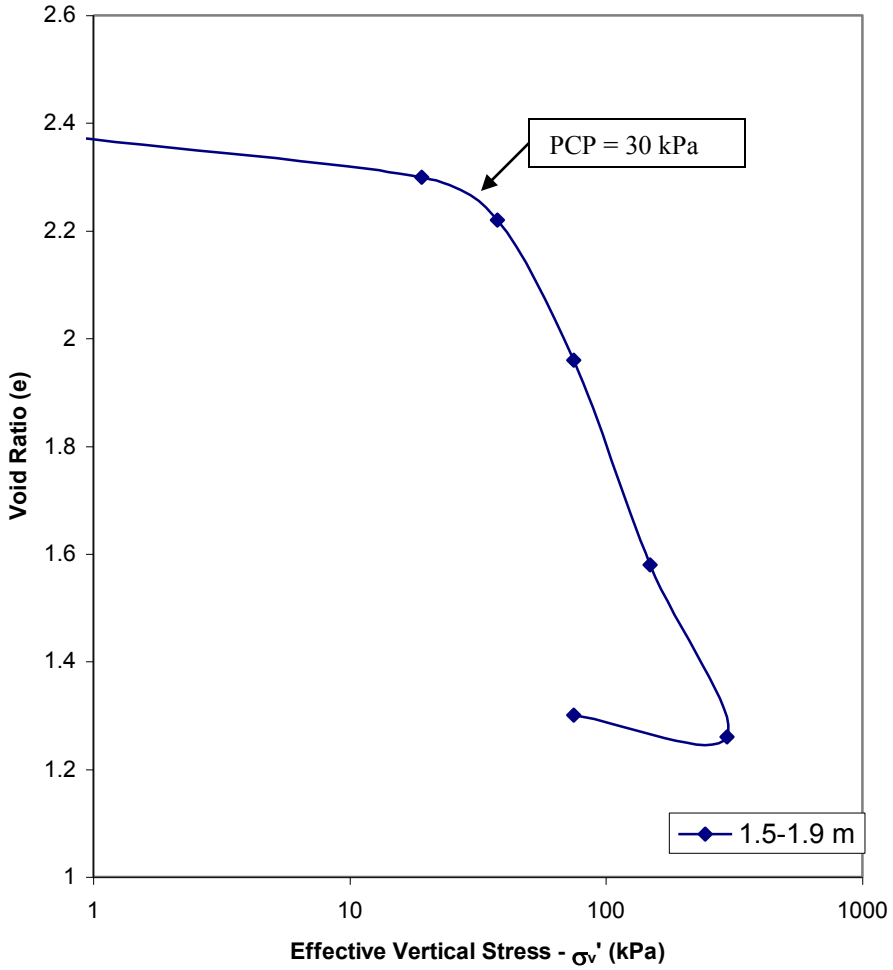

Figure B.19: Pressure versus void ratio plot for borehole 26B

Table B.19: Test results for borehole 26B

Av. Pressure (kPa)	9.85	28.35	56.15	111.72	222.82
m_v (m^2/MN)	1.33	1.08	1.95	1.39	0.77
c_v (m^2/year)	2.43	1.54		0.217	0.252
Description: Clay Silt Mixture (CH-MH)					

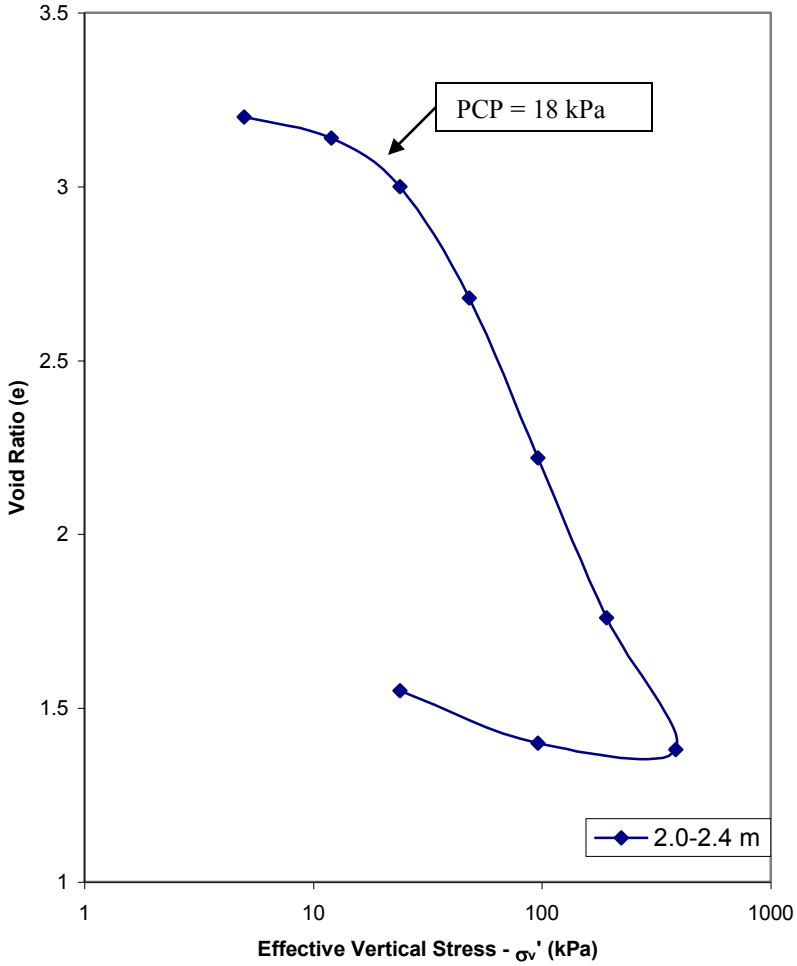

Figure B.20: Pressure versus void ratio plot for borehole 27C

Table B.20: Test results for borehole 27C

Av. Pressure (kPa)	8.5	18	36	72	144	288
m_v (m^2/MN)	1.806	2.537	3.811	2.457	1.448	1.49
c_v (m^2/year)	1.32	0.68	0.24	0.25	0.25	0.2
Description: Clayey Silt (MH)						

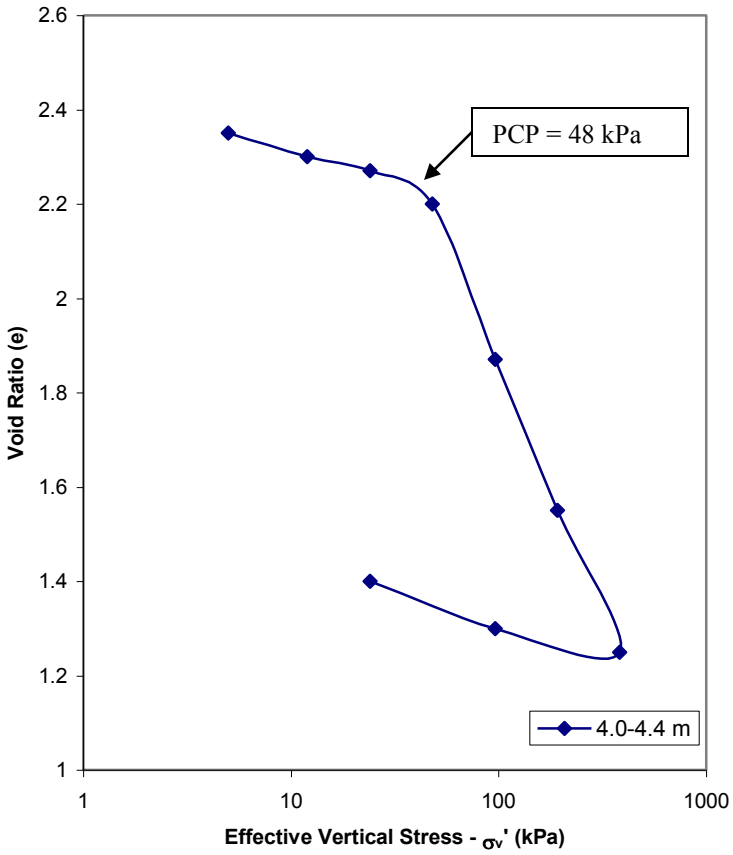

Figure B.21: Pressure versus void ratio plot for borehole 27G

Table B.21: Test results for borehole 27G

Av. Pressure (kPa)	8.5	18	36	72	144	288
m_v (m^2/MN)	1.1	1.54	1.53	1.95	1.19	0.56
c_v (m^2/year)	0.62	0.61	0.32	0.19	0.19	0.16
Description: Clayey Silty Sand (SC)						

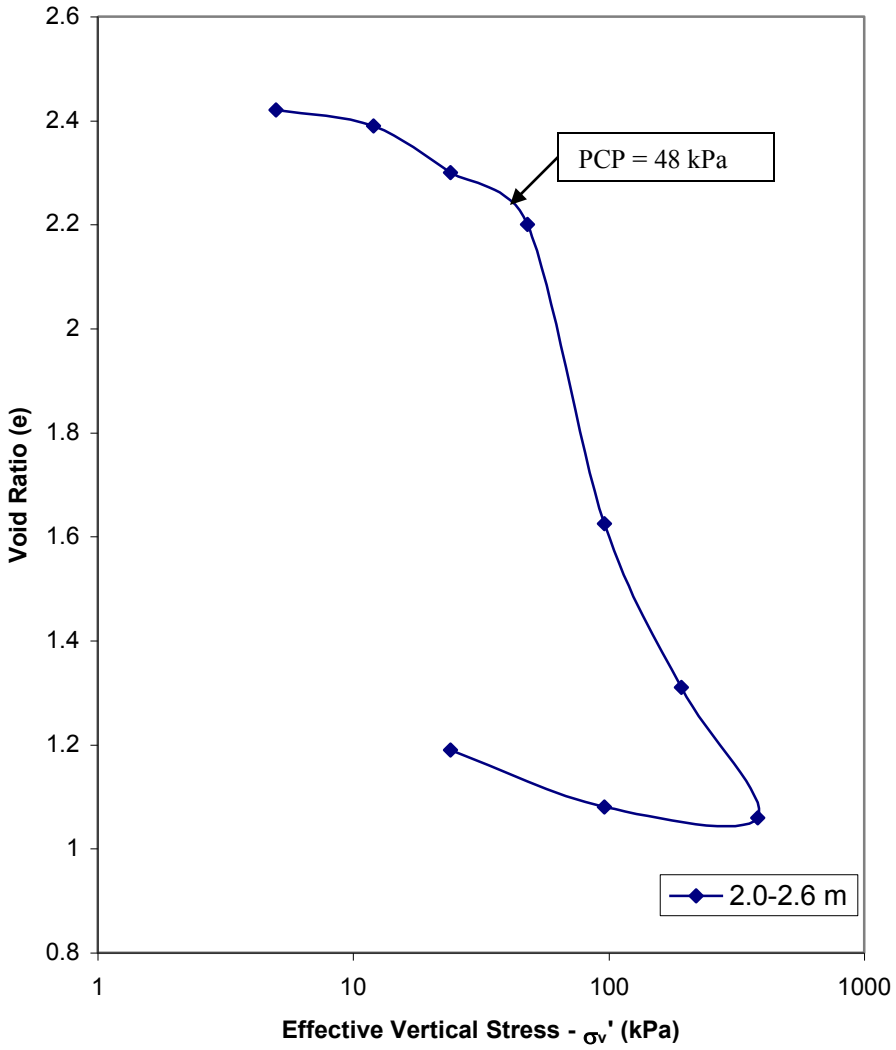

Figure B.22: Pressure versus void ratio plot for borehole 29C

Table B.22: Test results for borehole 29C

Av. Pressure (kPa)	8.5	18	36	72	144	288
m_v (m^2/MN)	1.21	2.23	3.44	2.8	1.25	0.59
c_v (m^2/year)	0.754	0.832	0.313	0.249	0.279	0.246
Description: Clayey Silt (MH)						

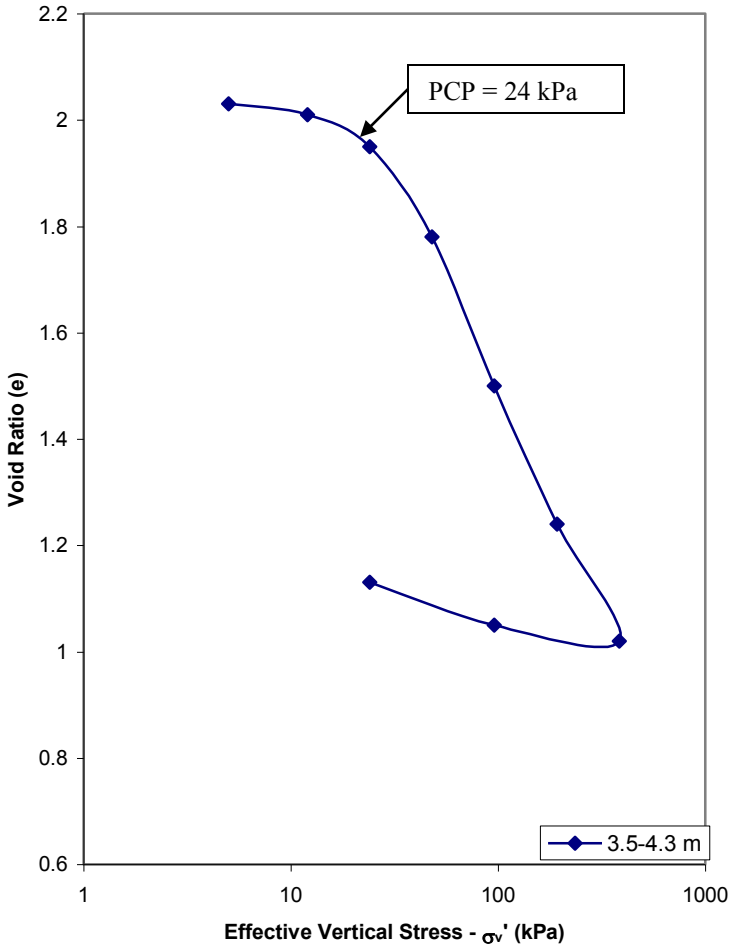

Figure B.23: Pressure versus void ratio plot for borehole 30E

Table B.23: Test results for borehole 30E

Av. Pressure (kPa)	8.5	18	36	72	144	288
m_v (m^2/MN)	1.18	1.75	2.41	2.07	1.08	0.51
c_v (m^2/year)	1.083	0.993	0.165	0.246	0.252	0.278
Description: Silty Clay (CH)						

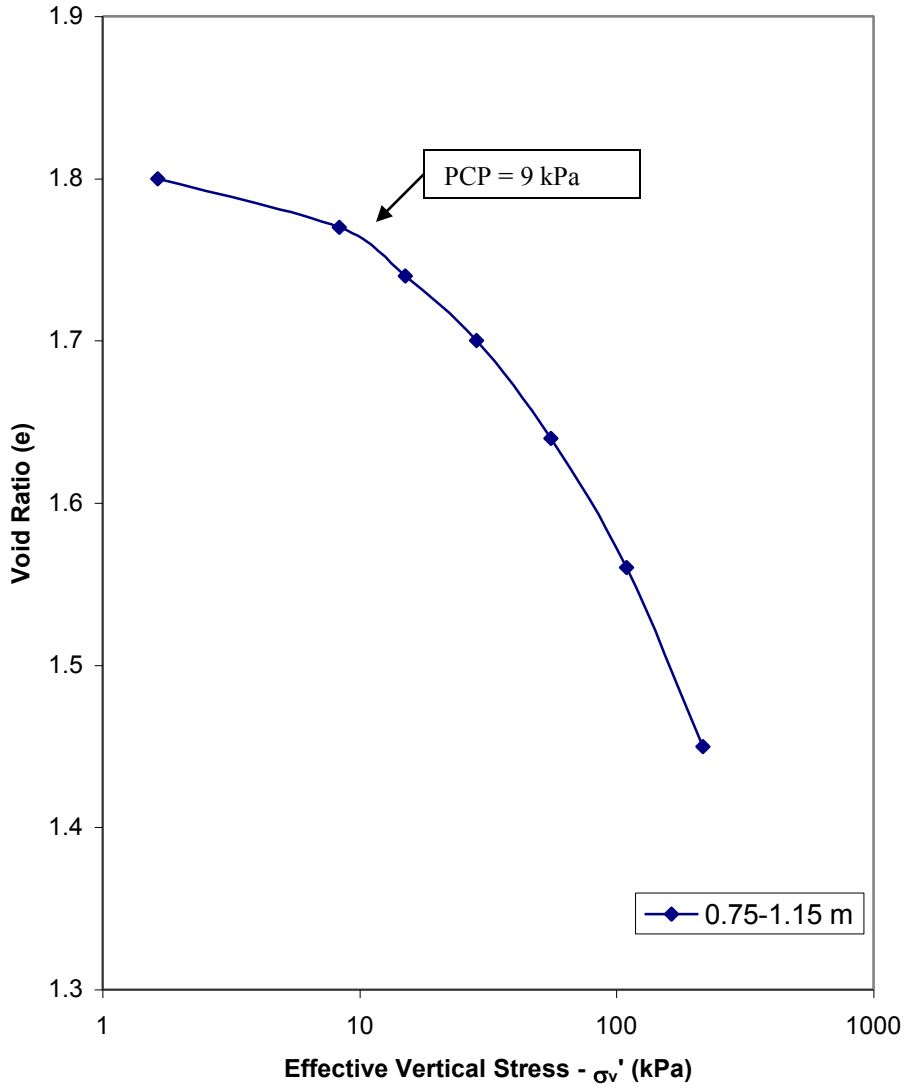

Figure B.24: Pressure versus void ratio plot for borehole 45A

Table B.24: Test results for borehole 45A

Av. Pressure (kPa)	5	11.72	21.82	42.03	82.42	163.19
m_v (m^2/MN)	1.86	1.03	0.88	0.67	0.48	0.34
c_v (m^2/year)	15.53	15.15	8.85	3.41	2.31	1.87
Description: Silty Clay (CH)						

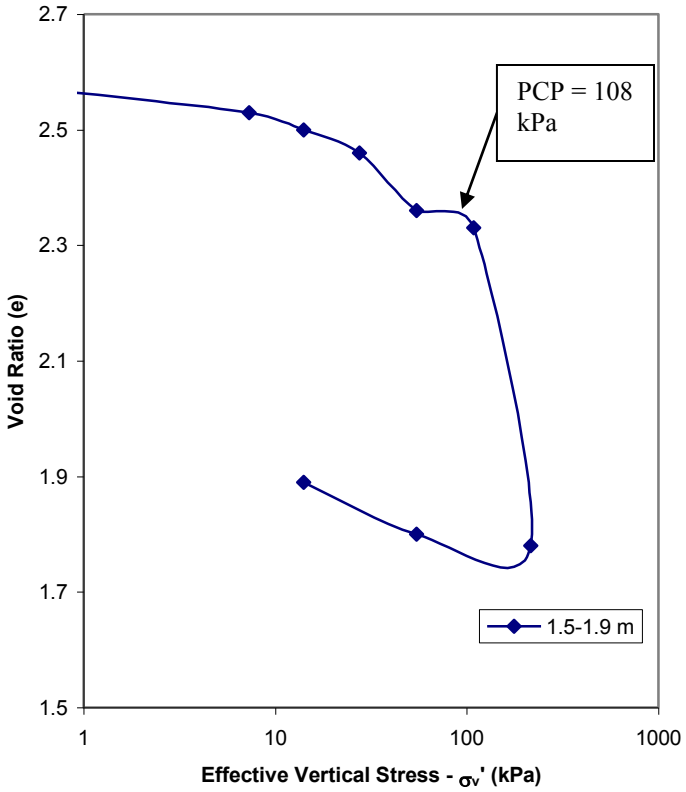

Figure B.25: Pressure versus void ratio plot for borehole 45B

Table B.25: Test results for borehole 45B

Av. Pressure (kPa)	3.98	10.7	20.8	41.01	81.39	162.15	135.24
m_v (m^2/MN)	1.57	0.79	0.68	0.87		0.77	0.17
c_v (m^2/year)	18.67	10.16	6.89	2.86	0.817	0.283	0.665
Description: Silty Clay Mixture (CH-MH)							

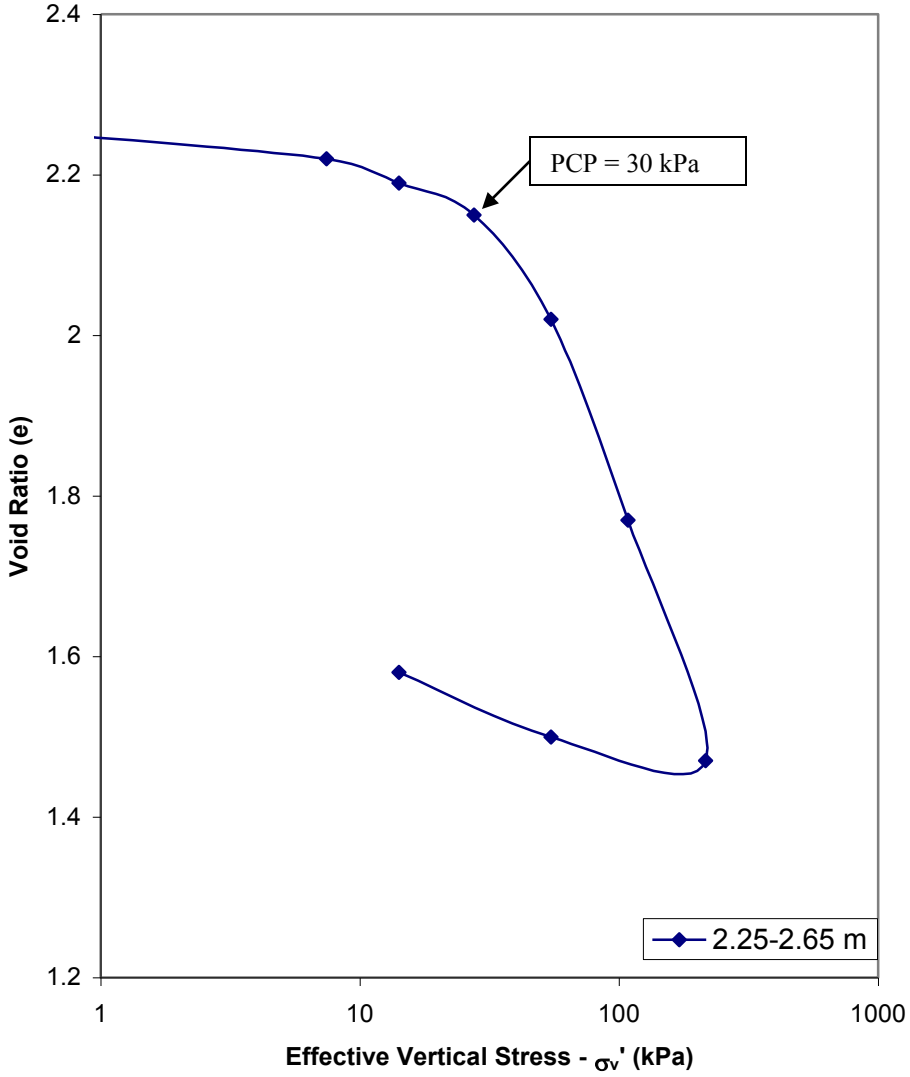

Figure B.26: Pressure versus void ratio plot for borehole 45C

Table B.26: Test results for borehole 45C

Av. Pressure (kPa)	4.07	10.79	20.89	41.1	81.49	162.26
m_v (m^2/MN)	1.34	0.79	0.72	1.3	1.32	0.76
c_v (m^2/year)	18.55	7.58	6.85	1.29	0.318	0.37
Description: Sandy Silty Clay (CH)						

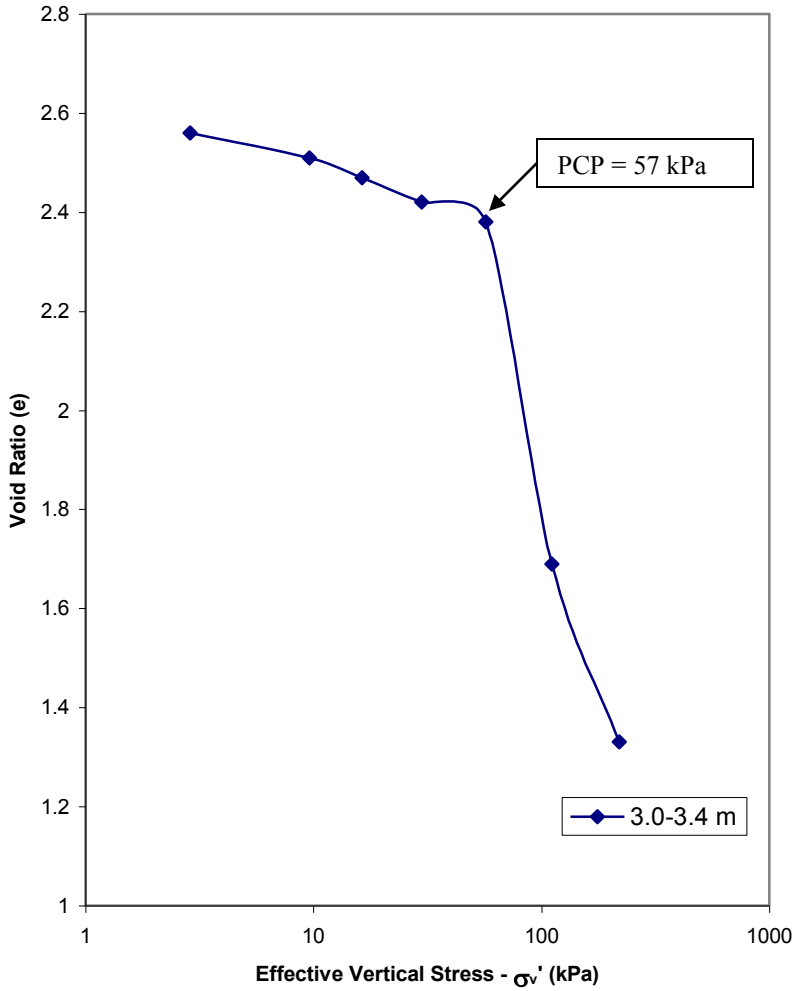

Figure B.27: Pressure versus void ratio plot for borehole 45D

Table B.27: Test results for borehole 45D

Av. Pressure (kPa)	6.25	13	23.15	43.44	83.99	165.1
m_v (m^2/MN)	2.06	1.04	0.77	0.06	2.22	0.96
c_v (m^2/year)	22.56	5.852	8.56	1.509	0.2	0.147
Description: Clayey Silt (MH)						

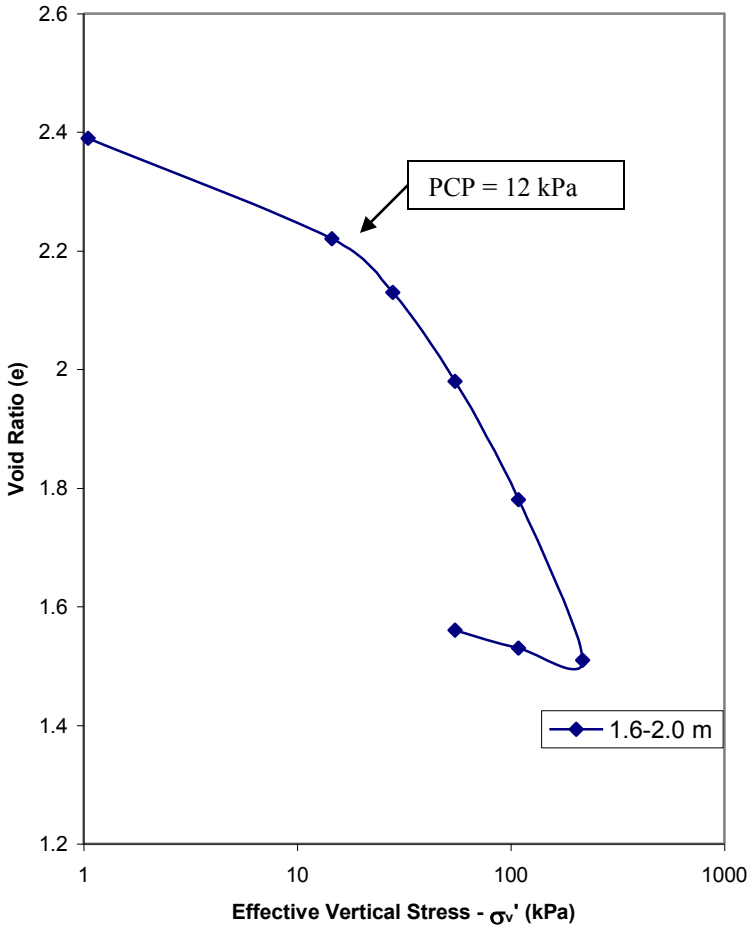

Figure B.28: Pressure versus void ratio plot for borehole 46E

Table B.28: Test results for borehole 46E

Av. Pressure (kPa)	7.77	21.23	41.44	81.82	162.6
m_v (m^2/MN)	3.69	2.1	1.56	1.03	0.73
c_v (m^2/year)	0.89	0.454	0.342	0.416	0.069
Description: Sandy Silty Clay (CH)					

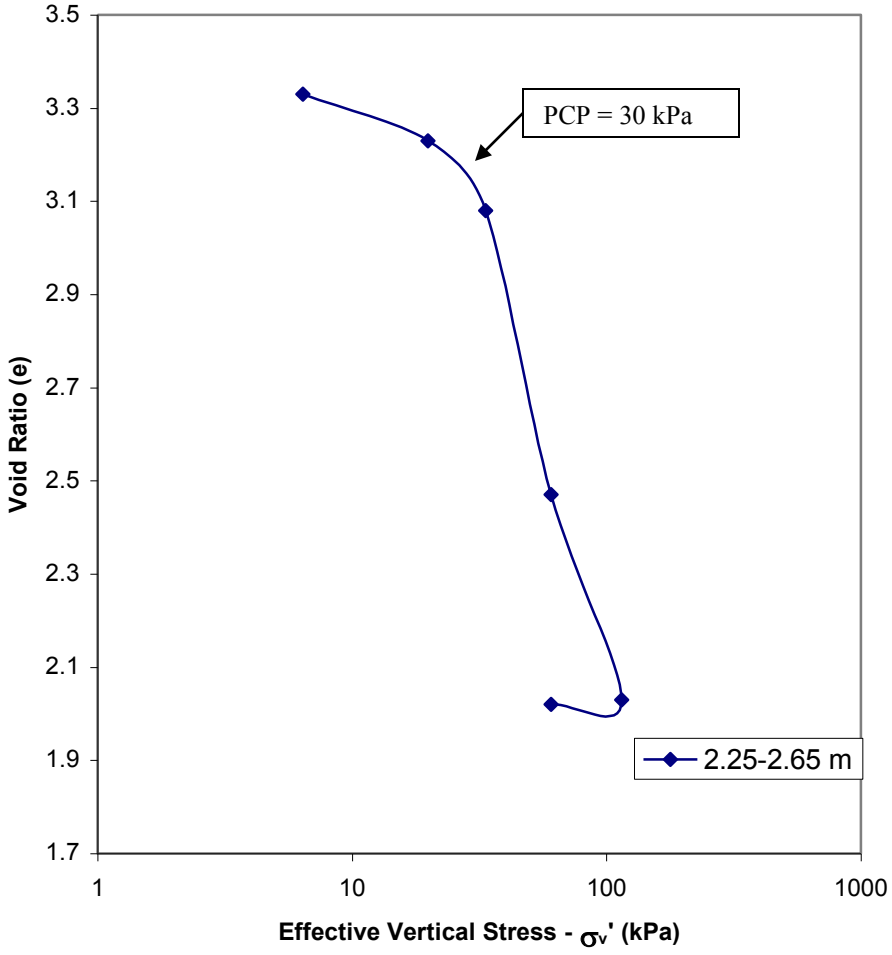

Figure B.29: Pressure versus void ratio plot for borehole 46F

Table B.29: Test results for borehole 46F

Av. Pressure (kPa)	13.16	26.68	46.97	87.52
m_v (m^2/MN)	1.6	2.13	4.6	2.18
c_v (m^2/year)	3.972	1.069	0.172	0.186
Description: Silty Clay (CH)				

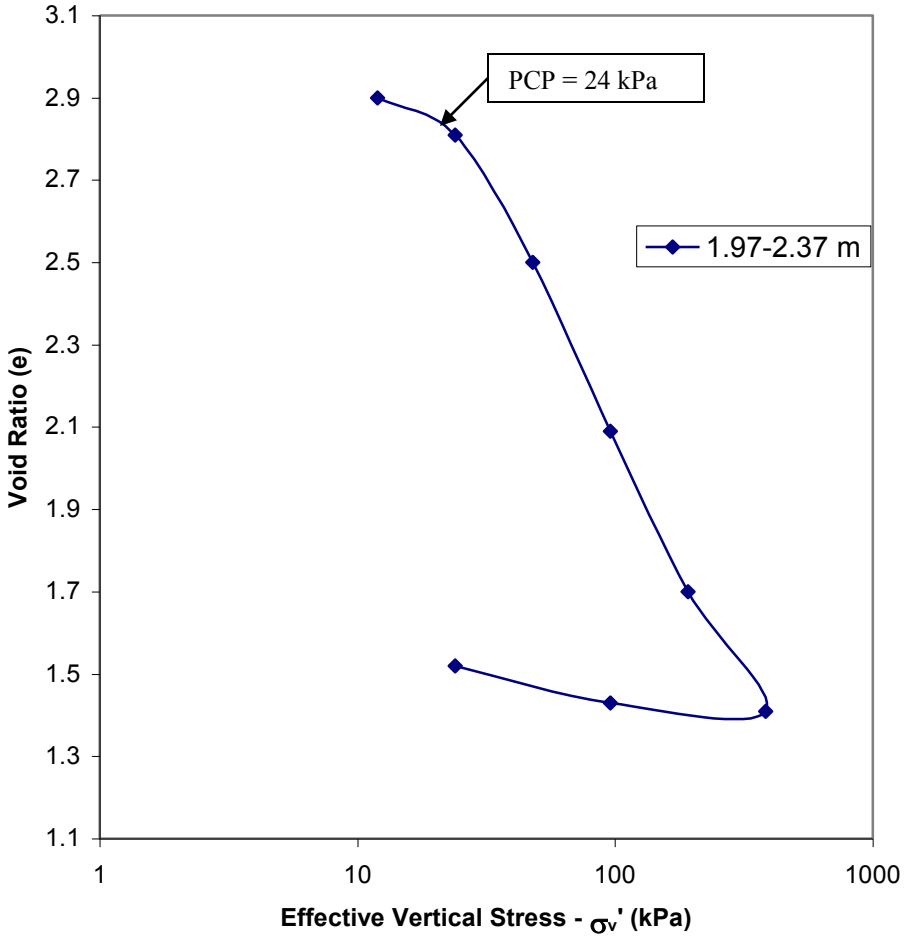

Figure B.30: Pressure versus void ratio plot for borehole 47B

Table B.30: Test results for borehole 47B

Av. Pressure (kPa)	8.5	18	36	72	144	288
m_v (m^2/MN)	1.27	1.88	3.33	2.47	1.28	5.74
c_v (m^2/year)	0.97	0.542	0.205	0.323	0.296	0.283
Description: Sandy Silty Clay (CH)						

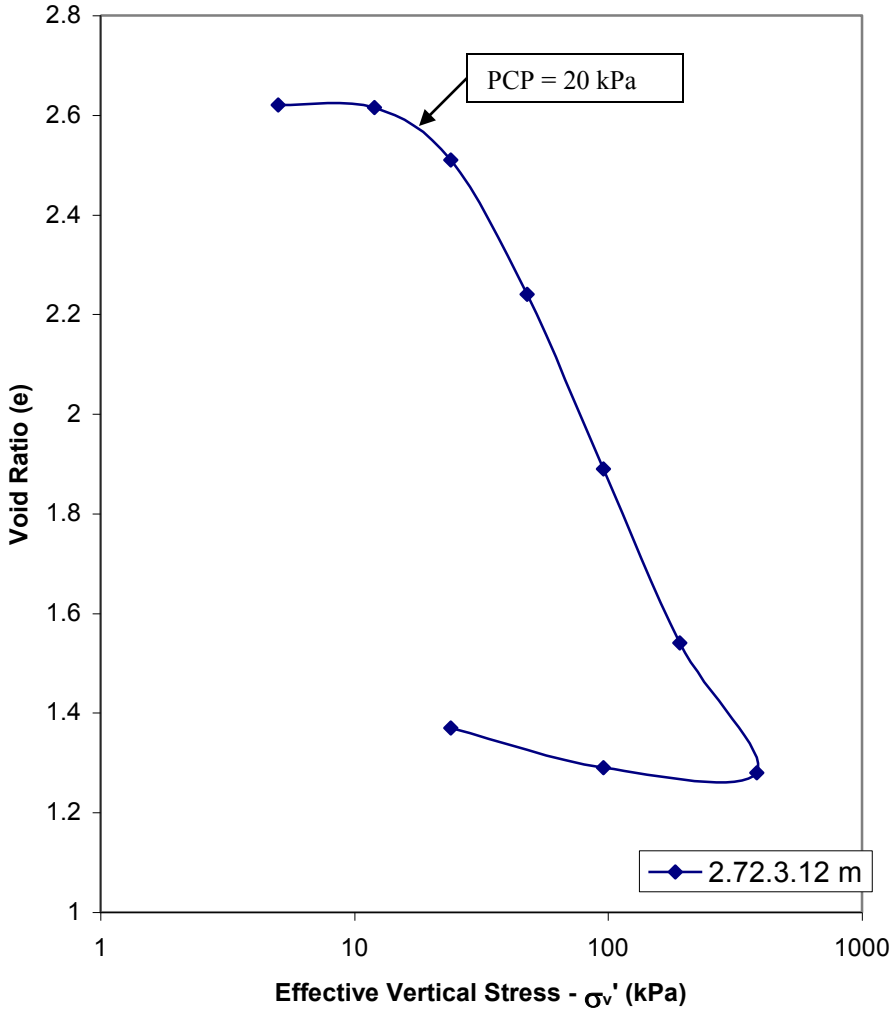

Figure B.31: Pressure versus void ratio plot for borehole 47C

Table B.31: Test results for borehole 47C

Av. Pressure (kPa)	8.5	18	36	72	144	288
m_v (m^2/MN)	0.59	0.24	3.17	2.39	1.23	0.53
c_v (m^2/year)	20.92	0.24	0.21	0.28	0.25	0.28
Description: Silty Clay (CH)						

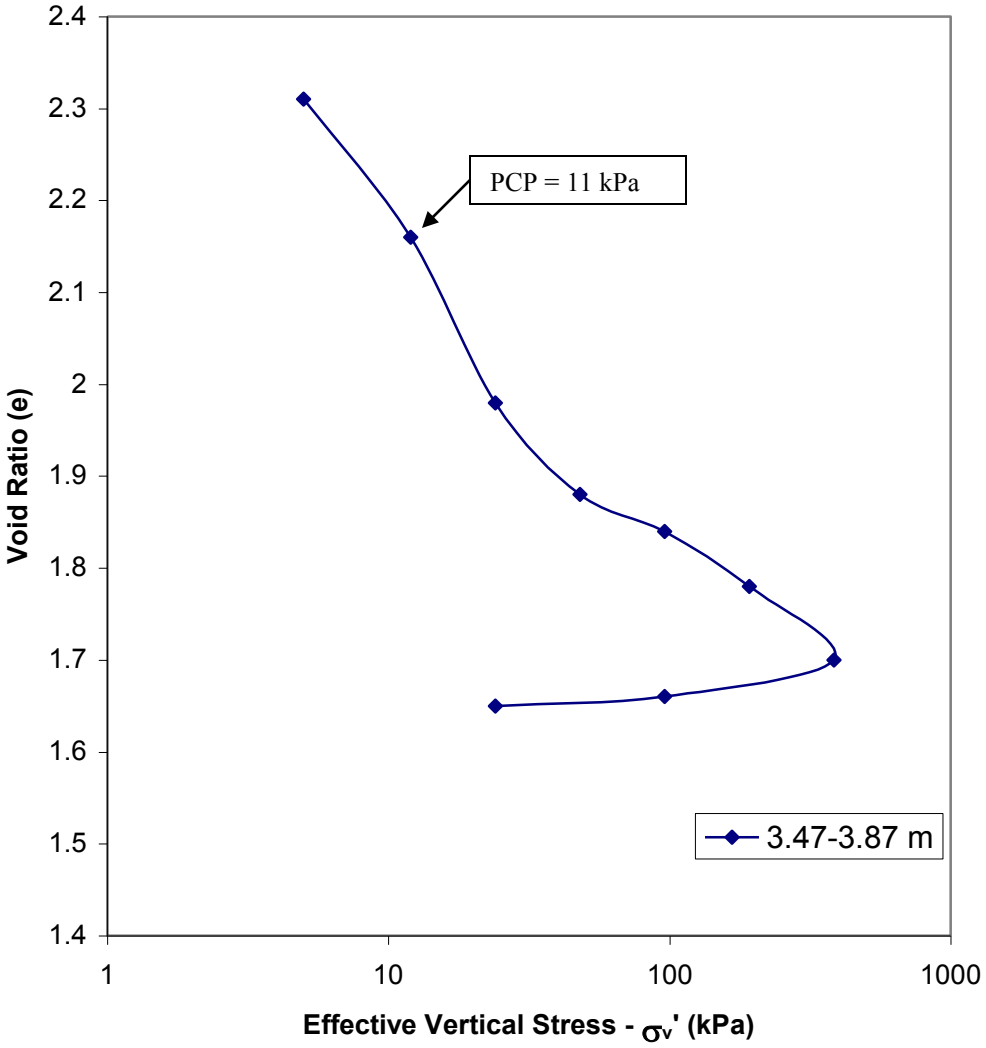

Figure B.32: Pressure versus void ratio plot for borehole 47D

Table B.32: Test results for borehole 47D

Av. Pressure (kPa)	8.5	18	36	72	144	288
m_v (m^2/MN)	8.56	3.61	1.3	0.42	0.21	0.13
c_v (m^2/year)	0.3	0.2	0.42	0.68	5.58	6.85
Description: Sandy Silt (MH)						

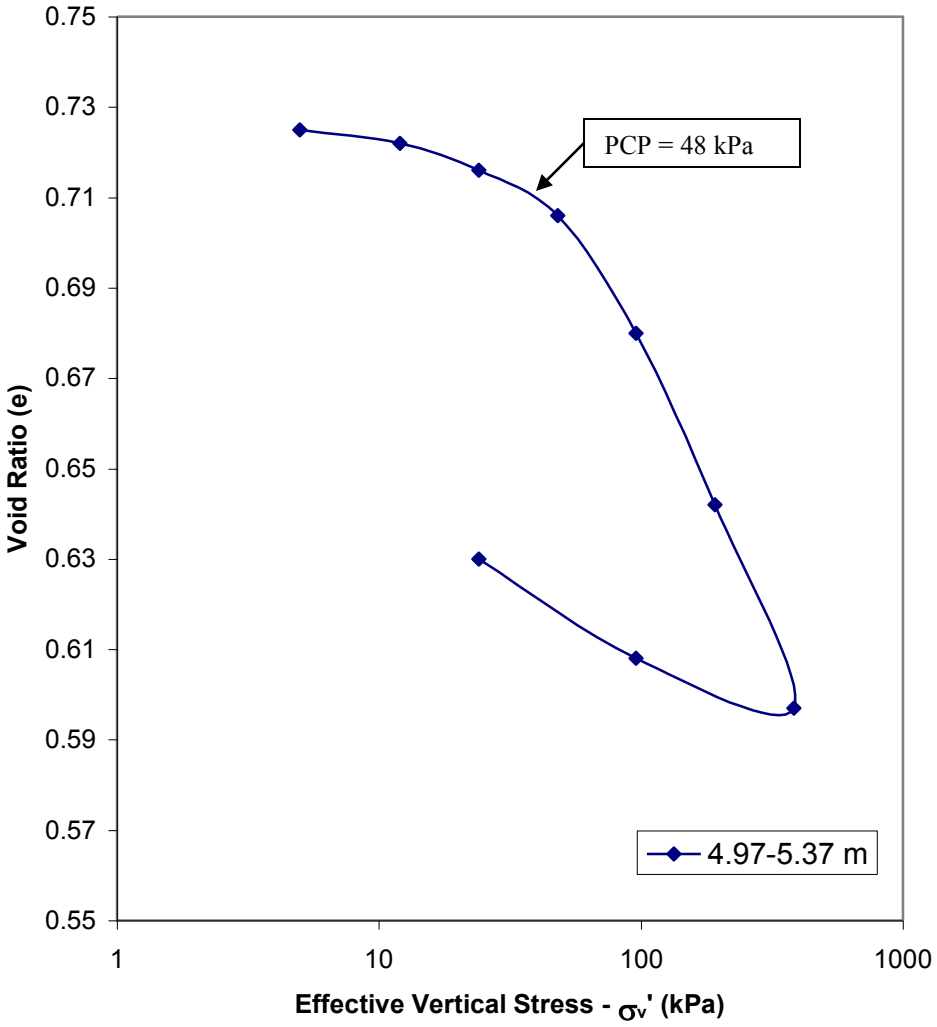

Figure B.33: Pressure versus void ratio plot for borehole 47F

Table B.33: Test results for borehole 47F

Av. Pressure (kPa)	8.5	18	36	72	144	288
m_v (m^2/MN)	0.25	0.34	0.29	0.28	0.24	0.14
c_v (m^2/year)	0.465	0.285	0.488	0.399	0.364	0.365
Description: Silty Sandy Clay (CL)						

Table B.34: Summary of test results for Sunshine Motorway

HOLE No.	LOCATION/ DEPTH (m)	w_n (%)	WET DENSITY (t/m^3)	DRY DENSITY (t/m^3)	w_L (%)	I_p (%)	C_c	ORGANIC CONTENT (%)	SPECIMEN DESCRIPTION / (UNIFIED SOIL CLASSIFICATION)
3R	15.75-16.15	36.2	1.82	1.34					SL SANDY CLAY
4N	9.25-9.70	76.8	1.52	0.86			0.1837		SANDY SILT (MH)
4N	9.25-9.70	77.6	1.52	0.86	61.2	23.6		14.5	SANDY SILT (MH)
4U	15.0-15.6	50.4	1.72	1.14	24.6	7			CLAYEY SILTY SAND (SC)
4W	16.75-17.2	60	1.6	1					CLAY TO CLAYEY SAND
5AD	1.5-1.9	70.2			45.2	22.6		7.05	SILTY SANDY CLAY (CL)
5AF	2.3-2.7	21.9	2	1.64	23	11	0.087201		CLAYEY SAND (SC)
9AE	1.6-2.0	43.4			38.2	20.6	0.211555		SILTY CLAYEY SAND (SC)
10B	1.5-1.9				43.6	20.8			SL SANDY CLAY (SC)
11B	1.5-2.0	111.2	1.46	0.7			1.394666		CLAYEY SILT
11B	1.5-2.0	120.6	1.42	0.64					CLAYEY SILT
11B	1.5-2.0	125.2	1.36	0.6					CLAYEY SILT
11F	4.5-4.9	21.2	2.1	1.74	29.4	15.4			SL SANDY CLAYEY SILT (ML)
11H	6.0-6.4	19.8	1.1	0.92	24	9			SANDY CLAYEY SILT (ML)
11K	7.5-5.9	24.8	2	1.6	73	24			SILTY CLAY (CH)
11R	12.0-12.4	42.2	1.76	1.24					SILTY CLAY
12C	2.25-2.65	126.8	1.4	0.62			1.199998	10.2	SILTY CLAY
12C	2.25-2.65	122.8	1.38	0.62	76	49.4			SILTY CLAY
12C	2.25-2.65	97.8							SILTY CLAY
12E	3.75-4.15	83.4	1.48	0.82	37	21.6		5.25	SL SANDY CLAYEY SILT (ML)
12E	3.75-4.15	57.4							SL SANDY CLAYEY SILT (ML)
13D	5.25-5.7	16.4	2.18	1.88					SANDY CLAY
13BC	1.6-2.4	79.8			48.6	25.4			SANDY SILTY CLAY (CL)
13BC	1.6-2.4	72.6	1.58	0.92					SANDY SILTY CLAY (CL)
13BD	2.4-3.2	55.2	1.92	1.24	55.8	28.4			SANDY SILTY CLAY (CL)
13BE	3.2-4.0	64.6	1.6	0.98	57.2	29.6			SL SANDY SILTY CLAY (CH)

14K	12.75-13.1	29.2	1.96	1.52					SILTY CLAY
14P	15.75-16.15	29	1.94	1.52					SL SANDY SILTY CLAY (CH)
16D	3.0-3.4	76.2	1.52	0.86	75	44			SILTY CLAY (CH)
17B	3.2-3.65	90.6	1.46	0.76	62.6	34			SILTY CLAY (CH)
17J	13.7-14.15	48.8	1.72	1.16	43	18			CLAY (CL)
18AA	1.0-1.5	40.5	1.78	1.26	41	18.6			CLAY (CL)
19A	0.0-0.8	33.2	1.82	1.36	61.4	45.4			SILTY SAND (SM)
19B	0.8-1.6	93.6	1.5	0.78	30.2	6.2			SL CLAYEY SANDY SILT (ML)
19C	1.6-2.4	106	1.42	0.7	68	41.2			SL SANDY SILT (MH)
19D	2.4-3.2	119.6	1.4	0.64	79.2	46.6			SL CLAYEY SILT (MH)
19E	3.2-4.0	84.8	1.54	0.84	61.6	33.8			SL CLAYEY SILT (MH)
19F	4.0-4.8	97.2	1.48	0.74	72.4	41.6			CLAYEY SILT (MH)
19G	4.8-5.6	84.8	1.5	0.82	67.4	37.6			CLAYEY SILT (MH)
19H	5.6-6.4	86.2	1.52	0.82	65.8	36.6			CLAYEY SILT (MH)
20A	0.2-1.0	64.4	1.64	1	36.8	20.6			SILTY CLAYEY SAND (CL)
20B	1.0-1.8	93.4	1.48	0.76	60.6	35.2			SANDY SILTY CLAY (CH)
20C	1.8-2.6	103.2	1.44	0.72	64.4	40			SANDY SILTY CLAY (CH)
20D	2.6-3.4	109.2	1.42	0.68	75.2	45.6			SANDY SILTY CLAY (CH)
20E	3.4-4.2	124	1.38	0.62	80.2	49.8	0.980217		SILTY CLAY (CH)
20E	3.4-4.2	121	1.44	0.64			0.729831		SILTY CLAY (CH)
20E	3.4-4.2	125.6	1.4	0.62					SILTY CLAY (CH)
20F	4.2-5.0	89.2	1.5	0.8	68.8	39			SILTY CLAY (CH)
20G	5.0-5.8	85.8	1.52	0.82	73.4	44.2			SILTY CLAY (CH)
20H	5.8-6.6	78.8	1.54	0.86	65.4	39.4			SILTY CLAY (CH)
20J	6.6-7.4	88	1.52	0.8	66.8	37			SILTY CLAY (CH)
20K	7.4-8.2	94.4	1.48	0.76	67.4	36.2			SILTY CLAY (CH)
20L	8.2-9.0	81.8	1.54	0.84	64.8	39.4			CLAYEY SILT (MH)
20M	9.0-9.8	73.6	1.52	0.88	60	32.8			CLAYEY SILT (MH)
20N	9.8-10.6	68.6	1.6	0.96	68.2	37.8			SILTY CLAY (CH)
22B	0.9-1.4	50.8	1.68	1.1	37.2	19		5.3	SANDY CLAY (CL)
22C	1.4-1.8				44	27	0.498289		CLAYEY SILTY SAND (SM)

22C	1.4-1.8	84	1.52	0.84					CLAYEY SILTY SAND (SM)
22C	1.4-1.8	64.6	1.646	1					CLAYEY SILTY SAND (SM)
22D	1.8-2.3	90.4			55.4	27.8			CLAY (CH)
22E	2.3-2.7				67	35.4	1.442448		CLAYEY SILTY SAND (SM)
22E	2.3-2.7	125.4	1.36	0.6					CLAYEY SILTY SAND (SM)
22E	2.3-2.7	124	1.38	0.62					CLAYEY SILTY SAND (SM)
22F	2.7-3.2				109	79.8	0.963359		CLAY (CH)
22F	2.7-3.2	119.6	1.4	0.64					CLAY (CH)
22F	2.7-3.2	85.6	1.37	0.74					CLAY (CH)
22G	3.2-3.6	128.8	1.34	0.58	74	40.4		10.7	CLAY (CH)
22H	3.6-4.0	103.2			93	55			CLAY (CH)
22J	4.0-4.4				77.8	45.4	1.420124		SANDY SILTY CLAY (CH)
22J	4.0-4.4	120.4	1.38	0.62					SANDY SILTY CLAY (CH)
22J	4.0-4.4	125	1.4	0.62					SANDY SILTY CLAY (CH)
22J	4.0-4.4	130.8	1.36	0.58					SANDY SILTY CLAY (CH)
22K	4.9-5.3	87.8			65.8	31			CLAY (CH)
22L	6.1-6.5	71.4	1.6	0.94	59.6	31.4			SILTY CLAY (CH/MH)
22M	6.8-7.2				60.2	33.4	0.632405		CLAYEY SILT (CH/MH)
22M	6.8-7.2	71.8	1.54	0.9					CLAYEY SILT (CH/MH)
22M	6.8-7.2	74	1.6	0.92					CLAYEY SILT (CH/MH)
22N	7.7-8.1	63			55	25.2			CLAY (CH)
22P	8.4-8.8				61	30.6	0.564728		CLAYEY SILT (CH/MH)
22P	8.4-8.8	60.8	1.64	1.02					CLAYEY SILT (CH/MH)
22P	8.4-8.8	60.6	1.64	1.02					CLAYEY SILT (CH/MH)
22P	8.4-8.8	57.8	1.63	1.03					CLAYEY SILT (CH/MH)
23B	1.0-1.5	62.4	1.64	1.02	31.6	17	0.60655		CLAYEY SILTY SAND (SM/SC)
23B	1.0-1.5	75.4	1.5	0.86					CLAYEY SILTY SAND (SM/SC)
23C	1.5-1.9	59	1.64	1.04	49	35	0.539813		SANDY CLAY (CH)
23C	1.5-1.9	62.4	1.58	0.97					SANDY CLAY (CH)
24A	0.5-0.9	61.4	1.6	1	24	5.2	0.138208		CLAYEY SILTY SAND (SC)
24A	0.5-0.9	36	1.84	1.36					CLAYEY SILTY SAND (SC)

24B	0.9-1.4	114	1.64	0.76	45	27.4	0.673797		SILTY CLAYEY SAND (SC)
24B	0.9-1.4	67.1	1.58	0.94				6.2	SILTY CLAYEY SAND (SC)
24C	1.4-1.8				32.8	16.4			SILTY CLAYEY SAND (SC)
25A	0.5-0.9							4.95	SILTY CLAYEY SAND (SC)
25C	1.3-1.7	42.6	1.78	1.24	25	6	0.37796		SILTY CLAYEY SAND (SP)
25C	1.3-1.7	43.2							SILTY CLAYEY SAND (SP)
25E	2.4-2.8	79.4	1.52	0.84	39	18.8		8.7	SILTY CLAYEY SAND (SC)
26A	0.75-1.15	85.4			65	30.4			SILTY CLAY
26B	1.5-1.9	106.2	1.44	0.7	72.2	44	1.069886		CLAYEY SILT (CH/MH)
26B	1.5-1.9	106.2	1.56	0.76					CLAYEY SILT (CH/MH)
26B	1.5-1.9	89.8							CLAYEY SILT (CH/MH)
26C	2.0-2.4	95.8							SILTY CLAY
26D	2.4-2.9	78.8			60.6	34.8			SILTY CLAY
26E	3.0-3.4	21							SILTY SAND
26F	4.0-4.4	29			57	35.8			SANDY CLAY
27A	0.75-1.15	84.4			66.6	38.2			SILTY CLAY
27C	2.0-2.4	125.8	1.38	0.6			1.345381		SILTY CLAY (CH)
27C	2.0-2.4	116.1	1.35	0.62	130	99			SILTY CLAY (CH)
27D	2.5-2.9	107.6			79.4	44.8			SILTY CLAY
27E	3.0-3.4	98.2			73	41.6			SILTY CLAY
27F	3.5-3.9	77.8			64.6	35.6			SILTY CLAY
27G	4.0-4.4	162.8	1.28	0.48			1.051944		SL SANDY SILTY CLAY (CH)
27G	4.0-4.4	102.4	1.42	0.7					SL SANDY SILTY CLAY (CH)
27G	4.0-4.4	107.2	2.84	1.37	123	93			SL SANDY SILTY CLAY (CH)
27J	5.0-5.4	51.6			55.4	31.2			SL SANDY SILTY CLAY
27K	6.0-6.4	32.8			53.6	30			SL SANDY SILTY CLAY
27L	7.0-7.4	22.8	2	1.64	46.6	27.8			CLAYEY SILT (SL/ML)
27L	7.0-7.4	24.4							CLAYEY SILT (SL/ML)
29A	0.6-1.2	77	1.52	0.86	63.4	37.2			SILTY CLAY
29B	1.2-2.0	117.6	1.42	0.66	72.8	45.2			SILTY CLAY
29C	2.0-2.6	126.6	1.38	0.62	77.8	48	1.262333		SILTY CLAY (CH)

29C	2.0-2.6	116	1.41	0.65					SILTY CLAY (CH)
29D	2.6-3.4	96.4	1.48	0.76	71.6	36.8			SILTY CLAY
29E	3.5-4.3	60.2	1.6	1	37	13.6			CLAYEY SANDY SILT (ML)
29F	4.3-5.1	28.2	1.92	1.5	42.8	22.4			SANDY SILTY CLAY (CL)
30A	0.7-1.1	69	1.56	0.92	58.6	29.6			SANDY SILTY CLAY (CH)
30B	1.1-1.9	90.8	1.44	0.76	66.2	34.8			SANDY SILTY CLAY (CH)
30C	1.9-2.7	128.6	1.36	0.6	78.2	46.6			SILTY CLAY
30D	2.7-3.5	104.2	1.46	0.72	73	44.2			SILTY CLAY
30E	3.5-4.3	132.4	1.36	0.58	72	39.2	0.772348		SILTY CLAY (CH)
30E	3.5-4.3	83	2.78	1.52					SILTY CLAY (CH)
30F	4.3-4.9	18.4			12.8	2.4			SANDY CLAY
30G	4.9-5.4	17.4	2.16	1.84	17.8	7.4			SANDY CLAY
37B	2.9-3.3	116.4			77.8	44.2			SILTY CLAY
37D	5.9-6.3				71.2	39.6			SILTY CLAY (CH)
37E	7.4-7.8	89.6			69	37.2			SILTY CLAY
44A	0.75-1.15	83.4			65.2	41.4			SANDY SILTY CLAY (CH)
44B	1.5-1.9	99.8			70.2	39.4			SANDY SILTY CLAY (CH)
44B	1.5-1.9	95	1.48	0.76					SANDY SILTY CLAY (CH)
44C	2.25-2.65	88.2			67.8	41.2			SL SANDY SILTY CLAY (CH)
44C	2.25-2.65	100.2	1.44	0.72					SL SANDY SILTY CLAY (CH)
44D	3.0-3.4	97.4			75.2	46			CLAYEY SILT (MH)
44D	3.0-3.4	79.6	1.44	0.8					CLAYEY SILT (MH)
44E	3.5-3.95	86.4			65.6	39.4			SL SANDY CLAYEY SILT (MH)
44E	3.5-3.95	87.6	1.5	0.8					SL SANDY CLAYEY SILT (MH)
44F	4.0-4.5	35.8			40	21.6			SL SANDY CLAYEY SILT (MH)
44F	4.0-4.5	45.4	1.74	1.2					SL SANDY CLAYEY SILT (MH)
45A	0.75-1.15	59			68	40	0.250406		SILTY CLAY (CH)
45A	0.75-1.15	66.8	1.6	0.96					SILTY CLAY (CH)
45A	0.75-1.15	63	1.5	0.92					SILTY CLAY (CH)
45B	1.5-1.9	94			63	34.6	1.834402		SILTY CLAY (CH)
45B	1.5-1.9	93.2	1.48	0.76					SILTY CLAY (CH)

45B	1.5-1.9	88.4	1.42	0.76					SILTY CLAY (CH)
45C	2.25-2.65	96.6			59.4	33.4	0.761245		SANDY SILTY CLAY (CH)
45C	2.25-2.65	99	1.46	0.74					SANDY SILTY CLAY (CH)
45C	2.25-2.65	82.2	1.46	0.8					SANDY SILTY CLAY (CH)
45D	3.0-3.4	70.4			71	39.4	1.793991		CLAYEY SILT (MH)
45D	3.0-3.4	92	1.48	0.78					CLAYEY SILT (MH)
45D	3.0-3.4	93	1.4	0.72					CLAYEY SILT (MH)
45E	3.75-4.15	27.2			38.4	21.2			CLAYEY SILT (ML)
45E	3.75-4.15	52.6	1.66	1.08					CLAYEY SILT (ML)
45F	4.5-4.9	26.4			38.4	19.8			CLAYEY SILT (ML)
45F	4.5-4.9	24.6	1.98	1.58					CLAYEY SILT (ML)
46A	0-0.4	20.8			53.2	20.6			SANDY SILTY CLAY (MH-CH)
46A	0-0.4	32.6	1.8	1.36					SANDY SILTY CLAY (MH-CH)
46B	0.4-0.8	58.2			68.2	25.4		14.95	CLAYEY SILT (MH)
46C	0.8-1.2	65			59	22.6			CLAYEY SILT (MH)
46D	1.2-1.6	118.6			70.8	36.2			SANDY SILTY CLAY (CH)
46D	1.2-1.6	113.2	1.42	0.66					SANDY SILTY CLAY (CH)
46D	1.2-1.6								SANDY SILTY CLAY (CH)
46E	1.6-2.0	87.6			51.2	25.6	0.697691	7.4	SANDY SILTY CLAY (CH)
46E	1.6-2.0	86.8	1.42	0.76					SANDY SILTY CLAY (CH)
46F	2.25-2.65	121.4			84.6	42.6	1.96395		SILTY CLAY (CH)
46F	2.25-2.65	123.4	1.38	0.62					SILTY CLAY (CH)
46F	2.25-2.65	118.8	1.28	0.58					SILTY CLAY (CH)
46G	2.65-3.05	134.2			80.2	45.2		11.15	SILTY CLAY (CH)
46G	2.65-3.05	126.6	1.4	0.62					SILTY CLAY (CH)
47B	1.97-2.37	133			78.6	45.2	1.162675		CLAYEY SILT (MH)
47B	1.97-2.37	127.8	1.38	0.62					CLAYEY SILT (MH)
47B	1.97-2.37	108.5	1.3	0.63					CLAYEY SILT (MH)
47C	2.72-3.12	111.8			75	42.6	1.021493		SILTY CLAY (CH)
47C	2.72-3.13	101.4	1.48	0.74					SILTY CLAY (CH)
47C	2.72-3.14	98.3	1.35	0.68					SILTY CLAY (CH)

47D	3.47-3.87	143	1.3	0.54	59.8	29.8	0.232535	11.3	SL SANDY SILT (MH)
47D	3.47-3.87	86.9	1.38	0.737					SL SANDY SILT (MH)
47E	4.22-4.62	21.6	2.08	1.72	31	16.4			SAND, SILT, CLAY MIXTURE
47F	4.97-5.37	29	1.94	1.5	40	24.4	0.120697		SANDY CLAY (CL)
47F	4.97-5.38	22.9	1.83	1.49					SANDY CLAY (CL)
47G	5.72-6.12	30			62.2	37.4			SILTY CLAY (CH)
47G	5.72-6.13	28.8	1.96	1.52					SILTY CLAY (CH)
47H	6.47-6.87	20.8			25.8	8.2			CLAYEY SILT (MH)
47H	6.47-6.88	19.4	2.08	1.74					CLAYEY SILT (MH)
47K	8.72-9.12	31.8			69.4	40.6			SILTY CLAY (CH)
49M	14.5-14.9	37.8			72.8	45.2			CLAY (CH)
51A	1.28-1.68	56.2			69.2	23			SILTY CLAY (CH)
52A	1.3-1.7	26.8	1.96	1.54					SILTY CLAY
52B	2.05-2.45	27.2	1.96	1.54	48.6	24.2			SL SANDY SILTY CLAY (CH-ML)
53A	1.29-1.69	78.2			60.4	31.8			SL SANDY CLAYEY SILT (MH)
53A	1.29-1.69	77	1.54	0.86					SL SANDY CLAYEY SILT (MH)
53B	2.04-2.44	111.6			63.2	32.4			SL SANDY SILTY CLAY (CH)
53B	2.04-2.44	107.6	1.46	0.7					SL SANDY SILTY CLAY (CH)
53C	2.79-3.19	129.4			99	36.4			SL SANDY CLAYEY SILTY (MH)
53C	2.79-3.19	156.2	1.3	0.5					SL SANDY CLAYEY SILTY (MH)

79.24737	1.584193	0.930348	60.12562	33.09091	0.848056	9.05	<- Average
162.8	2.84	1.88	130	99	1.96395	14.95	<- Max
16.4	1.1	0.48	12.8	2.4	0.087201	4.95	<- Min
83.7	1.52	0.82	63.2	34.8	0.761245	8.7	<- Median
190	135	135	121	121	33	13	<-No. sample
34.23466	0.259072	0.331565	19.42858	14.6403	0.515919	3.261783	<- Standard Deviation

APPENDIX C - PORT BRISBANE MOTORWAY

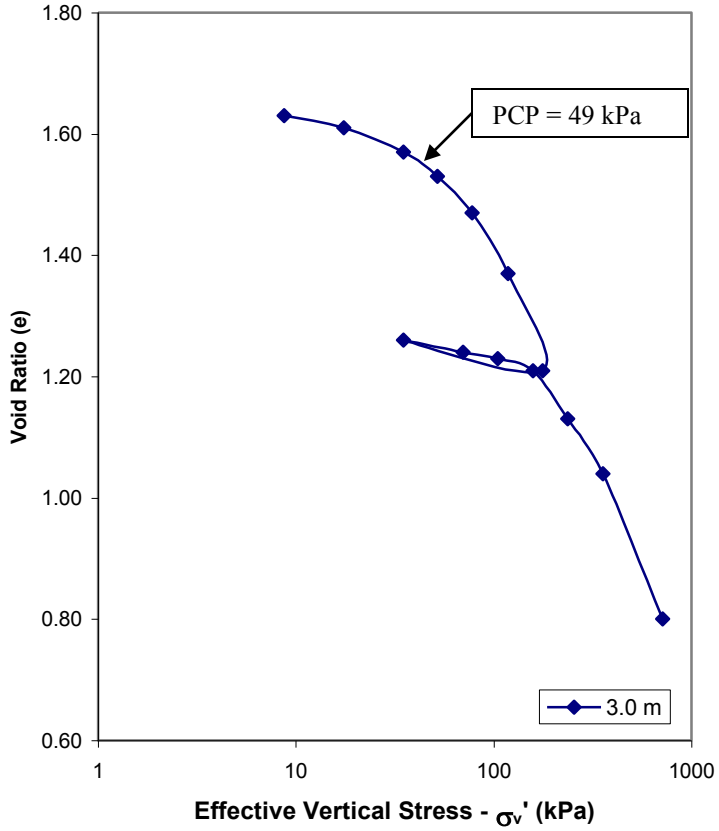

Figure C.1: Pressure versus void ratio plot for borehole 127B

Table C.1: Test results for borehole 127B

Av. Pressure (kPa)	4.4	13.1	26.2	43.4	64.9	97.9	147.4	296.6	534.0
m_v (m^2/MN)	1.16	0.81	0.78	0.84	0.87	0.98	0.97	0.50	0.24
c_v (m^2/year)	7.7	10.9	10.6	5.8	3.6	2.3	1.1	0.6	0.8
Description: Dark Grey Clay									

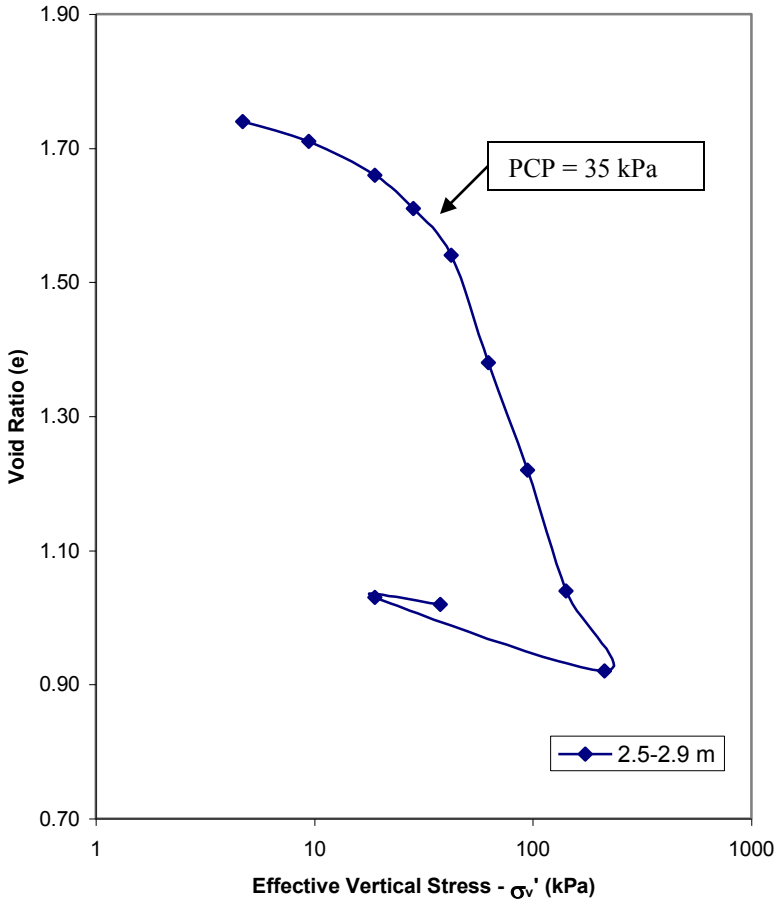

Figure C.2: Pressure versus void ratio plot for borehole 114

Table C.2: Test results for borehole 114

Av. Pressure (kPa)	2.4	7.1	14.2	23.6	35.4	52.5	78.4	118.2	177.7
m_v (m^2/MN)	1.13	2.17	1.94	1.76	1.95	2.33	2.53	1.45	0.89
c_v (m^2/year)	5.0	2.4	1.7	1.2	0.9	0.3	0.1	0.2	0.1
Description: Dark Grey Clay									

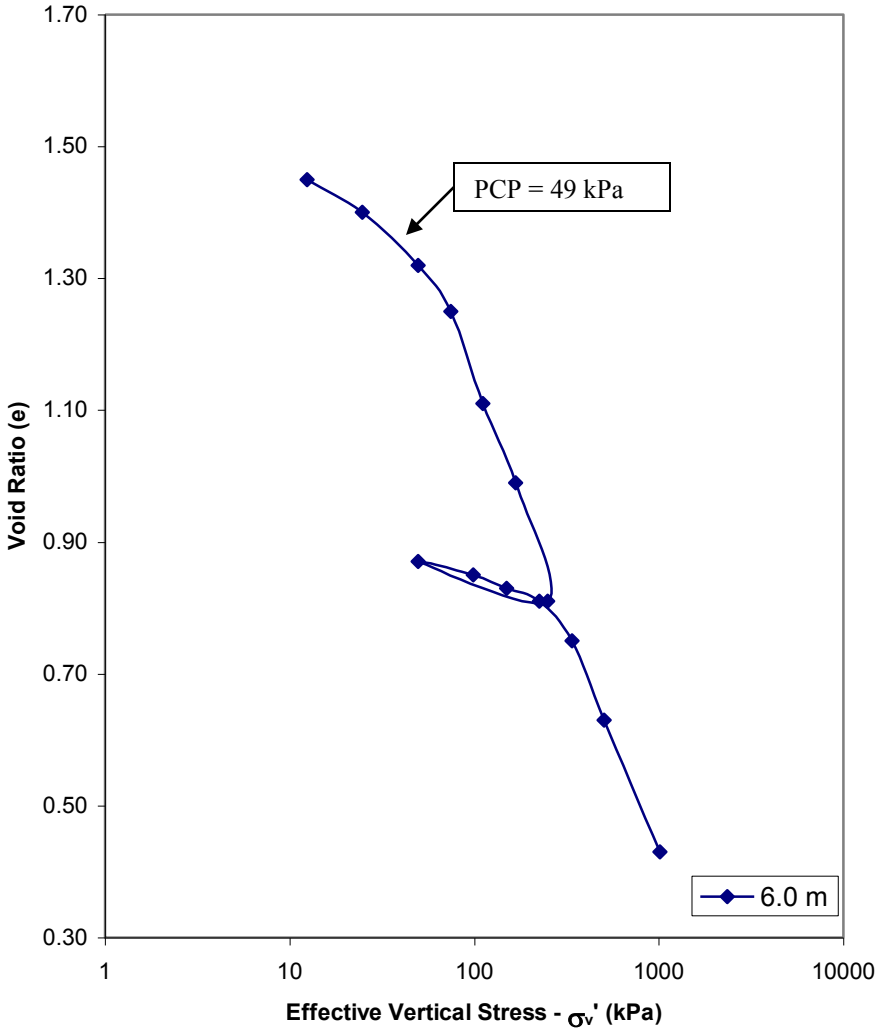

Figure C.3: Pressure versus void ratio plot for borehole 127D

Table C.3: Test results for borehole 127D

Av. Pressure (kPa)	6.2	18.6	37.2	62.0	92.7	139.3	208.9
m_v (m^2/MN)	2.47	1.77	1.09	1.45	1.49	1.26	0.79
c_v (m^2/year)	20.6	12.0	11.4	3.2	1.1	0.6	0.5
Description: Grey Sandy Clay							

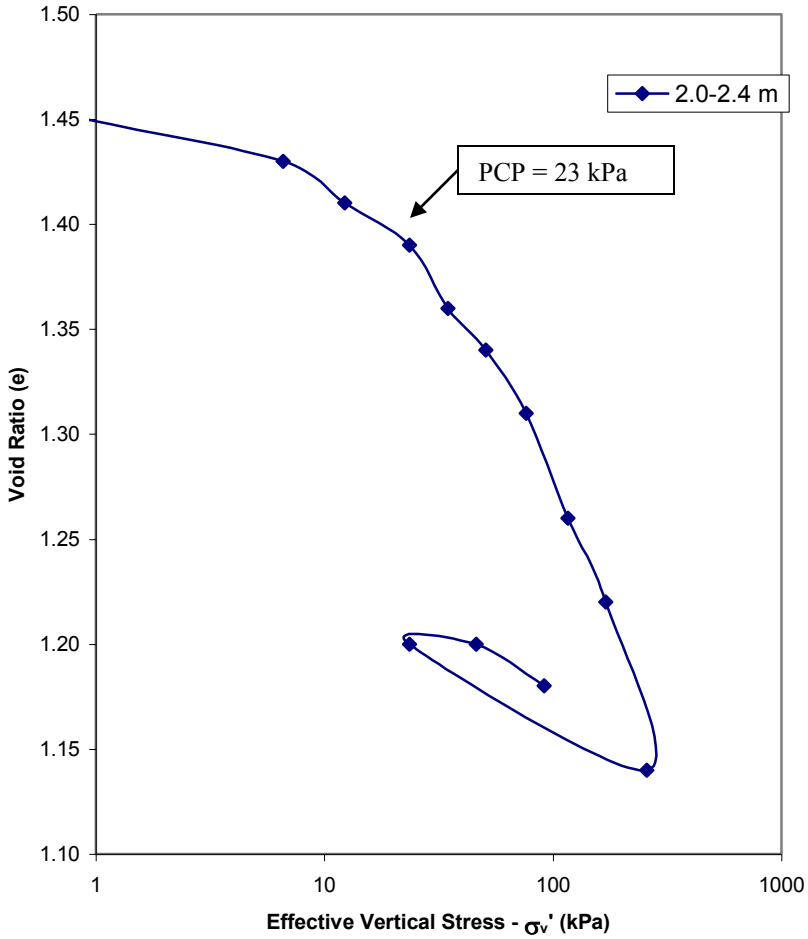

Figure C.4: Pressure versus void ratio plot for borehole 139B

Table C.4: Test results for borehole 139B

Av. Pressure (kPa)	3.8	9.4	17.9	29.2	42.9	63.6	96.4
m_v (m^2/MN)	0.85	1.13	0.91	0.97	0.62	0.44	0.37
c_v (m^2/year)	100.6	50.3	68.0	10.6	11.9	54.1	89.0
Description: Dark Grey Silty Clay							

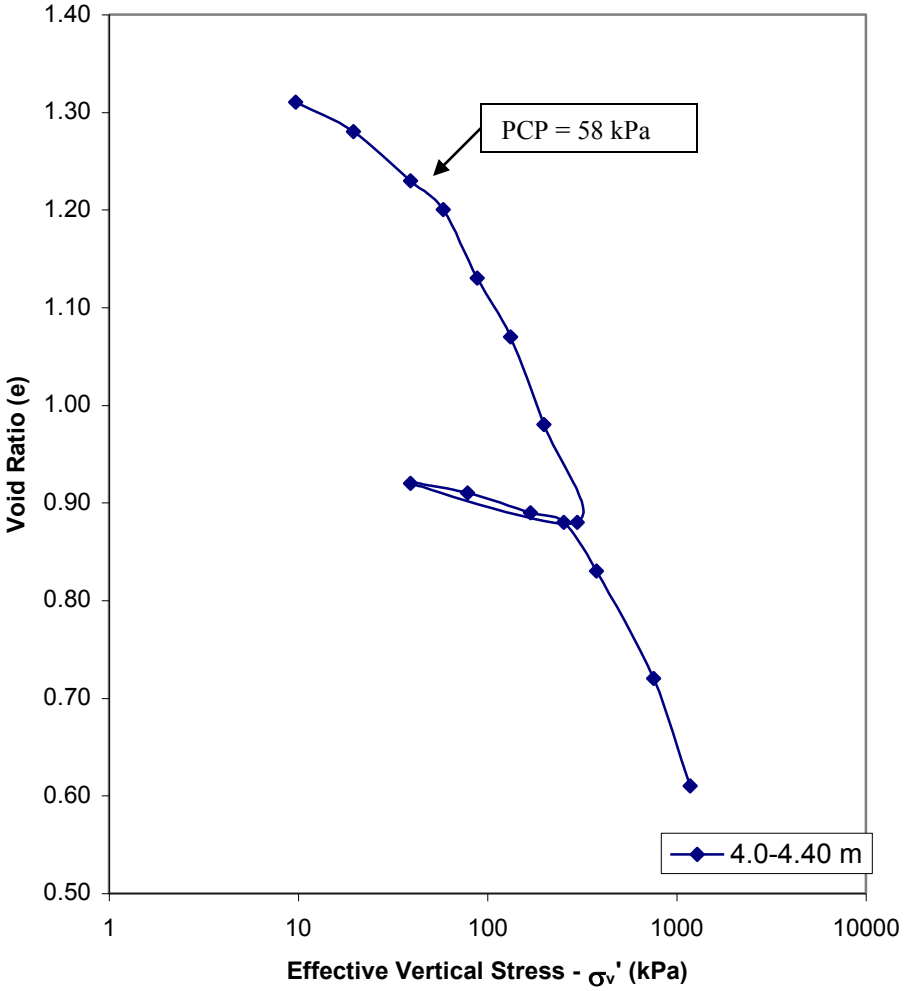

Figure C.5: Pressure versus void ratio plot for borehole 139D

Table C.5: Test results for borehole 139D

Av. Pressure (kPa)	4.9	14.7	29.4	48.9	73.4	110.3	165.3	315.2	566.6
m_v (m^2/MN)	0.99	1.25	0.95	0.78	0.68	0.64	0.65	0.13	0.16
c_v (m^2/year)	39.0	49.6	19.5	35.6	22.0	129.6	30.2	11.2	14.8
Description: Grey Sandy Clay									

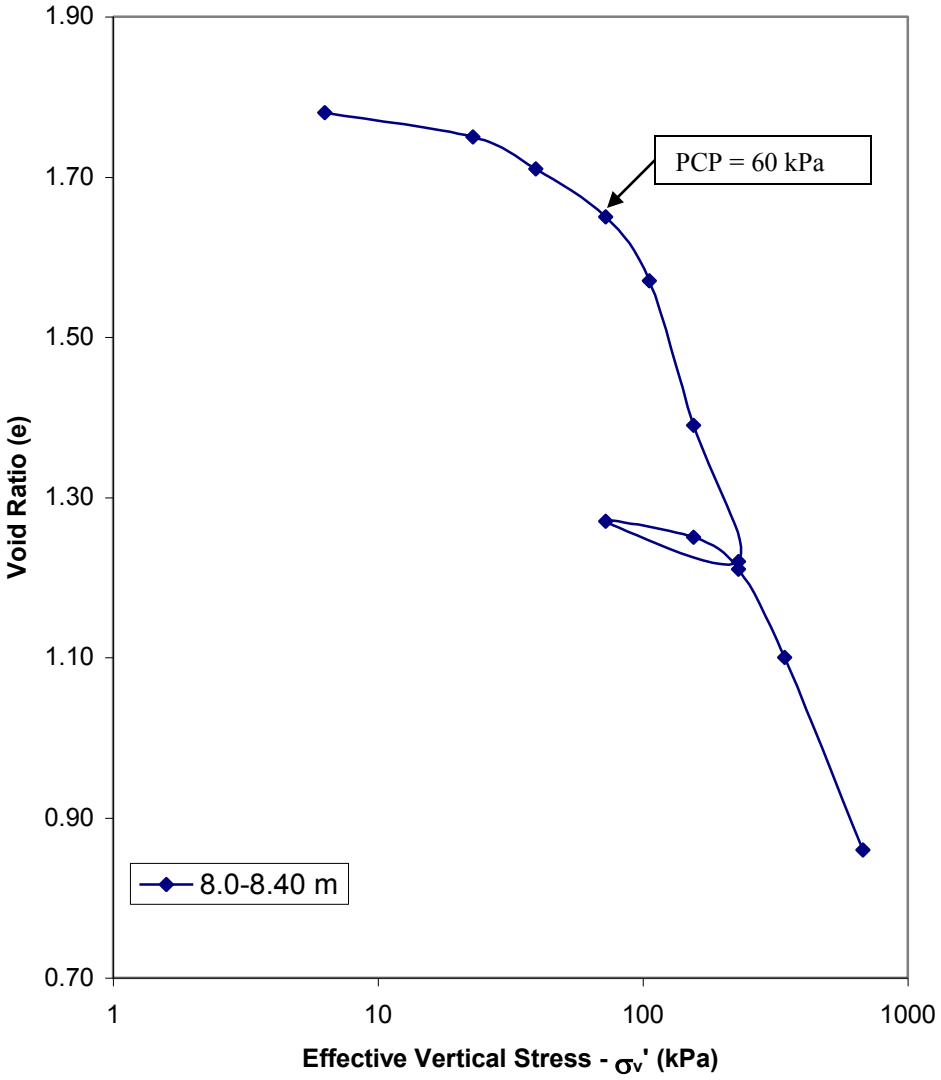

Figure C.6: Pressure versus void ratio plot for borehole 139H

Table C.6: Test results for borehole 139H

Av. Pressure (kPa)	14.6	31.1	56.0	89.1	130.5	192.5	285.9	509.5
m_v (m^2/MN)	0.42	0.84	0.75	0.90	1.23	1.00	0.47	0.35
c_v (m^2/year)	19.9	1.6	1.5	0.7	0.3	0.2	0.3	0.1
Description: Dark Grey Clay								

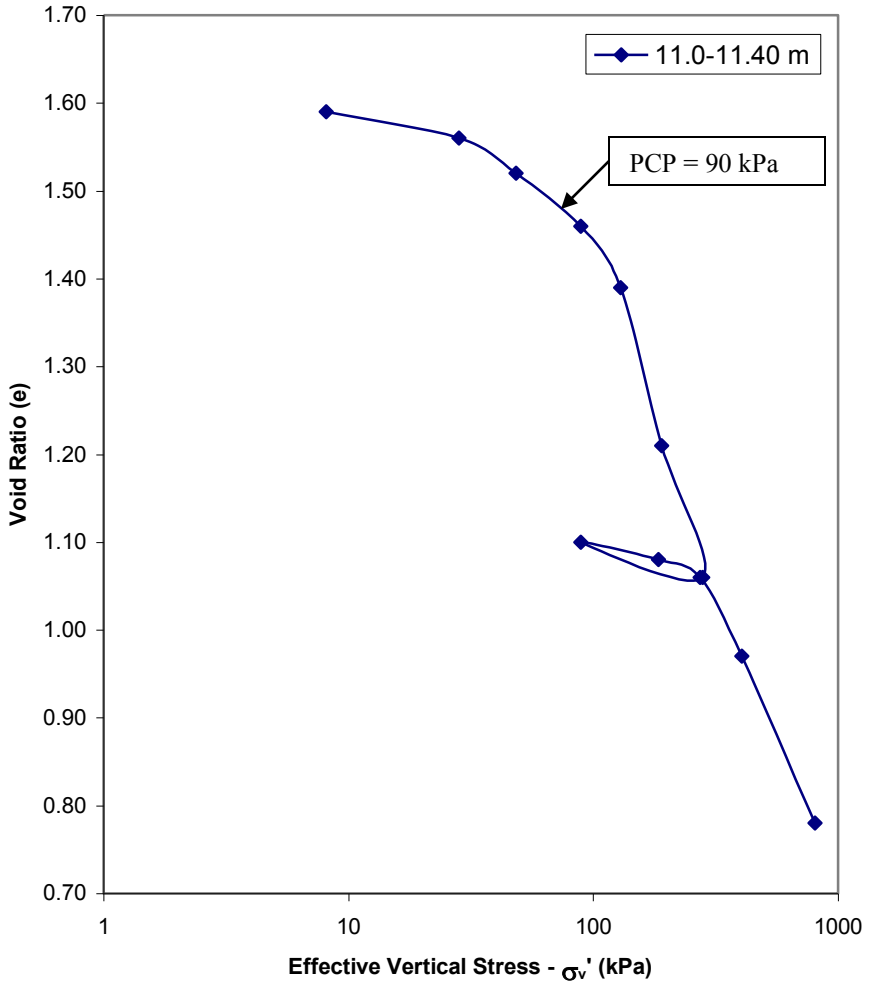

Figure C.7: Pressure versus void ratio plot for borehole 139L

Table C.7: Test results for borehole 139L

Av. Pressure (kPa)	18.2	38.4	68.7	109.2	159.7	235.3	339.4	604.1
m_v (m^2/MN)	0.55	0.64	0.56	0.69	1.18	0.73	0.29	0.24
c_v (m^2/year)	2.0	1.5	1.7	0.8	0.3	0.3	0.3	0.1
Description: Dark Grey Clay								

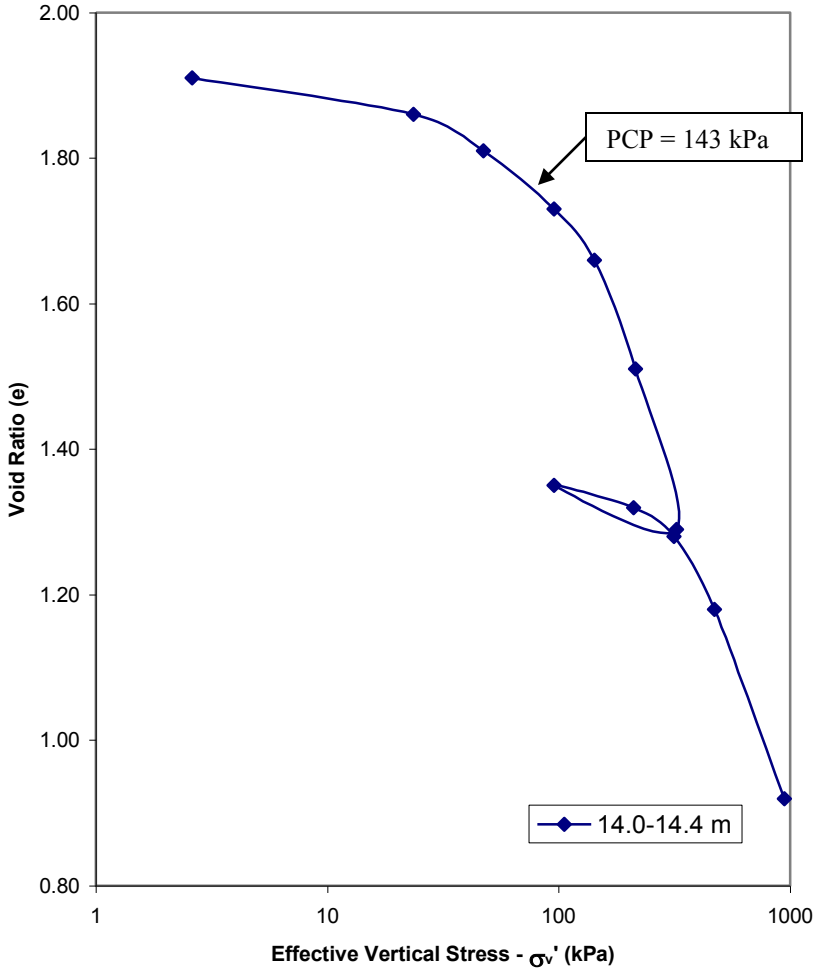

Figure C.8: Pressure versus void ratio plot for borehole 139P

Table C.8: Test results for borehole 139P

Av. Pressure (kPa)	13.1	35.4	71.4	119.4	179.0	269.1	393.1	707.0
m_v (m^2/MN)	0.63	0.85	0.58	0.56	0.72	0.66	0.28	0.19
c_v (m^2/year)	3.7	1.0	1.1	0.8	0.4	0.3	0.3	0.4
Description: Dark Grey Clay								

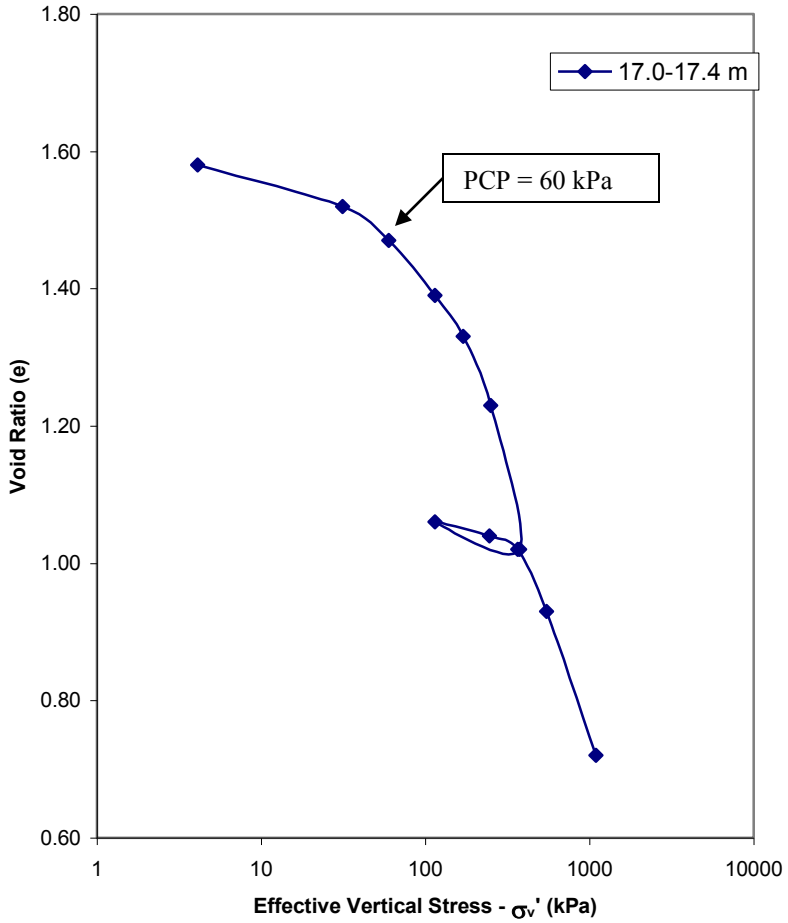

Figure C.9: Pressure versus void ratio plot for borehole 139S

Table C.9: Test results for borehole 139S

Av. Pressure (kPa)	17.7	45.5	86.9	141.9	210.5	313.9	456.4	818.3
m_v (m^2/MN)	0.45	1.03	0.50	0.46	0.62	0.57	0.23	0.18
c_v (m^2/year)	39.6	2.7	2.7	2.1	0.6	0.4	0.4	0.3
Description: Dark Grey Clay								

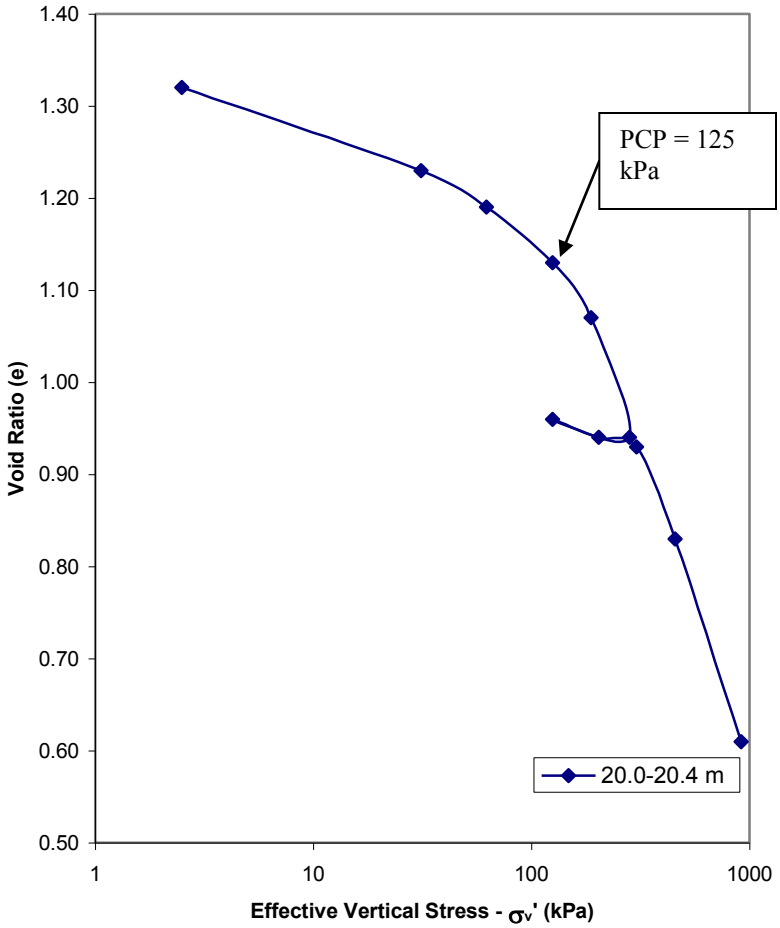

Figure C.10: Pressure versus void ratio plot for borehole 139U

Table C.10: Test results for borehole 139U

Av. Pressure (kPa)	16.9	46.8	93.6	156.5	234.6	380.7	685.3
m_v (m^2/MN)	0.83	0.94	0.38	0.47	0.47	0.36	0.20
c_v (m^2/year)	14.8	2.6	3.0	1.1	0.6	0.3	0.5
Description: Dark Grey Clay							

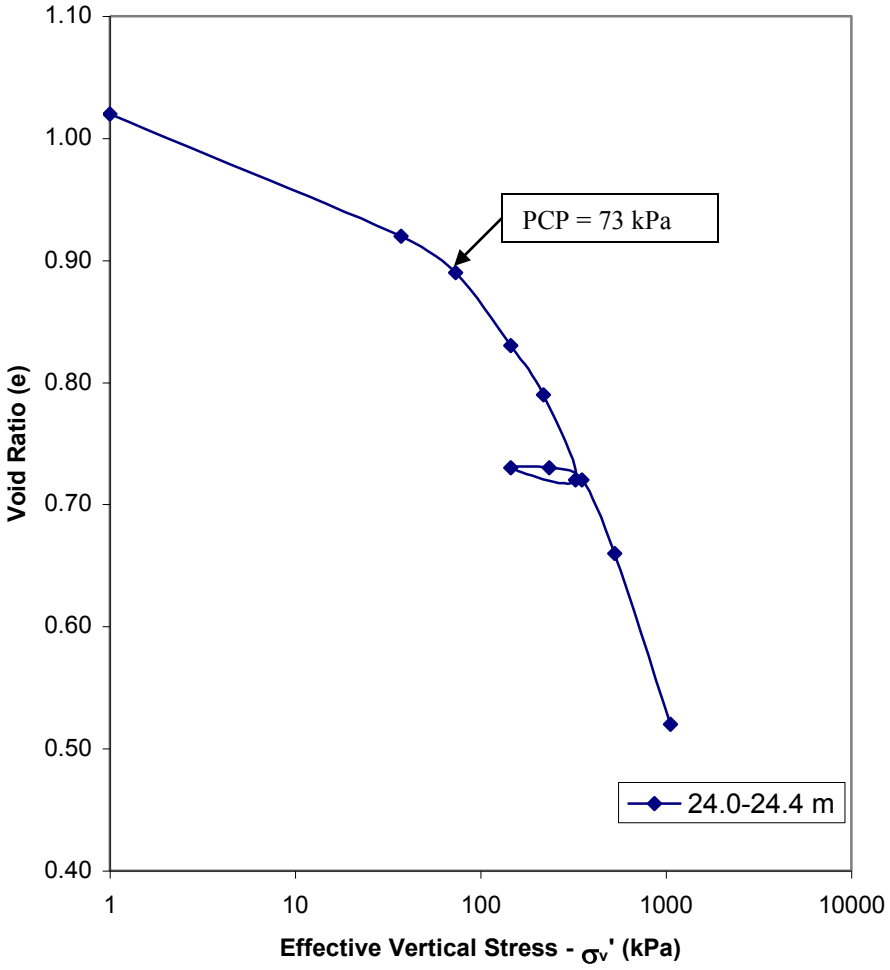

Figure C.11: Pressure versus void ratio plot for borehole 139AA

Table C.11: Test results for borehole 139AA

Av. Pressure (kPa)	19.2	55.3	109.5	181.9	272.2	441.2
m_v (m^2/MN)	1.17	0.59	0.34	0.33	0.29	0.16
c_v (m^2/year)	6.1	7.1	9.7	5.7	1.5	2.1
Description: Dark Grey Sandy Silty Clay						

Table C.12: Summary of test results for Port Brisbane Motorway

LAB NO. GS99 /	LOCATION/ DEPTH (m)	w_n (%)	WET DENSITY (t/m^3)	DRY DENSITY (t/m^3)	C_c	w_L (%)	I_p (%)	L.S. (%)	Description
546	2.5	63.8	1.56	0.96		70.6	43.4	18.4	
547	5.5	64.0	1.60	0.98		60.6	30.2	16.8	
548	8.5	71.0	1.54	0.90		80.4	44.8	21.0	
466	2.5-2.9	70.8	1.62	0.96		52.6	24.6	14.8	
467	6.5-6.9	63.6	1.64	1.00		55.9	29.2	16.2	
499	2.5-2.95	70.8	1.62	0.94		59.6	29.0	16.0	DARK GREY CLAY
499.A	2.5-2.95	75.6	1.56	0.88					
500	5.5-5.95								
501	8.5-8.95	81.6	1.52	0.84		74.6	36.8	19.0	DARK GREY CLAY
501.A	8.5-8.95	76.2	1.54	0.88					DARK GREY CLAY
502	11.5-11.95	73.8	1.54	0.88					DARK GREY CLAY
457	2.5-2.9	71.2	1.64	0.96	0.8834				
504	2.5	50.2	1.76	1.18		67.4	38.6	16.8	BROWN CLAY
504.A	2.5	53.4	1.70	1.10					BROWN CLAY
505	5.5	66.4	1.58	0.96		63.8	28.6	15.4	DARK GREY CLAY
505.A	5.5	70.4	1.56	0.92					DARK GREY CLAY
506	8.5	86.2	1.52	0.82		78.6	40.6	20.2	
458	2.5-2.9	98.6	1.48	0.74		35.8	14.8	9.8	
459	4.0-4.40	63.0	1.64	1.00		48.6	23.0	13.2	
461	7.0-7.40	77.8	1.56	0.88		58.4	29.4	16.6	
511	1.3-1.7	96.0	1.46	0.74		60.6	31.4	16.4	DARK GREY CLAY
512	2.7-3.1	47.6	1.48	1.00		70.4	35.6	19.6	DARK GREY CLAY
512.A	2.7-3.1	108.2	1.42	0.68					DARK GREY CLAY
513	4.2-4.6	83.0	1.52	0.82		59.8	29.8	17.0	DARK GREY CLAY
514	5.7-6.1	69.8	1.56	0.92		59.8	29.4	17.0	DARK GREY CLAY
514.A	5.7-6.1	71.6	1.54	0.90					DARK GREY CLAY

515	7.2-7.6	39.6	1.54	1.10		76.2	38.4	20.2	DARK GREY FIRM CLAY
515.A	7.2-7.6	77.8	1.50	0.84					DARK GREY FIRM CLAY
516	8.7-9.1	22.2	1.98	1.62		57.4	33.2	17.0	
519	2.5-2.95	48.8	1.22	0.82		71.8	38.4	19.8	
520	5.5-5.95	61.8	1.66	1.02		60.0	29.8	17.0	
521	8.5-8.95	69.8	1.56	0.92					
522	10.0-10.45					77.0	35.0	18.4	
517	3	59.0	1.64	1.02	0.6968	48.8	24.8	13.6	DARK GREY CLAY
518	6	49.8	1.70	1.14	0.7232	48.4	22.4	12.4	GREY SANDY CLAY with SHELLS
518.1	6	68.4	1.68	1.00					
544	5.0-5.4	25.6	1.76	1.40		56.6	24.0	16.0	
545	10.0-10.4	46.4	1.64	1.12		65.2	35.8	16.2	
508	2.50-2.90	93.6	1.48	0.76		64.2	33.0	17.4	
509	5.50-5.90	69.0	1.62	0.96		58.8	31.4	16.2	
510	8.50-8.90	33.6	1.92	1.44		72.6	46.2	17.6	
477	2.0-2.40	49.6	1.66	1.10	0.2403				DARK GREY SILTY CLAY
477.1	2.0-2.40	56.8	1.64	1.04					DARK GREY SILTY CLAY
478	3.0-3.40								
479	4.0-4.40	48.6	1.72	1.16	0.4522				DARK GREY SANDY CLAY
479.1	4.0-4.40	51.6	1.70	1.12					DARK GREY SANDY CLAY
480	5.0-5.4								
483	8.0-8.40	63.0	1.68	1.04	0.88				DARK GREY CLAY
483.1	8.0-8.40	70.4	1.62	0.96					DARK GREY CLAY
484	9.0-9.40								
485	10.0-10.40								
486	11.0-11.4	55.6	1.72	1.10	0.7119				DARK GREY CLAY, SHELL FRAGMENTS
486.1	11.0-11.4	61.6	1.68	1.04					DARK GREY CLAY, SHELL FRAGMENTS
523	14.0-14.4	58.4	1.70	1.08					DARK GREY CLAY
523.A	14.0-14.40	81.4	1.68	0.92	0.9042				DARK GREY CLAY

524	15.0-15.40								
526	17.0-17.40	60.2	1.68	1.04	0.6837				DARK GREY CLAY
526.1	17.0-17.4	38.4	1.64	1.20					DARK GREY CLAY
529	20.0-20.40	53.8	1.78	1.16	0.6699				DARK GREY CLAY
529.1	20.0-20.40	31.8	1.70	1.30					DARK GREY CLAY
533	24.0-24.40	37.6	1.82	1.32	0.3599				DARK GREY CLAY
533.A	24.0-24.40	40.8	1.84	1.30					

62.72	1.624	1.016	0.655045	62.56897	32.12414	16.75862	<- Average
108.2	2.0	1.6	0.9	80.4	46.2	21.0	<- Max
22.2	1.2	0.7	0.2	35.8	14.8	9.8	<- Min
63.6	1.6	1.0	0.7	60.6	31.4	16.8	<- Median
55	55	55	11	29	29	29	<-No. sample
17.85251	0.123017	0.18052	0.207969	10.23547	7.074659	2.412256	<- Standard Deviation

APPENDIX D – THEORY OF ONE-DIMENSIONAL CONSOLIDATION

THEORY OF ONE-DIMENSIONAL CONSOLIDATION

Saturated clay layer of thickness 2H place between two sand layers (Figure D.1) is subjected instantaneously by surface loading, σ. The pore water pressure, u increasing immediately equals to surface loading (u=σ).

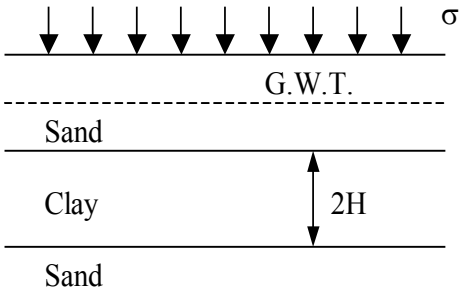

Figure D.1 Clay layer between two sand layers under groundwater table

Theory of consolidation for saturated clay was first proposed by Terzaghi (1925). The assumptions for mathematical derivation are based on

1. The clay layer is homogeneous.
2. The clay layer is saturated.
3. Darcy's law is valid.
4. The solid constituents of soil and water are absolutely incompressible.
5. The coefficient of consolidation (c_v) is constant through consolidation process.
6. The deformation occurs only in load applying direction.

The basic differential equation of Terzaghi consolidation theory is

$$\frac{\partial u}{\partial t} = c_v \frac{\partial^2 u}{\partial z^2} \quad \text{.....(D.1)}$$

Where c_v : coefficient of consolidation
u : pore water pressure
t : time
z : depth

The solution of equation D.1 requires boundaries conditions to solve the equation. The boundary conditions of this equation are as following:

1. At time $t = 0$, $u = u_i$
   Where u_i : initial pore water pressure at any depth
2. At time $t > 0$, $u = 0$ at $z = 0$

3.At time t > 0, u = 0 at z = 2H

Therefore, the solution of equation 2.1 correlating to above boundary conditions is

$$u = \sum_{n=1}^{n=\infty}\left(\frac{1}{H}\int_0^{2H} u_i \sin\frac{n\pi z}{2H}\,dz\right)\sin\frac{n\pi z}{2H}\,e^{\frac{-n^2\pi^2 T_v}{4}} \qquad \text{.....(D.2)}$$

Where T_v : time factor $\left(\frac{c_v t}{H^2}\right)$

n : an integer

H : the half length of clay thickness

u_i : initial excess pore pressure at any depth

The degree of consolidation, U_z at any depth, z is formulated by

$$U_z = \frac{u_i - u}{u_i} = 1 - \frac{u}{u_i} \qquad \text{.....(D.3)}$$

The average degree of consolidation for the whole clay layer can be defined as

$$U_{av} = \frac{\frac{1}{2H}\int_0^{2H} u_i dz - \frac{1}{2H}\int_0^{2H} u dz}{\frac{1}{2H}\int_0^{2H} u_i dz} \qquad \text{.....(D.4)}$$

The initial of excess pore pressure at any depth has many types. We will discuss 2 cases, constant of u_i with depth and linear variation of u_i with depth.

Case 1) Constant u_i with depth ($u_i = u_o$)

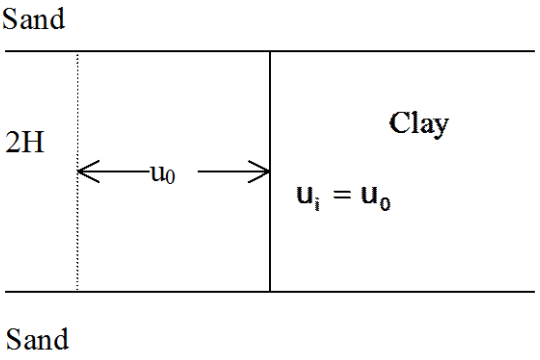

Figure D.2 u_i constant with depth

$$u = \sum_{m=0}^{m=\infty} \frac{2u_o}{M} \sin\frac{Mz}{H} e^{-M^2 T_v} \quad \text{.....(D.5)}$$

$$U_z = 1 - \sum_{m=0}^{m=\infty} \frac{2}{M} \sin\frac{Mz}{H} e^{-M^2 T_v} \quad \text{.....(D.6)}$$

$$U_{av} = 1 - \sum_{m=0}^{m=\infty} \frac{2}{M^2} e^{-M^2 T_v} \quad \text{.....(D.7)}$$

Where M : $\frac{(2m+1)\pi}{2}$

Case 2) Linear variation of u_i with depth

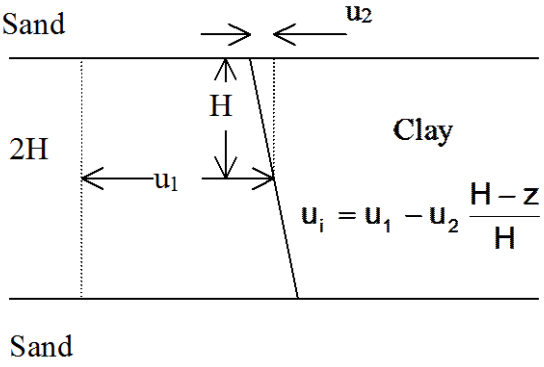

Figure D.3 Linear variation of u_i with depth

$$u = \sum_{n=1}^{n=\infty} \left[\frac{1}{H} \int_0^{2H} \left(u_1 - u_2 \frac{H-z}{H} \right) \sin\frac{n\pi z}{2H} dz \right] \sin\frac{n\pi z}{2H} e^{\frac{-n^2\pi^2 T_v}{4}} \quad \text{.....(D.8)}$$

The average degree of consolidation

$$U_{av} = 1 - \sum_{m=0}^{m=\infty} \frac{2}{M^2} e^{-M^2 T_v} \quad \text{.....(D.9)}$$

THEORY OF CONSOLIDATION UNDER TIME DEPENDENT SURCHARGE LOAD

Normally, surface loading does instantly not apply to clay layers but it will gradually increase with time (Figure D.2).

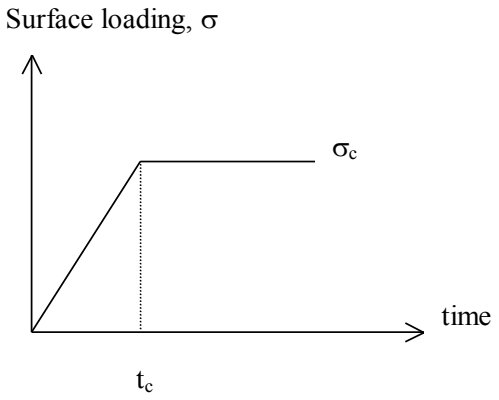

Figure D.4 Clay consolidation under time dependent surface loading

Olson (1977) introduced the mathematical solution of consolidation under time dependent surface loading as following:

When $T_v \le T_c$:

$$u = \sum_{m=0}^{m=\infty} \frac{2\sigma_c}{M^3 T_c} \sin\frac{Mz}{H}\left(1 - e^{-M^2 T_v}\right) \qquad \text{(D.10)}$$

$$U_{av} = \frac{T_v}{T_c}\left\{1 - \frac{2}{T_v}\sum_{m=0}^{m=\infty}\frac{1}{M^4}\left(1 - e^{-M^2 T_v}\right)\right\} \qquad \text{(D.11)}$$

When $T_v \ge T_c$

$$u = \sum_{m=0}^{m=\infty} \frac{2\sigma_c}{M^3 T_c}\left(e^{M^2 T_c} - 1\right)\sin\frac{Mz}{H} e^{-M^2 T_v} \qquad \text{(D.12)}$$

$$U_{av} = 1 - \frac{2}{T_c}\sum_{m=0}^{m=\infty}\frac{1}{M^4}\left(e^{M^2 T_c} - 1\right)e^{-M^2 T_d} \qquad \text{(D.13)}$$

Where T_c : $\left(\frac{c_v t_c}{H^2}\right)$

Alternatively, the incremental surface loading can be divided into step loads. The more step loads divided, the best accuracy of the solutions.

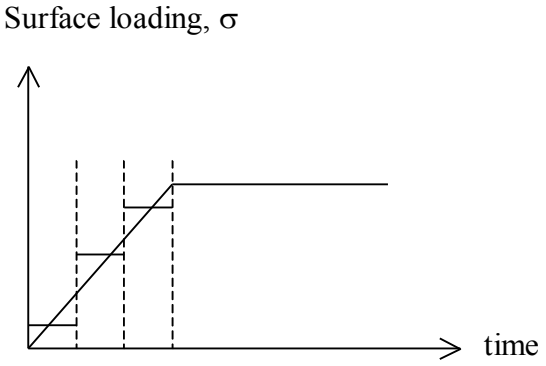

Figure D.5 Incremental surface loading by divided into step loads

THEORY OF ONE-DIMENSIONAL CONSOLIDATION SETTLEMENT

The settlement of clay layer can consider from the change of void ratio,

$$S = H\frac{\Delta e}{1+e_o} \qquad \text{.....(D.14)}$$

Where S : the magnitude of clay settlement
H : thickness of clay layer
e_o : initial void ratio at the beginning
Δe : change of void ratio

The change of void ratio can determine from the relationship between void ratio, e and pressure on semi-log scale. The correlations of e and log σ' depending on types of clay are as following:

1.Normally consolidated clay (NC)

$$\Delta e = C_c \log\left(\frac{\sigma_o' + \Delta\sigma}{\sigma_o'}\right) \qquad \text{.....(D.15)}$$

Where C_c, : the compression index
σ_o' : initial effective overburden pressure

$\Delta\sigma$: change of vertical pressure

2.Overconsolidated clay (OC)

$$\Delta e = C_s \log\left(\frac{\sigma_o' + \Delta\sigma}{\sigma_o'}\right) \quad \text{.....(D.16)}$$

Where C_s : the swell index
σ_o' : initial effective overburden pressure
$\Delta\sigma$: change of vertical pressure

3.Clay that $\sigma_o' < \sigma_c' < \sigma_o' + \Delta\sigma$

$$\Delta e = C_s \log\left(\frac{\sigma_c'}{\sigma_o'}\right) + C_c \log\left(\frac{\sigma_o' + \Delta\sigma}{\sigma_o'}\right) \quad \text{.....(D.17)}$$

Where C_c : the compression index
C_s : the swell index
σ_c' : the preconsolidation pressure
σ_o' : initial effective overburden pressure
$\Delta\sigma$: change of vertical pressure